ResearchOnline@JCU

JAMES COOK UNIVERSITY AUSTRALIA

This file is part of the following work:

**Shahriar, Mohammad Abu Naser (2014)** ***Settlement of shallow foundations due to rise of water table in granular soils.*** **PhD Thesis, James Cook University.**

Access to this file is available from:

https://doi.org/10.25903/9n49%2Drr36

Copyright © 2014 Mohammad Abu Naser Shahriar

The author has certified to JCU that they have made a reasonable effort to gain permission and acknowledge the owners of any third party copyright material included in this document. If you believe that this is not the case, please email researchonline@jcu.edu.au

# ResearchOnline@JCU

This file is part of the following reference:

**Shahriar, Mohammad Abu Naser (2014) *Settlement of shallow foundations due to rise of water table in granular soils.* PhD thesis, James Cook University.**

Access to this file is available from:

**http://researchonline.jcu.edu.au/41146/**

*The author has certified to JCU that they have made a reasonable effort to gain permission and acknowledge the owner of any third party copyright material included in this document. If you believe that this is not the case, please contact ResearchOnline@jcu.edu.au and quote* **http://researchonline.jcu.edu.au/41146/**

JAMES COOK UNIVERSITY AUSTRALIA

# Settlement of Shallow Foundations Due to Rise of Water Table in Granular Soils

Thesis submitted by

Mohammad Abu Naser Shahriar BSc. (Hons)

In November 2014

For the degree of Doctor of Philosophy
In the College of Science, Technology and Engineering
James Cook University

# STATEMENT OF ACCESS

I, the undersigned, the author of this thesis, understand that James Cook University will make it available for use within the University Library and, by microfilm or other means, allow access to users in other approved libraries.

All users consulting this thesis will have to sign the following statement:

> In consulting this thesis, I agree not to copy or closely paraphrase it in whole or in part without the written consent of the author; and to make proper public written acknowledgement for any assistance which I have obtained from it.

Beyond this, I do not wish to place any restriction on access to this thesis.

28/11/2014

---------- ----------

Signature Date

# STATEMENT OF SOURCES

## DECLARATION

I declare that this thesis is my own work and has not been submitted in any form of another degree or diploma at any university or other institution of tertiary education. Information derived from the published or unpublished work of others has been acknowledged in the text and a list of references is given.

28/11/2014

---------- ----------

Signature Date

## DECLARATION- ELECTRONIC COPY

I, the undersigned, the author of this work, declare that to the best of my knowledge, the electronic copy of this thesis submitted to the library at James Cook University is an accurate copy of the printed thesis submitted.

28/11/2014

---------- ----------

Signature Date

## ACKNOWLEDGEMENTS

I would like to express my deepest appreciation to all the professors, supervisors, friends and my family members for their incredible support, sincere guidance and encouragement throughout the tenure of my post graduate research study. I would like to express my special appreciation and thanks to my principal supervisor A/Professor Dr. Nagaratnam Sivakugan, who has been a tremendous mentor for me. I would like to thank my associate supervisors Dr. Vincent Wang and Professor Braja M. Das for encouraging my research and providing me excellent research training.

I want to thank Mr Warren O'Donnell for his valuable advice and guidance. I would also like to thank all my friends and colleagues, especially Hasan Mahmud, Shanka Widisinghe, Dhanya Ganesalingam for their ongoing support and valuable assistance. A special thanks to my family. I wish to express my sincere love and gratitude to my beloved wife Afrin Mehjabeen and my parents Abdul Latif Sarker and Nazma Ahmed for their understanding and endless love throughout the duration of my studies.

**ABSTRACT**

Shallow foundations are designed to limit settlements within tolerable limits. Rise of water level due to seasonal changes produce additional settlements of footings resting on granular soils and can threaten the integrity of the structure. Effect of water table rise on shallow foundation settlement was addressed by various researchers. Terzaghi's intuitive suggestion was to double the predicted settlement in dry sand to get the settlement in submerged condition. Analytical, experimental and numerical works by others were aimed at developing a correction factor to account for the effect of water table rise on foundation settlement. The objective of this study is to investigate the effect of water level rise on shallow foundation settlement in granular soils through numerical, analytical and experimental studies.

This study revisits Schmertmann's (1970) strain influence factor diagrams and modified influence factor diagrams for footings of various shapes (strip, circular, square, rectangular) are proposed using linear elastic models in FLAC and FLAC$^{3D}$. Then a rational method is proposed, based on proposed strain influence factors, to predict the additional settlement produced by the rise of water table on a footing resting on sands. The proposed method is validated by extensive laboratory test data where model footings of five different shapes were loaded in sand placed at two relative densities, where water level was raised from the bottom while the additional settlements were measured. This study also investigates how the additional settlement due to submergence is affected by various soil parameters. Nine different granular soils with wide range of variety in grain size distribution, uniformity and void ratio range were used for laboratory model study, and the results were analysed to determine the effect of different soil properties on settlement in submerged condition. Effect of fines content on settlement increment was investigated and additional settlements in loose and dense sands were compared. Particle shape parameters of the nine soils were determined by analysing microscopic images of soil grains and effect of particle shapes on additional settlement due to submergence was studied.

The study undertaken has also used explicit finite difference code FLAC and FLAC$^{3D}$ to simulate the rise of ground water table in granular soil and the resulting additional settlement was studied. The numerical results were compared with the laboratory test data and the proposed rational method for water table correction factor prediction. Elastic, nonlinear elastic and elasto-plastic constitutive models were used to investigate the variation of water

table correction factor with water table depth. Effect of various parameters (footing embedment depth, Poison's ratio, finite layer thickness and layered soil system etc.) on additional settlement due to water level rise is also discussed in this study.

The results obtained in this study will be valuable in understanding effect of different soil parameters and ground conditions on additional settlement that might occur as a result of water table rise. The rational method proposed herein will be useful for design engineers in predicting settlement correction factor for water table rise in granular soils.

The findings from this dissertation have been disseminated through the following technical papers, technical notes, and conference papers.

1. Shahriar, M. A., Sivakugan, N., Das, B.M. (2012a). "Strain Influence Factors for Footings on an Elastic Medium." *Proceedings, 11th Australia New Zealand conference on geomechanics,* Melbourne, 131-136.
2. Shahriar, M.A., Sivakugan, N., and Das, B.M. (2012b). "Settlements of shallow foundations in granular soils due to rise of water table – A critical review." *International Journal of Geotechnical Engineering*, J Ross Publishing, 6(4), 515-524.
3. Shahriar, M.A., Sivakugan, N., Urquhart, A., Tapiolas, M., and Das, B.M. (2013a) "A study on the influence of ground water level on foundation settlement in cohesionless soil*". Proceedings of the 18th International Conference on Soil Mechanics and Geotechnical Engineering: challenges and innovations in geotechnics,* Paris, 953-956
4. Shahriar, M. A., Sivakugan, N., and Das, B.M. (2013b). "*Settlement correction for future water table rise in granuular soils: a numerical modelling approach.*" *International Journal of Geotechnical Engineering*, Maney Publishing, 7 (2), 214-217.
5. Shahriar, M. A., Sivakugan, N., Das, B.M., Urquhart, A., Tapiolas, M. (2014). "Water Table Correction Factors for Settlements of Shallow Foundations in Granular Soils." *International Journal of Geomechanics,* ASCE (published online ahead of print).

# Contents

# List of figures

# List of Tables

# List of Symbols

| | | |
|---|---|---|
| $\beta$ | = | Gibson modulus ratio |
| $\gamma$ | = | Unit weight of sand |
| $\gamma_w$ | = | Unit weight of water |
| $\varepsilon$ | = | Axial strain |
| $\varepsilon_z$ | = | Vertical normal strain at depth *z* |
| $\epsilon_v$ | = | Volumetric strain potential |
| $\nu$ | = | Poisson's ratio |
| $\xi$ | = | Regularity |
| $\sigma'$ | = | Effective stress |
| $\sigma$ | = | Total stress |
| $\sigma_0^/$ | = | Effective overburden pressure at footing level |
| $\sigma_r$ | = | Radial stress increase due to applied load |
| $\sigma_1, \sigma_2, \sigma_3$ | = | Principal stresses in *x*, *y* and *z* direction |
| $(\sigma_1 - \sigma_3)_{max}$ | = | Asymptotic value of stress difference |
| $\sigma_z$ | = | Vertical stress increase due to applied load |
| $\sigma_{v0}^/$ | = | Overburden pressure at the depth where peak occurs |
| $\phi$ | = | Friction angle |
| $\varphi_c$ | = | Friction angle at zero dilation |
| $\Psi$ | = | Distance from critical state line |
| $A_t$ | = | Total area of the influence factor diagram |
| $A_w$ | = | Area of the influence factor diagram that is submerged |
| $B$ | = | Foundation width |
| $C$ | = | Footing shape factor |
| $C_1$ | = | Embedment depth correction factor |
| $C_2$ | = | Time correction factor |
| $C_c$ | = | Coefficient of curvature |
| $C_u$ | = | Coefficient of uniformity |
| $C_w$ | = | Water table correction factor |
| $C_{w,max}$ | = | Maximum value of water table correction factor |
| $d_{50}$ | = | Median grain size |

$d_{\max-in}$ = Maximum/largest inscribed circle within a sand particle

$d_{\max-in}$ = Minimum/smallest circumscribed circle of a sand particle

$d_{10}$ = Effective grain size

$D_f$ = Footing depth of embedment

$D_w$ = Water table depth

$D_r$ = Soil relative density

$e_{max}$-$e_{min}$ = Void ratio range

$E$ = Young's modulus of the dry sand

$E_0$ = Young's modulus of soil at the base of the footing

$E_i$ = Initial tangent modulus

$E_z$ = Elastic modulus of soil at depth $z$

$EI$ = Elongation index

$F_c$ = Percentage of fines content in soils

$h_f$ = Depth of thickness of the soil mass

$I_Z$ = Influence factor at depth $z$

$K_0$ = Coefficient of earth pressure at rest

$l_1$ = Length of major axis

$l_2$ = Length of intermediate axis

$n$ = Curve-fitting parameter

$(N_1)_{60}$ = Standard Penetration Test (SPT) number, corrected for overburden pressure and hammer efficiency

$N_{60}$ = SPT number, corrected for hammer efficiency

$N$ = Field Standard Penetration Number

$N_\gamma$ = Bearing capacity factor

$q$ = Applied pressure

$q_c$ = Cone resistance obtained from cone penetration test (CPT)

$q_{net}$ = Net applied pressure

$r_i$ = Radius of curvature of the of the particle corners

$R$ = Roundness

$s$ = Settlement of footing

$S$ = Sphericity

$S_r$ = Degree of saturation (%)

$t$ = Time (in years)

$z_a$ = Elevation above the water table in the unsaturated zone

$Z_I$ = Depth of influence zone

# Chapter 1 Introduction

## 1.1 General

Foundations are the lowest part of a structure which transmit the load from the structure to the underlying soil or rock. They have two major classes - shallow foundations and deep foundations. Foundations having the embedment depth lesser than the breadth are called shallow foundations. When the structural load is transferred deeper into the ground by piles or drilled shafts, they are called deep foundations.

Shallow foundations are usually of three types - pad, strip and raft foundations. Pad footings spread the column load uniformly into the ground, whereas strip footings carry the line load from the wall. Mat or raft foundations carry the loads from multiple columns and/or walls. Shallow foundations are the most economical, conventional foundations and are usually preferred by geotechnical engineers, when the soil conditions are suitable.

There are two main considerations in the design of shallow foundations - settlement and bearing capacity. The designers have to ensure that the foundation is safe with respect to bearing capacity failure into the underlying soil, and also the expected settlements are within tolerable limits. Shallow foundations are designed for specific column or wall loads and ideally they are designed such that their expected settlement is limited to 25 mm and there is safety factor of three against possible bearing capacity failure. It is believed that settlements are more critical than the bearing capacity for most foundations in granular soils, especially when the foundation width exceeds1.5 meters (this is often the case).

Settlement pattern in cohesive and cohesionless soil varies significantly. In granular soil, the settlement is almost instantaneous and there might be some long-term creep. In case of fine grained soil, settlement occurs in three stages - immediate settlement, primary and secondary consolidation settlement. Unlike cohesive soils, it is very hard to get undisturbed soil samples for granular soils, which makes the laboratory determination of soil stiffness extremely difficult. This is why in situ test results are used to get the soil stiffness in many settlement prediction methods.

There are more than 40 different settlement prediction techniques available to estimate settlements of shallow foundations in granular soils, many more than for cohesive soils. These can be divided into two major categories- 1) empirical or semi-empirical methods that

correlate settlements with in situ test results and 2) analytical methods based on elastic theory. In spite of all these different techniques and advancement in the computing power, the current state-of-the-art in the design of shallow foundations in granular soils remains very poor (Sivakugan and Johnson 2004).

The most important factors for shallow foundation design are applied pressure, soil stiffness, and width, depth and shape of the footing. Variation in the water table depth also plays an important role. When the water table is shallow, appropriate design parameters are used to account for the lower stiffness of the soil beneath the water table. When future rise in water table is expected, due to rain, floods or seasonal changes, the foundation settlements can increase substantially and jeopardize the integrity of the structure.

Terzaghi (1943) suggested that the soil stiffness (Young's modulus) of saturated granular soil is approximately 50% of that of the dry soil, without any strong experimental evidence. Usually a correction factor for the presence of water table is used in the design of shallow foundations. Various researchers proposed various correction factors to account for water table fluctuation below the footing. A few field investigations and some small scale laboratory experiments have been conducted so far to quantify the additional settlement due to submergence in granular soils. Predicting shallow foundation settlements on granular soils involve significant uncertainties, which can further increase if the ground water level rises below the footing level. Therefore, it is important to have a rational method to predict additional settlement due to water level rise, which should be verified by comprehensive experimental results and numerical analysis.

## 1.2 Effect of Water Table Rise on Settlement

Shallow foundations are designed such that their expected settlements are limited to 25 mm, and the safety factor against possible bearing capacity failure is three. When the water table is close to the footing, appropriate design parameters are used to reflect the less stiff soil beneath the water table. Owing to floods, heavy rainfall or seasonal fluctuations, the water table can rise below the footing and induce additional settlements that may not have been accounted for. There are various reasons for this additional settlement. Some soils contain soluble salts that can create strong bonding with soil grains in dry state. The salt gets dissolved when submerged and this can create significant additional settlement in cohesionless soils (US Army Corps of engineers, 1990). Fine grains presented in granular soil

create bonding with coarse grains in dry condition, which is lost when the soil is saturated. This results in additional settlement. Also, the lubrication mechanism of soil particle due to presence of water causes additional settlement (US Army Corps of engineers, 1990). However, the controlling factor for the settlement increment is the loss of soil stiffness due to saturation.

Terzaghi (1943) suggested intuitively that the soil stiffness (i.e. Young's modulus) of a saturated soil is 50% of that of the dry soil. He noted that the effective stresses within the soil, and hence the confining stresses, are reduced by 50% when the granular soil gets submerged. As a result, when water rises from very deep, and reaches the footing level, the settlement gets doubled. Fig. 1.1 shows the schematic diagram of a shallow foundation in granular soil. Throughout this thesis, the correction factor for water table, foundation width, depth of water table below the foundation and the depth of embedment of the footing are denoted by $C_w$, $B$, $D_w$ and $D_f$, respectively, as illustrated in Fig. 1.1.

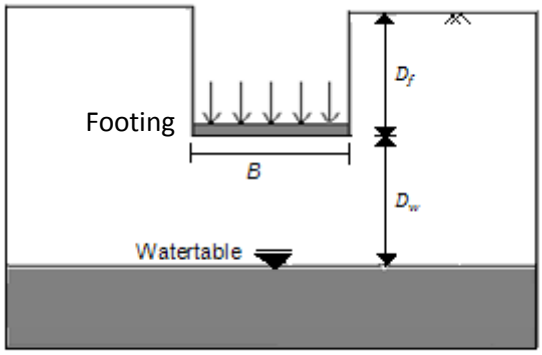


**Figure 1. 1 : Schematic diagram of foundation**

Very limited work has been conducted so far to study the effect of water table rise on shallow foundation settlement in granular soils. Some researchers accounted for the additional settlement due to fluctuating water table by using a correction factor, $C_w$, which varies with the water table height, reaching the maximum value when the water level reaches the base of the footing. The settlement calculated for dry sand is multiplied by this correction factor $C_w$, to get the settlement in submerged soil.

## 1.3 Current State-of-the-Art

The traditional approach to account for the additional settlement caused by rise in water level is to use a correction factor $C_w$. This is used as a multiplier to settlement in dry condition, to

get the settlement in submerged condition. The value of correction factor is greater than or equal to 1 and it increases with water table rise. It is defined as:

$$C_w = \frac{\text{settlement with water table below the footing level}}{\text{settlement in dry sand}} \tag{1.1}$$

Various researchers used the correction factor $C_w$ to account for the effect of rising ground water level on shallow foundation settlement (Terzaghi and Peck 1948; Teng 1962; Alpan 1964; Bazaraa 1967; Peck 1974; Bowles 1977; Department of the Navy 1982). The depth below the footing where the water table fluctuation will not have any effect is not unanimously agreed upon. The depth of embedment of the footing also affects the influence of water table on settlement, as the surcharge due to embedment increases the settlement in raised groundwater level. The different $C_w$ factors proposed by various researchers as function of the water table depth are summarised in Fig. 1.2. In all these cases, it is assumed that initially the water table is well below a depth where it can cause any effect on the settlement. Bazaraa (1967) suggested that the settlement increases by 75% when the water table rises to the footing level, and that there is no effect of the water table rise when it is at a depth greater than 0.5*B* below the footing. All others, in agreement with Terzaghi's (1943) recommendation, suggested that the settlement increase would be 100%, when the water table rises from very deep to the footing level. In other words, $C_w$ becomes 2.0 when the water table reaches the footing level. The depth at which the water table rise starts influencing the settlement varies from 1*B* (Teng 1962; Peck et al. 1974; Bowles 1977) to 2*B* (Terzaghi & Peck 1967; Alpan 1964). It can be seen from Fig. 1.2 that there is considerable variation in the suggested values for $C_w$. For example, when the water table rises to a depth of 0.5*B* below the footing, the suggested factors range from 1.00 to 1.75.

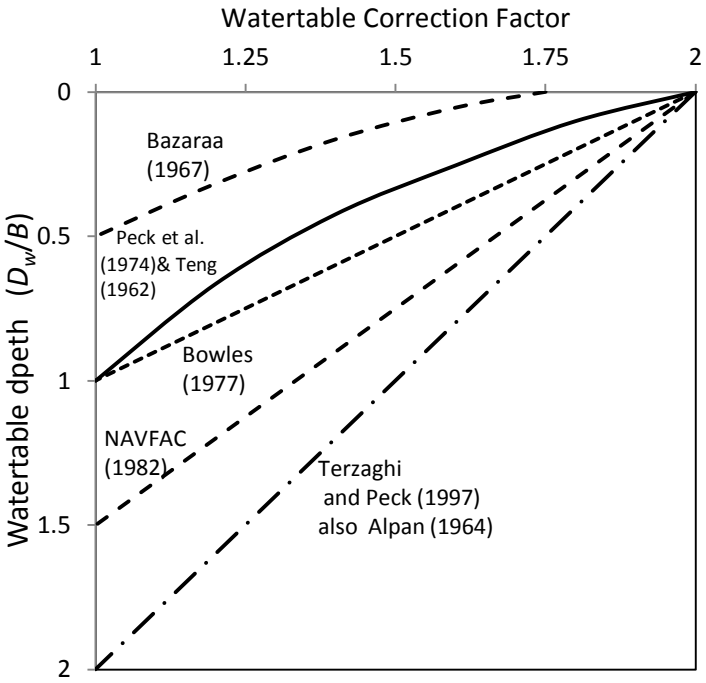


**Figure 1. 2 : Water table correction factors proposed by various researchers, when $D_f$ =0 (adapted after US Army Corps of Engineers,1991)**

Various researchers have investigated the effect of submergence on settlement of shallow foundations by analytical studies, field tests and laboratory model tests. Bazaraa (1967) used settlement prediction methods proposed by Vargas (1961) and Brinch Hansen (1966) to quantify the effect of submergence, and found that the maximum value of correction factor $C_w$ can be 1.7, when the water table reaches the footing level. Limited field investigations (Khanna et al. 1953; Ferreira and Da Silva 1961) reported in the literature show that the settlement gets doubled when the soil below the footing gets saturated, suggesting a correction factor of 2.0, supporting Terzaghi's suggestion.

A few laboratory experiments have been conducted so far to investigate the effect of rising water level on settlement, and contradictory results were reported. Agarwal and Rana (1987) used three square model footings in their experiments and the results suggested a correction factor of 2.0 at complete submergence, which support Terzaghi's (1943) proposition. Three different sizes of square model footings were used by Murtaza et al. (1995) at three different soil densities, who observed significantly higher additional settlements, up to 8 to 12 times more than that in the dry sand when the sand beneath the footing is fully submerged. This implies maximum $C_w$ values of 8-12, which are significantly higher than the values reported by the others. Morgan et al. (2001) used a single model square footing at very dense and very loose condition, and reported that the settlement increase in submerged soil can be 5.3 times

(i.e. $C_w$=5.3) more than the settlement in dry condition. However, the contradictory results obtained from these small scale experiments justify the need for a systematic laboratory model study on the effects of the water table rise on the settlements of footings on sands.

## 1.4 Objectives and Scope of the Research

The primary goal of this dissertation is to investigate the effect of water table rise on settlement of shallow foundation resting on cohesionless soils, based on numerical modelling, comprehensive laboratory testing and theoretical analysis. The scope of the study includes the following:

- To revisit Schmertmann's (1970) influence factors and develop strain influence factor diagrams for footings of various shapes (strip, circular, square, rectangular) using explicit finite difference codes, and the theory of elasticity.
- To propose a rational method, based on strain influence factors and experimental results, to predict the additional settlement produced by the rise of water table on a footing resting on sands.
- To simulate the rise of ground water table in granular soil by using explicit finite difference code FLAC and FLAC$^{3D}$ and study the resulting additional settlement.
- To quantify the effect of varying footing shapes, water table depth, ground conditions and relevant soil parameters on additional settlement of footings due to submergence through laboratory modelling and numerical simulation.

The study will involve numerical modelling, laboratory modelling and theoretical analysis. While simulating the water table rise in granular soils using FLAC and FLAC$^{3D}$, laboratory modelling of the footings will be performed concurrently and the results will be compared to verify the accuracy of the proposed method. The research will result in:

- Better understanding of the effect of water table rise on shallow foundation settlement resting on granular soils.
- A rational methodology to predict the water table correction factor that will have the flexibility to account for the varying soil properties, footing shapes and water table depths.
- Simple design charts and tables to assist the designers in selecting appropriate water table correction factors, which are based on sound fundamentals and verified by numerical and experimental results.

## 1.5 Relevance of the research

A large number of settlement prediction methods for foundations resting on cohesionless soil are available in the literature, mainly due to the difficulties involved in determining soil compressibility. Yet the current state-of-the-art for settlement prediction is very poor. This is well documented in the literature. The additional settlements produced by the rise of water table below the footing can bring in further uncertainties. Therefore, it is desirable to have some rational method for determining the additional settlements induced by the water table rise that can occur due to floods, rain fall or rise in sea level. There is no widely accepted procedure to quantify the increase in settlement due to rise in water table. Various researchers proposed correction factors for water table depth based on theoretical analysis, laboratory modelling and field test results. These factors differ from each other in magnitude and also vary with water table depth.

Theoretical studies conducted by Vargas (1961), Brinch Hansen (1966b) and Bazaraa (1967) suggest that when water table rises up to the footing level, the correction factor is 1.7. A few field investigations performed by Ferreira and Da Silva (1961) and Khanna et al. (1953) suggest that the correction factor is 2.0, which support Terzaghi's (1943) prediction. A few small scale laboratory experiments by Murtaza et al. (1995) and Morgan et al. (2010) have reported significantly higher values of correction factor. None of these investigated the effect of foundation shape on additional settlement caused by rising water level. Therefore, it is important to conduct a comprehensive laboratory experimental program to investigate the additional settlement induced by water table rise with varying footing shape, soil density and water table depth. The tests should be conducted with granular soils of various grain size distributions, representing well graded and poorly graded soils, in a wide range of grain sizes. The results can be analysed to determine the effect of different soil properties on settlement in submerged condition.

Most of the past studies on settlement increment due to submergence are based on analytical and experimental results, and there is a lack of research efforts involving numerical modelling. Footings of different shapes can be modelled using FLAC and FLAC$^{3D}$. Circular footing can be modelled as an axisymmetric problem and strip footing as plain strain problem in FLAC. For square and rectangular footings the problem becomes three dimensional and FLAC$^{3D}$ can be used. Settlement behaviour of model footings can be observed by simulating water table rise below the footings and the results can be compared with the experimental results in order to fully understand the effect of submergence on shallow foundation

settlement. Influence of foundation embedment depth, Poisson's ratio, finite layer thickness and other parameters can also be studied by numerical modelling.

# Chapter 2 Literature Review

Settlements play a critical role in the designs of shallow foundations in granular soils. Future rise in water table below the foundation can produce additional settlements, which can threaten the integrity of the structure. The tolerable settlements of shallow foundations are generally small, in the order of 25 mm, and hence any such additional settlements have to be estimated with good care. A critical review of the current state-of-the-art for estimating settlements due to water table rise is presented in this Chapter. This includes analytical studies, laboratory model tests and field tests. Terzaghi's (1943) hypothesis that settlement is doubled in granular soils when the water table rises to the ground level is supported by some analytical studies and limited field data. Laboratory model tests suggest that the settlement increase can be significantly larger, especially at higher stress-levels.

## 2.1 General

Shallow foundations include pad, strip and raft foundations. These are often the most economical and conventional foundations that are the preferred choice of geotechnical engineers when the soil conditions are favourable. Settlements and bearing capacity are the two main considerations in the design of shallow foundations. While ensuring that the foundation is safe with respect to bearing capacity failure into the underlying soil, it is also necessary to ensure that the expected settlements are within tolerable limits. Generally, shallow foundations are designed to limit the settlements to 25 mm and to have a safety factor of at least three against bearing capacity failure. For most foundations in granular soils, it is believed that settlements are more critical than the bearing capacity, especially when the foundation width is greater than 1.5 meters, which is often the case.

Settlement of a structure is not a big concern when the entire structure settles evenly. But if differential settlement occurs, that is, the adjacent footings experience a considerable difference in settlement values, there is a serious threat to the structure. The differential settlements can be controlled by limiting the total settlements of the various isolated footings that support the columns and walls.

In case of shallow foundations in granular soils, the most important factors that govern the settlements are the applied pressure, soil stiffness, and the dimensions including the width, depth and shape of the footing. Variation in the water table also plays an important role as it

causes fluctuation in the settlement of the shallow foundations. The soil below the water table has less stiffness, and this induces additional settlement. The groundwater level can rise up to or beyond the footing level, due to flood or rain, causing substantial additional and unforeseen settlements which can exceed the tolerable limits. The *N* value from standard penetration test (SPT) is used widely by geotechnical engineers for settlement prediction. Rise of water table also affects the blow count in SPT in granular soils.

There is no widely accepted procedure to quantify the increase in settlement due to the rise of water table. Terzaghi (1943) intuitively proposed that the stiffness of granular soil reduces to half as it gets saturated, which in turn doubles the settlement. When the watertable rises to some depth below the footing, a correction factor for the new location of watertable is used in the design of shallow foundations. Various researchers (Terzaghi 1948; Teng 1962; Alpan I. 1964; Bazaraa 1967; Peck 1974; Bowles 1977; Department of the Navy 1982) proposed correction factors to quantify the additional settlement due to the watertable rise below the footing. These correction factors are multiplied by the settlement in dry sands, to get the settlement in submerged sands. These correction factors differ from each other in magnitude and also vary with water table depth reaching the maximum value when the water table reaches the foundation level. Limited field investigations suggest that submergence of granular soil doubles the settlement when compared to dry condition, agreeing with Terzaghi's proposition. However, only limited laboratory studies have been conducted so far (Agarwal and Rana 1987; Murtaza et al. 1995; Morgan et al. 2010), and contradictory results have been found showing that the settlements increase by 12 times due to submergence. The extensive laboratory model tests carried out by the author in this dissertation also support these findings. These are critically reviewed in this Chapter.

## 2.2 Settlement prediction methods for shallow footings on granular soils

In the design of shallow foundations, two major criterions are taken into consideration - bearing capacity and settlement. When the foundation breadth is more than 1.5 m, settlement becomes more important than bearing capacity. Settlement of shallow foundations has two major components - elastic settlement and consolidation settlement. If the foundation is resting on granular soils, only the elastic settlement needs to be considered. In case of granular soil, it is very hard to get undisturbed soil sample which creates difficulty in determining the compressibility of the soil mass. This is why a large number of settlement prediction methods are available in the literature for footings on sand, much more than for

clays. Douglas (1986) reported 40 different settlement prediction methods for cohesionless soil. These can be classified in two general categories:

1. Empirical or semi-empirical methods based on observed settlement of structures. These methods correlate settlement with various in situ tests, for example, standard penetration test (SPT), cone penetration test (CPT), dilatometer test, etc.
2. Methods that use theoretical relationships obtained from the elastic theory. Methods of this category use the Young's modulus to predict foundation settlement.

Some of the most popular settlement methods were proposed by Terzaghi and Peck (1967); Schmertmann et al. (1978); Burland and Burbidge (1985); Berardi and Lancellotta (1994); Mayne and Poulos (1999). These methods were reviewed by Das and Sivakugan (2007) who also listed the empirical correlations that can be used for determining the soil stiffness.

The settlement prediction exercise carried out in Texas in 1994 clearly demonstrated the inadequacy in the current state-of-the-art for settlement predictions of footings in sands (Briaud and Gibbens 1994). Here, 31 international experts were given soil data from a very extensive laboratory and in situ testing program, and were required to predict the column loads that would produce 25 mm and 150 mm settlements of the five footings prior to the load test. The predictions were quite poor, with significant difference between the predicted and actual loads.

Settlements predicted by the different methods have been compared by Jeyapalan and Boehm (1986); Tan and Duncan (1991); Papadopoulos (1992); Berardi and Lancellotta (1994); and Sivakugan et al. (1998). The general observation is that most of the settlement prediction methods are conservative and hence overestimate the settlements and underestimate the allowable bearing pressures. Noting the uncertainty associated with the different methods, Sivakugan and Johnson (2004) proposed probabilistic design charts that can be used with some settlement prediction methods. These charts quantify the probabilities that the actual settlements can exceed specific values. Some researchers tried to develop settlement prediction methods using artificial neural network (Sivakugan et al. 1998; Shahin 2003).

## 2.3 Rise of water table and its effect on shallow foundation settlement

Rise of water table in cohesionless soil causes additional settlements. This can be attributed to various reasons. Some soils have soluble salts which, due to their ionic nature, create

strong bonding with the soil grains when dry. Rise in water table makes the salt get dissolved and the bonding is lost. This might create large additional settlement in loose granular soils (U S Army Corps of Engineers 1990). Presence of fines in granular soil mass can induce additional settlement when the water table rises. These fines create bonding with coarse grains in dry state, which is lost when they are saturated. Moreover, the lubrication mechanism of soil grains by water can result in additional settlement (US Army Corps of Engineers 1990). Another important reason for the increased settlement is the loss of capillary tension when the granular soil gets saturated. Capillary tension exists in partially saturated soil that exist above the water table. This causes an apparent cohesion in the granular soil mass, increases the effective stress and hence the shear strength. When the water table rises, the capillary suction is lost and additional settlement occurs (US Army Corps of Engineers 1990). But the most important cause for the additional settlement is the loss of soil stiffness which is described in the following section.

Terzaghi and Peck (1948) suggested that settlement of a footing in sand depends on initial tangent modulus of soil (slope of the initial straight segment of the stress-strain curve) and increases with the decrease in the tangent modulus. As the initial modulus depends on the confining stress and confining stress is roughly proportional to effective vertical stress, it can be said that the soil modulus changes with change in effective vertical stress. In the presence of water table, the effective stress reduces roughly to half when compared to the dry condition, which in turn lowers the soil stiffness (elastic modulus) to half. Hence, the settlement gets doubled.

Meyerhof (1956, 1965) noted that Terzaghi and Peck (1948) settlement calculation method is conservative and hence the correction for the presence of ground water table is not necessary. He also suggested that the effect of water table is already reflected on the value of the field standard penetration number *N*, and that is why further correction is not required. But if the water table rises after the determination of *N* value, there might be a significant increase in settlement value.

Peck and Bazaraa (1969) also supported Meyerhof's (1965) view about correction for water table, but they recognised the existence of field evidence of doubling the settlement due to water table rise to the footing level. They suggested that, when the water table rises into the influence zone in the vicinity of the foundation, the settlement on dry soil should be multiplied by the following factor

$$C_w = \frac{\sigma_{0\ in\ dry\ sand}}{\sigma'_{0\ in\ submerged\ sand}} \tag{2.1}$$

where, $\sigma_0$ = total overburden pressure at 0.5$B$ below the footing base

$\sigma'_0$ = effective overburden pressure at 0.5$B$ below the footing base

Burland and Burbridge (1985) proposed a settlement prediction method based on the statistical analysis of 200 settlement records of foundations, tanks and embankments on granular soil. In majority of the cases, water table was close to the foundation level. Among those, a few cases were noted where significantly larger settlement occurred when compared with the dry sand. Burland and Burbridge (1985) carried out a statistical analysis on 15 cases where the depth of water table was more than five meters, and found that their settlement was only about 13% less when compared to the complete data set. Another analysis was carried out on 24 plate load tests where water table was deeper than the depth of $B$ below the plates. It gave 25% less settlement value than the best estimate of all settlement records. Based on these, Burland and Burbridge (1985) concluded that there is no statistically significant effect of the water table depth on settlement value. But it does not mean that there is no effect of water level rise on settlement. While the presence of water table is reflected on the value of the field standard penetration number $N$, any future rise in water table can still cause significant increase in settlement.

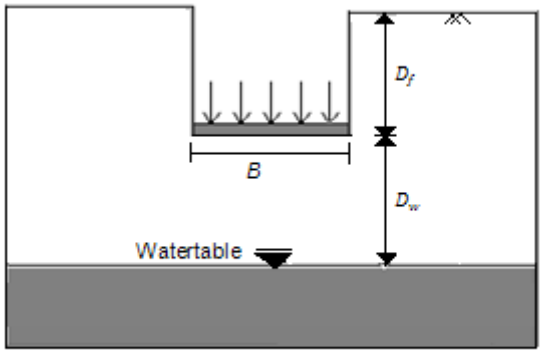


**Figure 2. 1 : Schematic diagram of foundation**

Various researchers have taken into account the effect of water table on foundation settlement in their settlement estimation methods. Usually, the effect is reflected as a correction factor

$C_w$ which is greater than 1. The correction factor is used to multiply the settlement calculated in dry condition to get the settlement in submerged condition. It is not unanimously agreed on the depth below which the rise in water table will have no effect on settlement. Generally it is taken as one to two times the width of the footing below the base of the footing. Depth of embedment also influences the effect of water table on settlement. The surcharge due to embedment results in increasing the settlement caused by water table fluctuation. In this thesis, the water table correction factor, foundation width, depth of embedment and water table depth will be denoted by $C_w$, $B$, $D_f$ and $D_w$, respectively (as shown in Fig. 2.1). Table 2.1 summarises the correction factors ($C_w$) proposed by various researchers, and some of these are also shown graphically in Fig. 2.2 for $D_f / B$ = 0, 0.5 and 1.

## 2.4 Effect of watertable on *N* value

The *N* value from standard penetration test is widely used in many settlement prediction methods. Hence, it is important to understand the effect of water table on the *N* value. The soil stiffness gets reduced when the soil gets saturated from dry state. Water lubricates the soil grains which reduce the intergranular shear resistance and increases slip potential. Also the apparent cohesion caused by capillary suction which contributes to the measured resistance, gets lost upon saturation. These affect the blow count in SPT test.

Table 2.1: Equations for water table correction factors

| **Reference** | **Equation for Water table Correction Factor,** $C_w$ |
|---|---|
| Teng (1962) | $C_w = \dfrac{1}{0.5 + 0.5[\dfrac{D_w - D_f}{B}]} < 2.0$ for water at end below footing base |
| Alpan (1964) | $C_w = 2.0 - 0.5(\dfrac{D_w}{B})$ for $D_w = D_f$ (approximately)>1.0 |
| Terzaghi and Peck (1967) | $C_w = 2 - \dfrac{D_w}{2B}$ (for surface footings) >1.0 |
| Bazaraa (1967) | $C_w = \dfrac{\gamma'(D_f + B/2)_{no\ water}}{\gamma'(D_f + B/2)_{water\ present}}$ |
| Peck, Hanson and Thornburn (1974) | $C_w = \dfrac{1}{0.5 + 0.5[\dfrac{D_w}{D_f + B}]}$ >1.0 |
| Bowles (1977) | $C_w = 2 - \dfrac{D_w}{D_f + B}$ >1.0 |
| NAVFAC(1982) | $C_w = 2 - \dfrac{D_w - D_f}{1.5B}$ >1.0 |
| Agarwal and Rana (1987) | $C_w = 1.95 - 0.57\dfrac{D_w}{B}$ >1.0 |

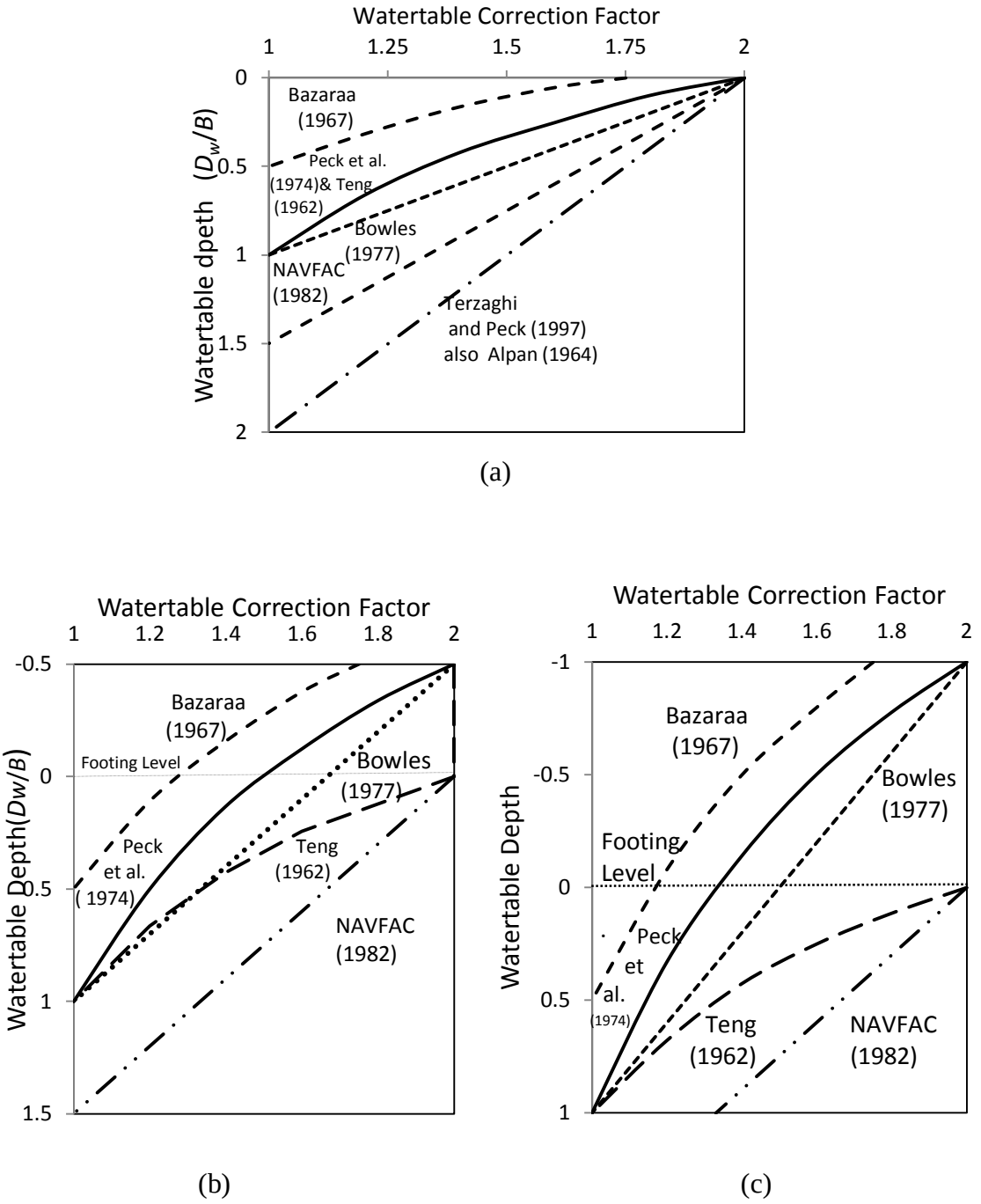


**Figure 2. 2 : Water table correction factors proposed by various researchers, (a) when $D_f$=0, (b) when $D_f$=0.5$B$, (c) when $D_f$=$B$ (adapted after US Army Corps of Engineers, 1991)**

Schultze and Menzenbach (1965) and Bazaraa (1967) have shown that submergence has little effect on $N$ value in the case of coarse granular soil. However, there are contradicting observations for fine and silty sands. Terzaghi and Peck (1948) suggested reducing the $N$ value for dense submerged fine or silty sand by the following,

$$N' = 15 + 0.5(N-15), \text{ when } N>15 \qquad (2.2)$$

This was contradicted by the laboratory test results of Gibbs and Holtz (1957) and Schultz and Melzer (1965). They investigated the effect of submergence on dynamic penetration value in very fine sands and observed that the penetration value gets substantially reduced in submerged sands. A large scale SPT test above and below the watertable was conducted by Bazaraa (1967) and he concluded that the *N* value for all fine and silty sands should be corrected by the following which is applicable for any value of *N*,

$$N' = 0.6N, \tag{2.3}$$

Burland and Burbridge (1985) conducted statistical analysis with 8 cases of submerged fine and silty sands. Applying correction for *N* value suggested by Terzaghi and Peck (1948) gives better results, whereas applying Bazaraa's correction yields poorer compressibility assessment. Hence, based on the limited evidence, Burland and Burbridge (1985) concluded that Terzaghi and Peck (1948) correction gives better assessment of foundation subgrade compressibility.

## 2.5 Further Developments

In addition to the above semi-empirical multiplication factors provided by various researchers, there were few more rational analytical studies as well as field and laboratory model tests. These are discussed in this section.

### 2.5.1 Theoretical Analysis

Vargas (1961) proposed a method to describe the settlement behaviour of Brazilian sand. The method assumes that the elastic modulus of soil ( $E_z$ ) at any depth *z* depends on the vertical and radial stresses at that point by:

$$E_z = \frac{(\sigma_z - \sigma_r)}{\varepsilon_z} = \alpha(K_0.\gamma z + \sigma_r) \tag{2.4}$$

where, $\sigma_z$ = vertical stress increase due to applied load

$\sigma_r$ = radial stress increase due to applied load

$\varepsilon_z$ = vertical normal strain at depth *z*

$\alpha$ = a constant which varies with soil type

$K_0$ = coefficient of earth pressure at rest

$\gamma$ = unit weight of sand

The settlement ($s$) of soil mass can be obtained by integrating the vertical strain $\varepsilon_z$ in Eq. 2.4, which gives:

$$s = \frac{1}{\alpha}\int_0^{\infty} \frac{\sigma_z - \sigma_r}{K_0.\gamma z + \sigma_r} dz \tag{2.5}$$

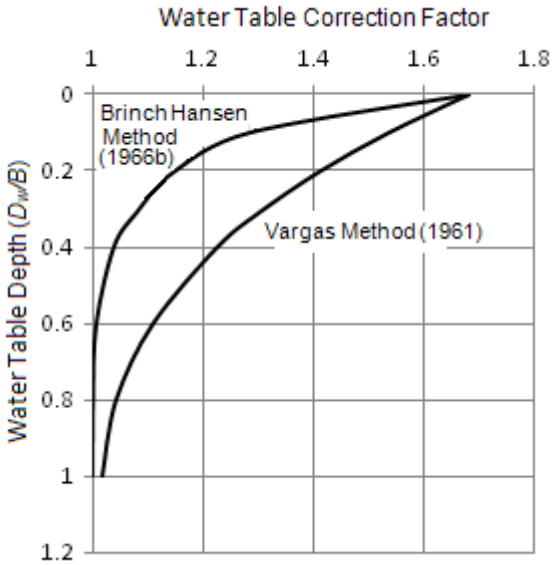


**Figure 2. 3 : Water table correction factors obtained by analytical methods (adapted after Bazaraa, 1967)**

Bazaraa (1967) used the method proposed by Vargas (1961) to study the effect of submergence on granular soil. He assumed the pressure on a circular footing resting on ground surface varies as a function of foundation width. Moreover, the pressure was chosen in such a way that it matches those of the buildings in Brazil and sufficient safety factor was maintained against bearing capacity failure. The vertical and radial stress changes were calculated using elastic theory assuming the Poisson's ratio as 0.3. The settlement values were calculated for different positions of water table below the foundation and the values are shown in Fig. 2.3. It was found that the settlement increases approximately by 70% when the water table rises up to the footing level.

Brinch Hansen's (1966b) method can also be used to quantify the effects of submergence. This method requires the values of some constants that can be obtained from oedometer and triaxial tests. Brinch Hansen proposed that the vertical strain $\varepsilon_1$ of sand can be obtained from general stress-strain relationship by using following equations:

$$\varepsilon_1 = f(\sigma_1 + \sigma_2 + \sigma_3)^s (1 + C_{12} + C_{13}) \tag{2.6}$$

$$f = \frac{be^r}{(1+2K_o)^s (1+2K_0 K_c)} \tag{2.7}$$

$$K_0 = 1 - \sin\phi \tag{2.8}$$

$$K_c = \tan^2(45^0 + \frac{\phi_c}{2}) \tag{2.9}$$

$$C_{12} = \frac{(m-1)K_c \frac{\sigma_1}{\sigma_2}}{\frac{m}{d_{12}^n} - 1} \tag{2.10}$$

$$d_{12} = (\cos ec\phi - 1)(\frac{\sigma_1}{\sigma_2} - 1) \tag{2.11}$$

$$C_{13} = \frac{(m-1)K_c \frac{\sigma_1}{\sigma_3}}{\frac{m}{d_{13}^n} - 1} \tag{2.12}$$

$$d_{13} = (\cos ec\phi - 1)(\frac{\sigma_1}{\sigma_3} - 1) \tag{2.13}$$

$$\phi = \sin^{-1}(\frac{\sigma_1 - \sigma_3}{\sigma_1 + \sigma_3}) \tag{2.14}$$

where, $\sigma_1, \sigma_2, \sigma_3$ are principal stresses, $\phi_c$ is the friction angle at zero dilation and *s, b, r, m, n* are constants. These constants depend on soil type, and Brinch Hansen (1966b, 1966a) gave the values for Asnoes sand in Denmark (*s* = 0.46, *b* = 2.6, *r* = 2.25, *m* = 4.5, *n* = 2). Bazaraa (1967) considered a surface tank resting on semi-infinite soil medium having similar properties as Asnoes sand and investigated the effect of water table rise on settlement. The tank was assumed to be circular with a diameter of *B* (m) and subjected to a pressure of *q*

($kN/m^2$) = 1.57*B*. Additional settlement due to water table rise was calculated using Brinch Hansen's method (1966b) for various positions of water table. The result also exhibits that settlement in submerged condition is 1.7 times the settlement in dry condition as shown in Fig. 2. 3.

### 2.5.2 Field Investigations

There are limited data available on field investigation of settlements in submerged and dry conditions. Khanna et al (1953) conducted some plate loading tests on square plate having an area of 928 $cm^2$ embedded to 0.305 meter. The tests were conducted in dry and rainy periods. The results indicated that submergence increases the settlement to around 2.1 times in case of sandy loam, and 1.4 times for coarse gravelly soil.

Ferreira and Da Silva (1961) conducted three plate loading tests on marine sand in Angola. The first test was conducted on sand at natural moisture content in dry weather (curve "a" of Fig. 2.4). The second one was carried out at the same natural moisture content for up to 98.07 kPa and then in submerged condition for higher loads (curve "c"). The last test was run on submerged sand (curve "b"). The results reveal that the submerged condition reduces the bearing capacity significantly and causes 2.5 times more settlement when compared to the natural moisture content. Moreover, the comparison of curve "a" and "b" indicates that the additional settlement due to submergence is much higher at high footing pressures. Ferreira and Da Silva (1961) have found iron and aluminium compounds in that soil which broke down in submerged condition and contributed to additional settlements.

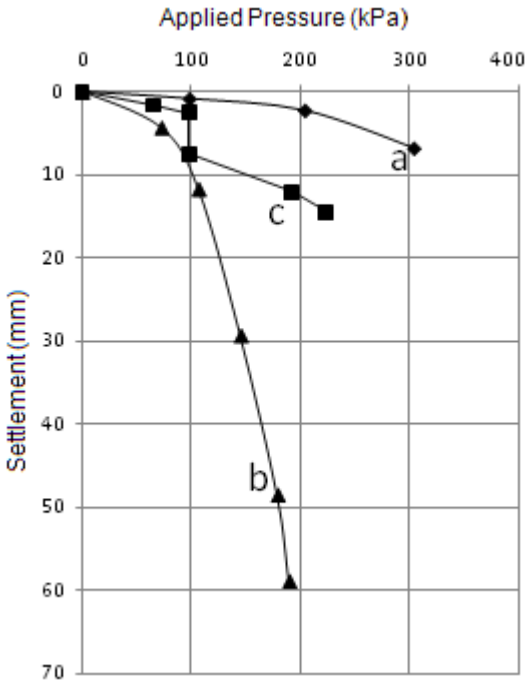


**Figure 2. 4 : Load-settlement curve obtained from field investigation by Ferreira and Da Silva (1961)**

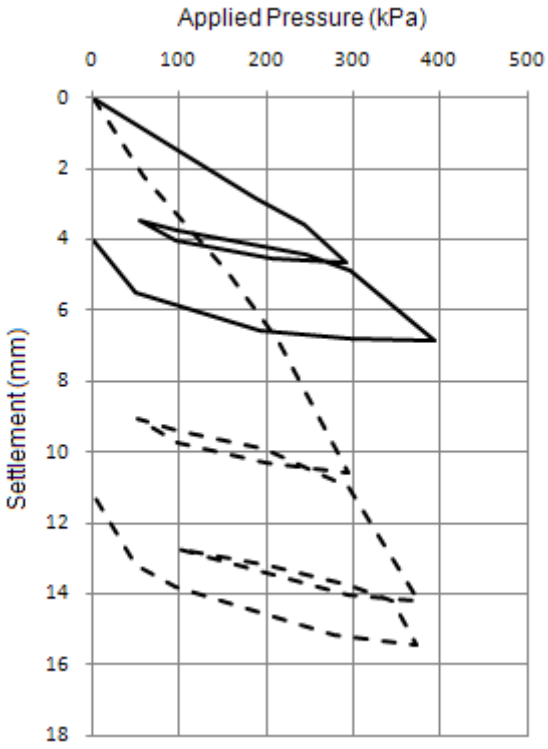


**Figure 2. 5 : Load-settlement curve for circular plates on clayey sandy gravel in dry (solid line) and submerged (dotted line) condition (adapted after Dvorák, 1963)**

Dvorák (1963) conducted plate loading tests on clayey sandy gravel. The soil was composed of more than 60% gravel and the rest was clayey sand. He used a square plate measuring

0.707 m X 0.707 m and carried out tests in dry and submerged condition. Fig. 2.5 shows the results of the tests. The solid line shows the load-settlement curve for dry soil, and the dotted line is the curve for submerged soil. The settlement in submerged sand was approximately 2.2 times than of the dry sand.

In general, these limited field investigations suggest that submergence almost doubles the settlement in granular soil, supporting Terzaghi's (1943) proposition. Bazaraa (1967) collected some field investigation data for situations where the sand was partially submerged. However, these failed to give any clear picture on the effect of water table rise at different depths.

### 2.5.3 Laboratory Model Tests

Agarwal and Rana (1987) investigated the effect of water table on foundation settlement in sand and proposed an equation for water table correction. In this series of model tests, settlement under a given load was measured for different depth of water table underneath the footing. They conducted tests on square footings of size 20 cm x 20 cm, 15 cm x 15 cm and 10 cm x 10 cm. The sand used was poorly graded, air dried and was deposited to dry unit weights of 15.5 kN/m$^3$ and 15.7 kN/m$^3$. Uniform density throughout the layer was ensured by applying rainfall method. First, an initial settlement of a specific value was applied on the footing placed on dry sand, which was followed by gradual rise of water table from the bottom of the tank up to the base of footing, and the increment in settlement was observed. A correction factor $C_w$ was proposed which is the ratio of settlement value at different water table level to the settlement on a dry soil. Fig. 2.6. shows the variation of water table correction factor at different water table depths ( $D_w$ ). The data points plotted in Fig. 2.6 were fitted along with the line of best fit given by:

$$C_w = 1.95 - 0.57\frac{D_w}{B} \tag{2.15}$$

The equation shows that the settlement increases by a factor of 1.95 when the water table rises up to the footing level. The correction factor is 1.67 when $D_w$ = 0.5 $B$ and 1.38 when $D_w$ = 1.0 $B$. These experimental findings support Terzaghi's (1943) proposal that the settlement doubles when water table rises to the base of the footing and that the increase is linear.

Murtaza et al (1995) conducted a settlement test on three model footings to observe the effect of submergence on settlement at different stress levels. They used three square footings of 6 cm x 6 cm, 8 cm x 8 cm and 10 cm x 10 cm placed on sand in a circular tank of 50 cm diameter and 25 cm height. Vertical load was applied in increments, and the corresponding settlement was measured. From the load-settlement curve of the dry sand, ultimate bearing capacity in each case was determined by double tangent method. The double tangent method requires that tangents be drawn to the pressure-settlement plot at the two linear segments. The intersections of these two tangents define the ultimate bearing capacity. This was divided by 1.5, 2.0 and 3.0 to get the working load at different factors of safety. These working loads were then applied on each of the footings under dry and submerged conditions. The results showed that settlement increased significantly, in the order of 8 to 12 times in wet sands. In submerged condition, settlement increased eight times for a factor of safety of 3 and twelve times for a factor of safety of 1.5 when compared to the dry conditions. Fig. 2.7 shows the applied pressure vs. settlement curves for 6 cm x 6 cm footing in submerged and dry conditions, for loose, medium and dense sands.

Rekowski (2001) investigated the additional settlements at various depths of ground water level. He used uniformly graded sand (soil A) and uniform gravels (soil B) for the research. The soils were tested at different relative densities ranging from 20% to 95%. A square model footing of 100 mm width was used. Soil was placed in the test tank by pouring from a funnel held vertically. The footing was loaded to one third of its bearing capacity and the settlement at dry state was recorded. Then water level was raised and the additional settlement corresponding to different water level was recorded. The results showed that the water table correction factor $C_w$ varied from 1.42 to 3.28 for soil 1 and from 1.51 to 2.52 for soil 2, with looser soils having higher correction factor value and vice versa. The plot of correction factor vs. water table depth was convex upwards for all cases in his study, showing higher rate of increment in the additional settlements with the water table rise.

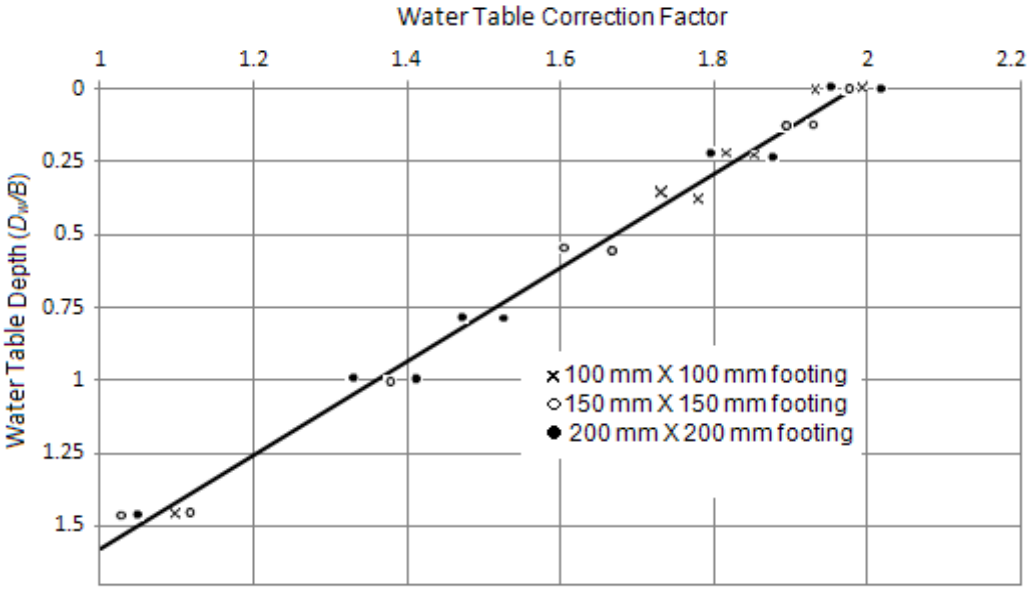


**Figure 2. 6 : Correction factor for varying water table depth from laboratory model tests of Agarwal and Rana (1987)**

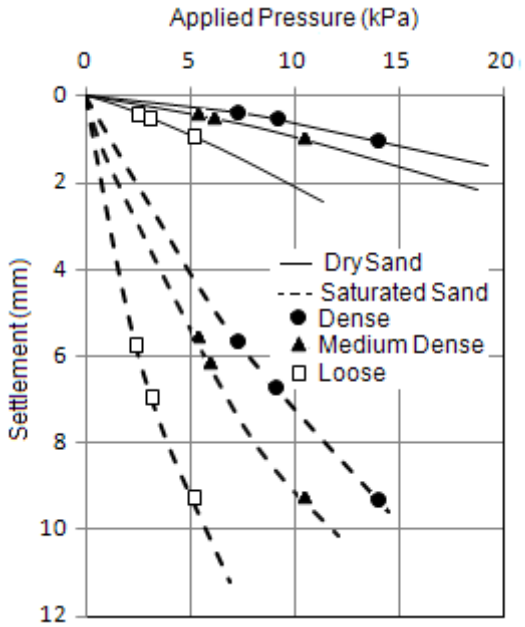


**Figure 2. 7 : Settlement of 6 cm x 6 cm model footing in dry and submerged condition (adapted after Murtaza et al, 1995)**

Morgan et al. (2010) carried out settlement and oedometer tests to investigate the additional settlement caused by water table rise in granular soil. They filled a cubical glass tank of 500 mm side length with granular soil and placed a model square footing measuring 100 mm X 100 mm on the surface. Two types of soil were used- soil 1 was coarse sand with very little

silt, and soil 2 was gravelly sand of sub-rounded grains. The test was carried out in very loose and very dense state with relative density $D_r$ =0% and 100%, respectively. Water was poured into the tank through a hollow section at the corner of the tank and the additional settlement was measured. Fig. 2.8 shows the additional foundation settlement compared to dry soil caused by the presence of water table at various depths. The results indicate that the additional settlement due to submergence can be as high as 5.3 times the settlement in dry soil.

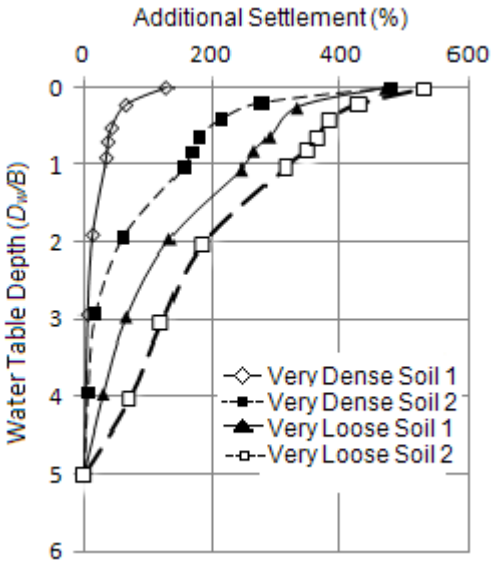


**Figure 2. 8 : Additional settlement due to water table rise obtained from laboratory experiments by Morgan et al. (2010)**

Mohamed et al. (2012) conducted plate load tests (PLT) and model cone penetration tests (CPT) in saturated and unsaturated conditions and proposed a settlement estimation method based on the test results. They used 150 mm x 150 mm plates (i.e., model footings) placed on the sand surface, at a embedment depth equal to footing width. A test tank with plan dimensions of 1500 mm x 1200 mm and 1060 height was used. The test was carried out at different water level and matric suction values. The test results were analysed along with stress-settlement relationship proposed by Mohamed and Vanapalli (2006) considering the influence of average matric suction within the influence zone (which was taken as 1.5 *B*). A series of CPT tests were also carried out with the same sand under saturated and unsaturated conditions. Based on the results they proposed a modification of Schemertman et al. (1978) settlement prediction method. Schemertman et al. (1978) proposed the following equation for predicting shallow foundation settlement resting on granular soils-

$$s = C_1 C_2 q_{net} \sum_{0}^{2B} \frac{I_z d_z}{E_z} \quad (2.16)$$

where, $C_1$ = embedment depth correction factor $= 1 - 0.5 \frac{\sigma_0'}{q}$

$\sigma_0'$ = effective overburden pressure at footing level

$q$ = applied pressure

$C_2$ = time correction factor

$$= 1 + 0.2 \log\left(\frac{t}{0.1}\right)$$

$t$ = time (in years)

Bowles (1996) suggested an expression to obtain elastic modulus *E*, from cone penetration resistance,

$$E = C_3 + C_4 (q_c) \quad (2.17)$$

where, $C_3 = 0$

and, $C_4$ =2.5-3.0 for normally consolidated sand

Mohamed et al. (2012) proposed a modification to Eq. 2.17 suggested by Bowles (1996). They proposed to replace the parameter $C_4$ by two correlation factors, namely, $f_1$ and $f_2$. These factors were obtained by regression analysis and are dependent on relative density ( $D_r$ ) of the soil. The soil condition (saturated or unsaturated) determines which factor should be used, this means

$f_1 = 1.5 * \left( (D_r/100)^2 + 3 \right)$ , for saturated sands

$f_2 = 1.2 * \left( (D_r/100)^2 + 3.75 \right)$, for unsaturated sands with $D_r < 50\%$

$f_2 = 1.7 * \left( (D_r/100)^2 + 3.75 \right)$, for unsaturated sands with $D_r \geq 50\%$

## 2.6 Conclusion

The effect of water table rise on settlement of shallow foundation in sand was firstly discussed by Terzaghi (1943) who suggested that the saturation halves the soil stiffness and doubles the settlement. Since then, many researchers tried to investigate how the shallow foundation settlement changes due to the variation of water table depth. Various correction factors have been proposed based on analytical and experimental studies. These factors differ from each other in magnitude and with water table depth. Theoretical studies (Vargas 1961; Brinch Hansen 1966b; Bazaraa 1967) described in this Chapter suggest a correction factor of 1.7, when the water level reaches the footing surface. A few field investigations (Ferreira 1961; Khanna 1953) support Terzaghi's (1943) prediction that the water table correction factor should be two when the water table rises to the base of the footing. Some small scale laboratory experiments (Murtaza et al 1995; Morgan et al. 2010) have reported significantly higher values of additional settlements, whereas experiments conducted by Agarwal and Rana (1987) and Rekowski (2001) suggested lower water table correction factors. However, none of these studies considered the effect of footing shapes or soil properties on the additional settlements due to water table rise. In summary, the absence of any widely accepted procedure to account for the effect of water table rise in the literature, very limited field and laboratory tests and scarcity of numerical modelling studies on the effects of water table rise indicate the need for further research in this area.

# Chapter 3 Strain Influence Factor Diagrams for Footings on an Elastic Medium

## 3.1 General

Settlement is one of the key considerations in designing shallow foundations. Shallow foundations in granular soils are designed such that the settlements are within tolerable limits, usually in the range of 25 mm in the case of isolated footings. Schmertmann's (1970) method is one of the most rational methods for computing settlements of footings in granular soils, and is commonly used world-wide. The method relies on a strain influence factor that varies with depth. To consider the effect of footing shape on foundation settlement, Schmertmann et al. (1978) proposed separate strain influence factors for axi-symmetric and plane strain loading situations, representing circular and strip footings, respectively. It was further modified by Terzaghi et al. (1996). The literature suggests that the researchers were not in unanimous agreement upon on the magnitude of influence factor below the footing, the depth at which it reaches the maximum and the depth it is extended below the footing.

In this Chapter, Schmertmann's influence factors were revisited using FLAC and FLAC$^{3D}$, explicit finite difference codes used widely in geotechnical modelling, and the theory of elasticity. Linear elastic and non-linear elastic constitutive models were used in the analysis. The influence factors derived are compared with those proposed by Schmertmann. For square and rectangular footings, the problem becomes three-dimensional and therefore FLAC$^{3D}$ was used in the analysis. The strain influence factors are developed for footings with breadth/length ratios of 0.25, 0.50, 0.75 and 1.0. The strain influence factors for the rectangular footings are presented along with those for the circular and strip footings. The effect of Poisson's ratio is also investigated. The strain influence factors proposed for the rectangular footings will be valuable in the design of shallow foundations on granular soils. The use of non-linear elastic constitutive model is more realistic than the traditional linear elastic model, and the differences are discussed. For practical use of geotechnical engineers, a mathematical form of derived strain influence factor is proposed along with a table showing influence factor values at different depth below the footing.

## 3.2 Strain Influence Factor Diagrams

In the design of shallow foundations, two major criteria's are taken into consideration- bearing capacity and settlement. If the foundation is resting on granular soil, settlement is

believed to be more critical than bearing capacity in most cases. Usually, an acceptable limit of 25 mm settlement is maintained in the design of shallow footings. In case of cohesionless soil, it is hard to get undisturbed soil sample which creates difficulty in determining compressibility of the soil mass. As a result, a large number of settlement prediction methods are available in the literature for footings on granular soil, much more than cohesive soils. Schmertmann (1970) proposed a settlement prediction method which is based on cone penetration test results and relies on strain influence factor which is a function of depth. This method is used by geotechnical engineers all over the world for its simplicity and reliability. Burland and Burbridge (1985) proposed a semi-empirical method for settlement calculation which is being more commonly used recently.

The concept of strain influence factor is straightforward and simple. If a uniform pressure $q$ is applied over a large area on an elastic half space, the resulting strain at any depth $z$ becomes $q/E_z$. If the load is applied over a limited width $B$, the resulting strain at a depth $z$ along the centreline will obviously be less and can be expressed as:

$$\varepsilon_z = \frac{q}{E_z} I_z \tag{3.1}$$

where, $E_Z$ = elastic modulus at depth $z$

$I_Z$ = influence factor at depth $z$

The strain influence factor can be used to determine the vertical settlement $s$ of shallow footing resting on granular soil. Schmertmann (1970) considered elastic theory, finite element analysis and load test on model footings and proposed a settlement prediction approach using the following equation,

$$s = C_1 C_2 q_{net} \sum_{2B}^{0} \frac{I_z d_z}{E_z} \tag{3.2}$$

where, $C_1$ = embedment depth correction factor $= 1 - 0.5\frac{\sigma_0^{/}}{q}$

$\sigma_0^{/}$ = effective overburden pressure at footing level

$q$ = applied pressure

$C_2$ = time correction factor

$$=1+0.2\log\left(\frac{t}{0.1}\right)$$

$t$ = time (in years)

After careful observation of theoretical and experimental results, Schmertmann (1970) proposed a simplified 2*B*-0.6 diagram as shown in Fig. 3.1(a). This shows that the influence factor is zero at the foundation level, increases linearly to peak at 0.6 at a depth of 0.5 *B*, and then decreases linearly to 0 at a depth of 2*B*.

The Young's modulus $E_z$ can be obtained by using the equation

$$E_z = 2q_c \tag{3.3}$$

where, $q_c$ = cone resistance obtained from cone penetration test (CPT)

To account for the effect of foundation shape on settlement, Schmertmann et al.(1978) modified the 2*B*-0.6 diagram as shown in Fig. 3.1(b). For square and circular footing, the value of $I_Z$ at the footing level is 0.1; it reaches its peak at a depth of 0.5*B* and reduces to zero at 2*B*. In case of strip footing, $I_Z$ value is 0.2 at foundation level, peaks at $z = B$ and becomes zero at $z = 4B$. The influence factor diagram for a rectangular foundation can be obtained by interpolating between these two. The peak value of influence factor can be calculated by:

$$I_{z,peak} = 0.5 + 0.1\sqrt{\frac{q_{net}}{\sigma'_{vo}}} \tag{3.4}$$

where, $q_{net}$ is the net applied pressure and $\sigma'_{v0}$ is the overburden pressure at the depth where peak occurs.

The relationship of Young's modulus with penetration resistance was also modified by:

$E_z = 2.5q_c$, for square/ circular footing (3.5)

$E_z = 3.5q_c$, for strip footing (3.6)

Terzaghi et al. (1996) suggested a simpler influence factor diagram as shown in Fig. 3.1(c). They proposed $I_Z$ = 0.2 at footing level and peak of 0.6 at 0.5$B$ depth for all footings. The depth of influence ($Z_I$) was kept same as Schmertmann et al. (1978) for circular and strip footing but for rectangular footing, it should be interpolated by:

$$Z_I = 2B[1+\log(\frac{L}{B})] \; for L/B \le 10 \tag{3.7}$$

Mayne and Poulos (1999) proposed a spreadsheet integration technique to obtain the strain influence factor at various depths to calculate the foundation settlement. This technique can be used in settlement calculation on homogeneous to non-homogeneous soils having finite to infinite soil layer thicknesses.

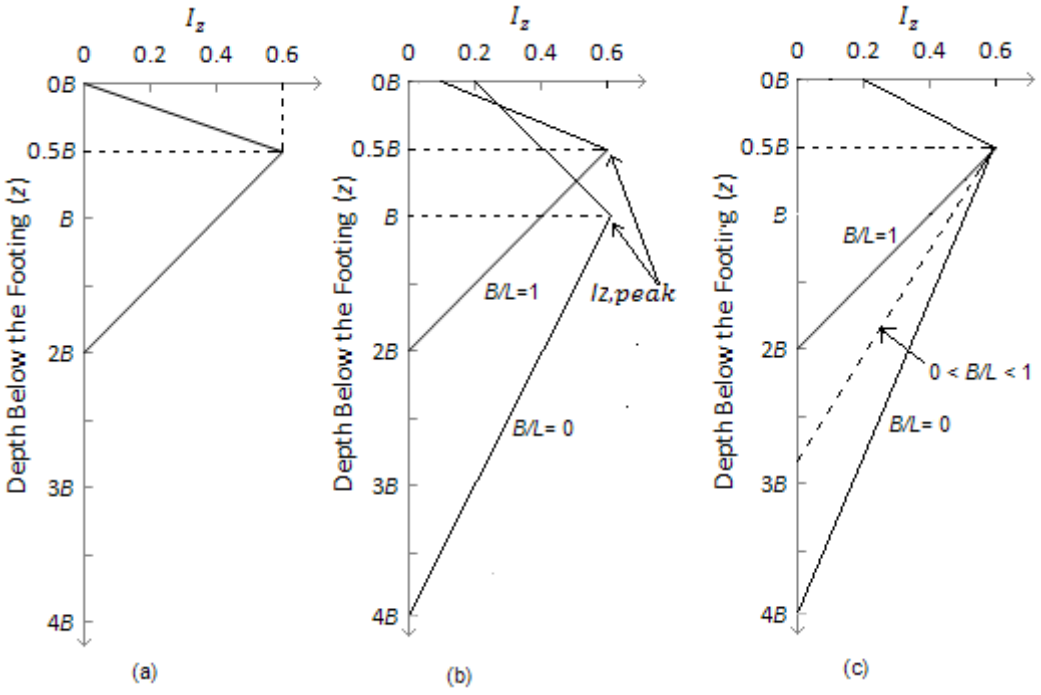


**Figure 3. 1 : Strain influence factor diagrams- a) Schmertmann (1970), b) Schmertmann et at. (1978), c) Terzaghi et al. (1996) (adapted after Sivakugan and Das 2010)**

Despite the popularity of Schmertmann's strain influence factor method, it is very conservative (Sivakugan et al. 1998) and lacks accuracy (Tan and Duncan 1991). So, there is plenty of scope to work further on the influence factor diagrams, thus improving the settlement prediction method. In this study, linear and non-linear elastic models in FLAC$^{3D}$ and FLAC to derive strain influence factors for all regular foundation shapes. Also, the depth to maximum strain, depth of influence and the effect of Poisson's ratio were investigated.

## 3.3 Derivation of Strain Influence Factor Diagrams using FLAC and FLAC$^{3D}$

### 3.3.1 Linear elastic analysis

In this study, explicit finite difference codes FLAC and FLAC$^{3D}$ and the elastic theory were used to revisit Schmertmann's strain influence factors. Influence factors for all regularly shaped footings (including circular, square, rectangular and strip footings) were derived using linear elastic model. FLAC was used to model axi-symmetric and plane strain loading conditions and FLAC$^{3D}$ to model square and rectangular cases. The strain influence factors were developed for footings with breadth/length ratios of 0.25, 0.5, 0.75 and 1.0. The modelling was done keeping the horizontal and rectangular boundaries 6.0 *B* away from the centreline of the footing and the footing width was fixed at 1.0 m. The elastic modulus was taken as 30 MPa and Poisson's ratio ($\nu$) was fixed at 0.2 for all cases. The footings were placed on ground surface and a uniform pressure of 100 kPa was applied.

Using FLAC and FLAC$^{3D}$, vertical and horizontal stresses were obtained at various depths along the centreline below the footing, which were then used to calculate the vertical strain using the constitutive relationship of Hooke's Law:

$$\varepsilon_z = \frac{1}{E_z}[\sigma_z - \nu(\sigma_x + \sigma_y)] \tag{3.8}$$

where, $\varepsilon_z$ and $E_z$ are the vertical normal strain and elastic modulus respectively at a depth $z$ below the centreline of the footing, and $\sigma_x, \sigma_y, \sigma_z$ are the normal stresses along $x$, $y$ and $z$ directions.

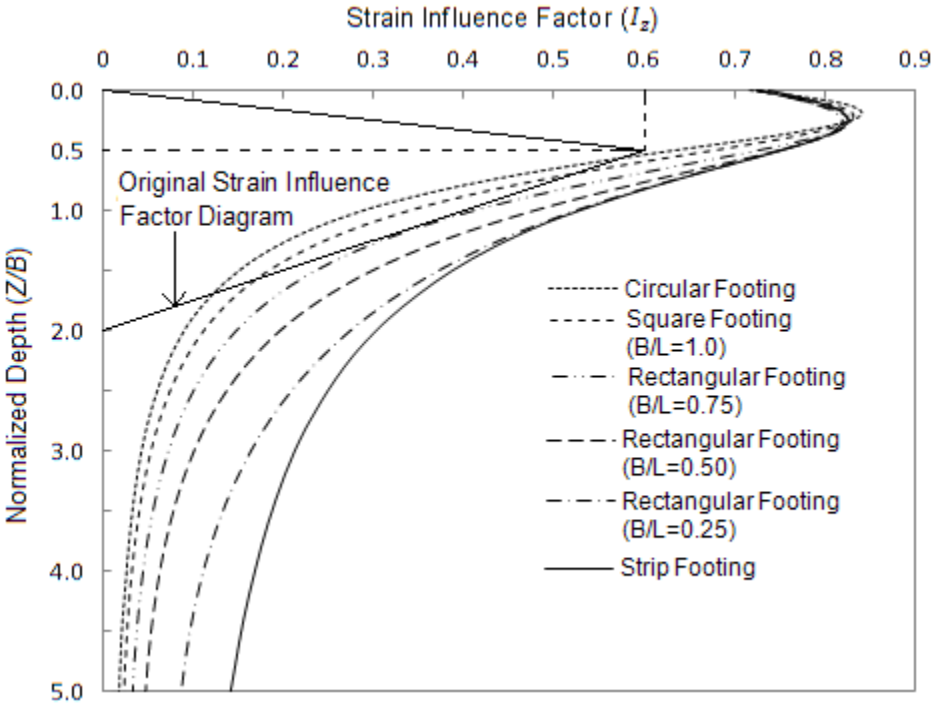


**Figure 3. 2 : Strain influence factor diagrams obtained from linear elastic analysis**

The influence factor was then obtained by:

$$I_z = \frac{\varepsilon_z E_z}{q} \tag{3.9}$$

Fig. 3.2 shows the strain influence factor diagrams for footings of various shapes obtained from linear elastic analysis. The diagrams show some variations when compared to Schmertmann's (1970) originally proposed influence factor diagram as shown in the figure. Unlike the original diagram, the influence factors range between 0.72-0.74 at the base of the footing, peak at around 0.83 at a depth of 0.2-0.25 and extend to a greater depth. The strain influence factors extend to depth well below 4*B* proposed by Schmertmann for strip footing, and the factors are significantly larger. For rectangular footings also, there are noticeable strains at depths of $z$ = 2*B* to 4*B*, and beyond. The shape of the strain influence factor plot was very similar for all footing shapes. The strain influence factor diagrams obtained from linear elastic analysis do not vary with Young's modulus, but their value changes with Poisson's ratio which is discussed in the next section.

### 3.3.2 Effect of Poisson's ratio

There are some difficulties involved in laboratory triaxial testing (for example, capping problems, seating errors, non-uniformity of stress etc.) which result in higher Poisson's ratio value, ranging from 0.25-0.45 (Lo Presti1995). Nowadays, these can be avoided by mounting

local strain devices at midlevel of soil specimen and measuring strain internally (Tatsuoka and Shibuya 1992). Tatsuoka et al. (1994) showed that the drained value of Poisson's ratio for elastic continuum solutions ranges from 0.1 to 0.2 in sands. Therefore, strain influence factors for $\nu$ = 0.1 and 0.2 were derived using linear elastic model in FLAC. Fig. 3.3 shows the effect of Poisson's ratio on the strain influence factors in circular and strip footings. The figure shows that variation of Poisson's ratio affects the influence factor diagram up to a depth of 0.5 *B* in circular footing. For strip footing, it affects the influence factor for a depth of 1.0 *B* below the footing.

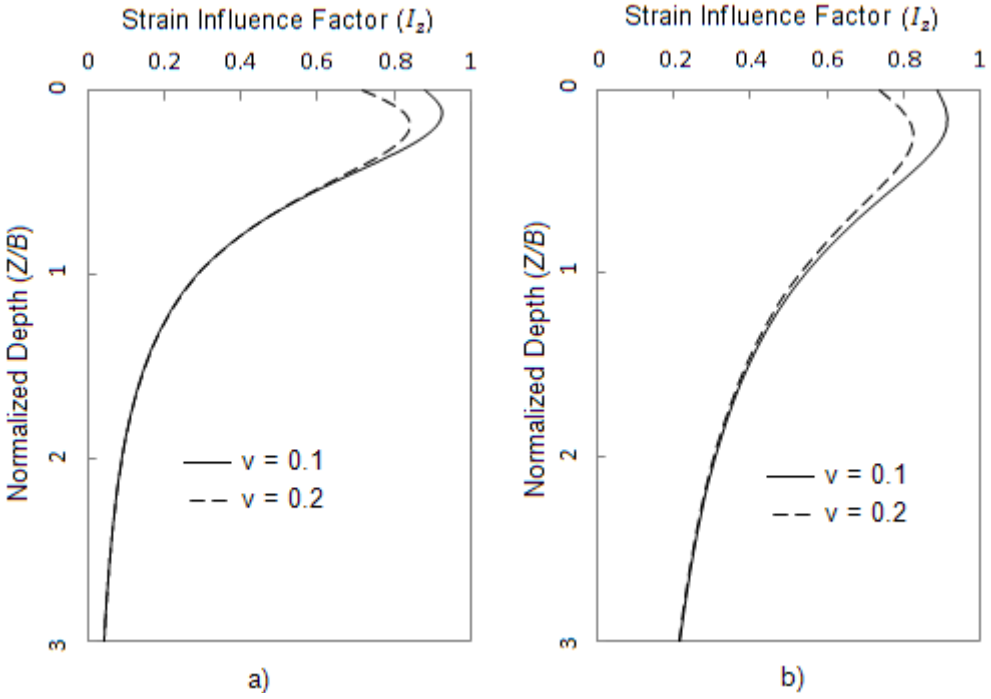


**Figure 3. 3 : Effect of Poisson's ratio on strain influence factor diagrams- a) circular footing, b) strip footing**

### 3.3.3 Non-linear elastic analysis

Hyperbolic nonlinear elastic soil model in FLAC was used to investigate the variation of vertical strain with depth. The nonlinear elastic soil model is based on the hyperbolic stress-strain relationship proposed by Kondner and Zelaska (1963):

$$(\sigma_1 - \sigma_3) = \frac{\varepsilon}{\frac{1}{E_i} + \frac{\varepsilon}{(\sigma_1 - \sigma_3)_{max}}} \tag{3.10}$$

where: $(\sigma_1 - \sigma_3)_{max}$ = asymptotic value of principal stress difference

$\varepsilon$ = axial strain

$E_i$ = initial tangent modulus

Fig. 3.4 shows the vertical strain distribution below the centreline of a circular footing resting on the surface of a homogeneous granular soil. Three different loading conditions were considered- 0.5, 1.0 and 1.5 times the working load of the soil (one-sixth, one-third and half of the bearing capacity of the soil). The results show that the depth of maximum vertical strain occurs at a depth of 0.3 *B* below the footing for all cases. This is little higher than what was obtained from linear elastic modelling (0.2 *B*) but less than Schmertmann's (1970) simple triangular approximation (0.5 *B*). Fig. 3.4 shows that $I_{z,peak}$ occurs at 0.3*B* in nonlinear elastic analysis.

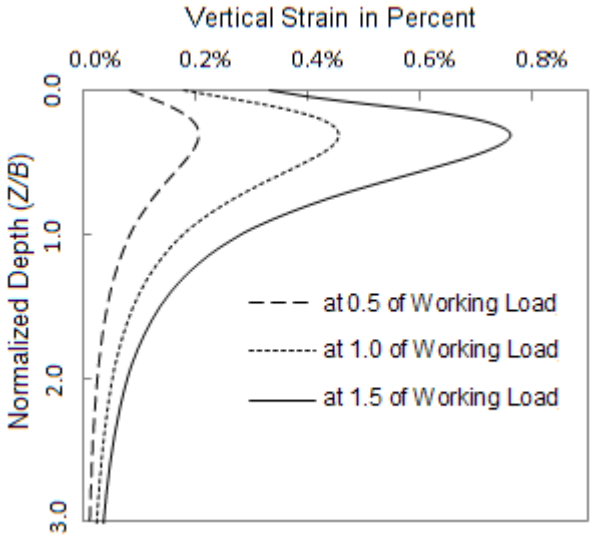


**Figure 3. 4 : Vertical strain at different loading conditions in nonlinear elastic analysis**

## 3.4 Equation for Modified Strain Influence Factor Diagrams

For the benefit of practising engineers, it is important that the strain influence factor diagrams can be used easily in routine design. The strain influence factor diagram proposed by Schmertmann (1970) was simple and has a mathematically defined shape which makes it easy to use for routine design. Further modifications proposed by Schmertmann et al. (1978) and Terzaghi et al. (1996) also have simple mathematically defined shapes. For strain influence factor diagrams proposed in this Chapter, an equation is proposed based on several curve fitting trials. The strain influence factor $I_z$ at a depth $z$ can be expressed as-

$$I_z = \frac{0.438}{(z+0.2)} e^{C(z-0.16)-0.59\left[\ln(z+0.2)+0.22\right]^2} \tag{3.11}$$

where, *C* is the footing shape factor and can be defined as

$$C = 0.56 - 0.56\left(\frac{B}{L}\right) \tag{3.12}$$

Eq. 3.11 can be used for any rectangular, strip or circular footing and influence factor at any given depth can be determined by substituting the depth and appropriate footing shape factor in Eq. 3.12.

Fig. 3.5 shows how the influence factor diagrams using Eq. 3.11 match with the diagrams derived in this Chapter. A careful observation of the diagrams clearly indicates that equation Eq. 3.11 and 3.12 can be used for proposed influence factor diagrams with reasonable accuracy.

Strain influence factors for different footings at various depths are also given in Table 3.1. Anyone who is interested in using the proposed strain influence factor diagrams can either use the diagrams in Fig. 3.2 or strain influence factor equation given in Eq. 3.11, or the values given in Table 3.1.

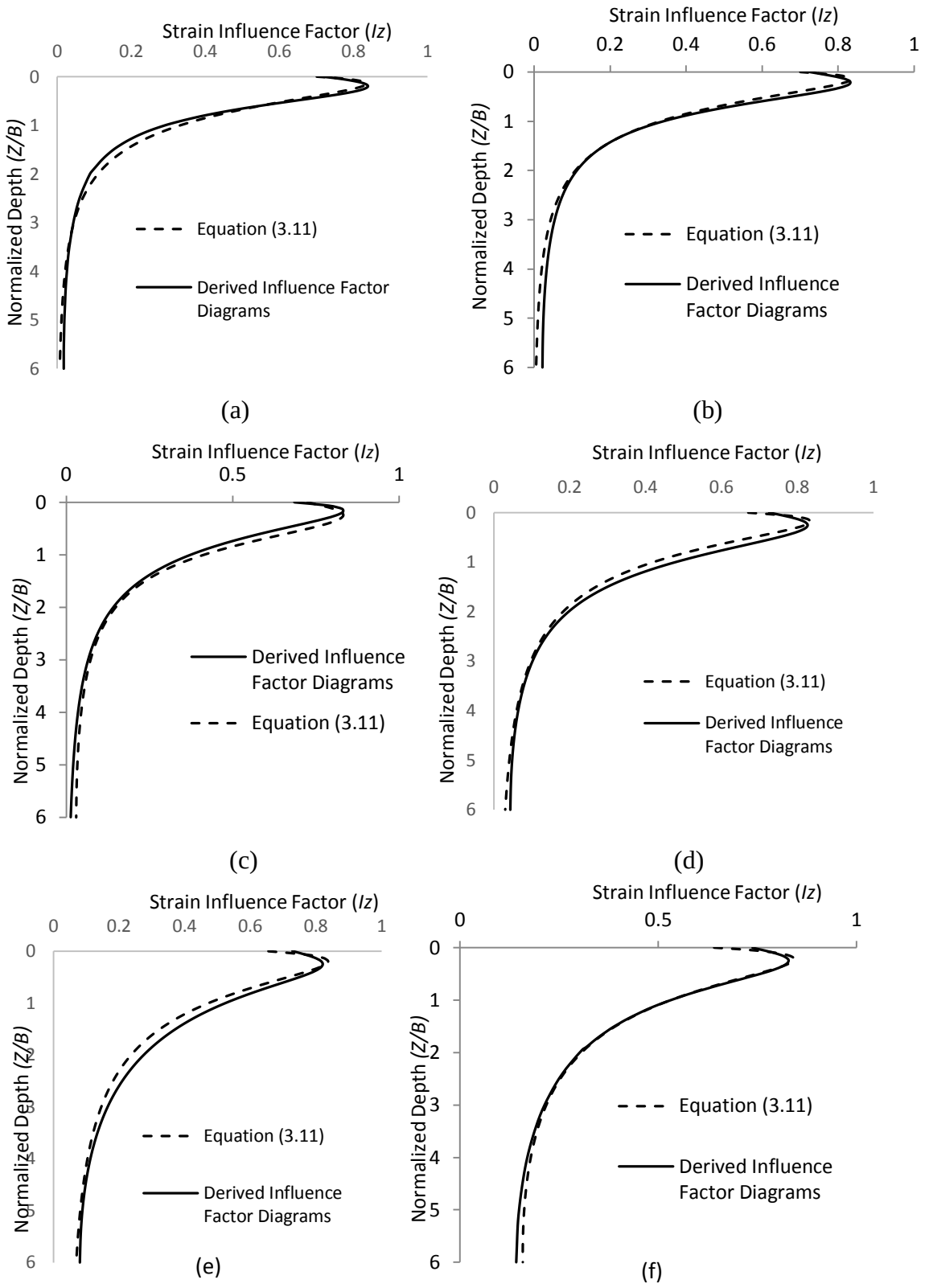


**Figure 3. 5 : Comparison of derived influence factor diagrams and diagrams based on Eq. 3.11 for, a) circular footing, b) square footing (B/L = 1.0), c) Rectangular Footing (B/L = 0.75), d) Rectangular Footing (B/L = 0.50), e) Rectangular Footing (B/L = 0.25), f) strip footing**

Table 3.1: Values of strain influence factors at various depths for different footing shapes

| Normalized Depth ($z/B$) | Strain Influence Factor ($I_z$) | | | | | |
|---|---|---|---|---|---|---|
| | Circular Footing | Square Footing | Rectangular Footing ($B/L$=0.75) | Rectangular Footing ($B/L$=0.50) | Rectangular Footing ($B/L$=0.25) | Strip Footing |
| 0.00 | 0.717 | 0.725 | 0.725 | 0.725 | 0.728 | 0.739 |
| 0.20 | 0.841 | 0.83 | 0.827 | 0.821 | 0.815 | 0.825 |
| 0.30 | 0.804 | 0.812 | 0.822 | 0.821 | 0.815 | 0.823 |
| 0.50 | 0.633 | 0.677 | 0.727 | 0.749 | 0.751 | 0.754 |
| 0.75 | 0.427 | 0.483 | 0.556 | 0.608 | 0.631 | 0.635 |
| 1.00 | 0.289 | 0.341 | 0.413 | 0.479 | 0.525 | 0.530 |
| 1.50 | 0.151 | 0.185 | 0.237 | 0.299 | 0.373 | 0.389 |
| 2.00 | 0.090 | 0.113 | 0.149 | 0.197 | 0.275 | 0.304 |
| 2.50 | 0.061 | 0.076 | 0.101 | 0.138 | 0.21 | 0.251 |
| 3.00 | 0.043 | 0.055 | 0.068 | 0.095 | 0.156 | 0.213 |
| 3.50 | 0.033 | 0.041 | 0.056 | 0.079 | 0.134 | 0.188 |
| 4.00 | 0.027 | 0.034 | 0.043 | 0.061 | 0.108 | 0.169 |
| 4.50 | 0.022 | 0.028 | 0.038 | 0.054 | 0.097 | 0.155 |
| 5.00 | 0.018 | 0.024 | 0.033 | 0.047 | 0.085 | 0.142 |

## 3.7 Conclusion

Strain influence factor diagrams for footings of various shapes (strip, circular, square, rectangular) were developed using linear elastic models in FLAC and FLAC$^{3D}$. The diagrams were then compared with Schmertmann's (1970) simple triangular approximation. Unlike the original strain influence diagram, the proposed diagrams start at 0.72-0.74 at footing level,

rises up to 0.83 at 0.2*B*-0.25*B* depth and extend to a greater depth. Effect of Poisson's ratio on the diagrams was discussed and presented graphically for circular and strip footings. It was observed that the variation of Poisson's ratio affects the influence factor diagram up to a depth of 0.5 *B* in circular footing, and up to 1.0 *B* for strip footing. Also a simple hyperbolic nonlinear model was used to investigate the depth at which maximum vertical strain occurs. The result shows that the peak occurs at 0.3*B* (whereas $I_{z,peak}$ occurs at 0.2*B* in linear elastic modelling) for axi-symmetric loading at any stress level. At the end, an equation is proposed that can be used to obtain strain influence factor at any depth for different footing types. Also, influence factors at various depths are given for different footing shapes in tabular form.

# Chapter 4 Laboratory Modelling of Shallow Footings and the Effects of Water Level Rise on Granular Soils on Settlements

## 4.1 General

Various researchers used different techniques, namely analytical, field tests and laboratory model studies to investigate the effect of water table rise on shallow foundation settlement resting on granular soils (Bazaraa, 1967; Vargas 1961; Brinch Hansen 1966a; Khanna et al. 1953; Ferreira and Da Silva 1961; Agarwal and Rana 1987; Murtaza et al. 1995; Morgan et al. 2001). Very little laboratory studies have been conducted so far and contradictory results have been found. Agarwal and Rana (1987) conducted tests on square footings of three different sizes (20 cm x 20 cm, 15 cm x 15 cm and 10 cm x 10 cm). Their results support Terzaghi's proposition that the settlement gets doubled when the sand gets submerged. Murtaza et al. (1995) also used three different sized square footings (6 cm x 6 cm, 8 cm x 8 cm and 10 cm x 10 cm) and conducted the tests with loose, medium dense and dense sands. The results showed 8 to 12 times more settlement in submerged condition. Morgan et al. (2010) carried out settlement tests with a square footing in two different types of soils and found that the increase in settlement in submerged sand can be 5.3 times the dry sand. However, these experimental programs were small in scale and none of these considered the effect of varying footing shapes and soil grain size distribution. An important objective of this study is to conduct comprehensive laboratory model testing and develop a rational method for predicting additional footing settlement due to water table rise based on the experimental results.

This Chapter describes the experimental program that was designed to include the effect of footing shape, soil gradation and varying water table depth on settlement increment of shallow footings subjected to water level rise. For successful modelling of shallow footings, scale effect and effect of capillary rise on the test results were considered, and the experimental program was developed in such a way that their effects can be avoided.

## 4.2 Properties of granular soils used in the test

The experimental program was divided into two parts. Firstly, model tests were performed in a rectangular tank 600 mm high and 800 mm x 800 mm plan dimensions. Model footings of different shapes were used to rest on a uniformly graded granular soil and settlements were measured in dry and submerged condition. The objective of the test was to propose a rational

method to predict water table correction factor based on the test results that can incorporate the effect of footing shape. Also the variation of water table correction factor with depth of water table below the footing level was investigated in this test. Once a rational method to predict water table correction factor is proposed and the variation of correction factor with water table depth is established, the next aim was to investigate how the water table correction factor varies for different soils, when the water table is at the footing level. This was investigated in the second part of the laboratory test program, where a small cylindrical mould was used to carry out model tests on nine different cohesionless soils. The soils were chosen so that there is wide variety of grain size distributions, void ratio ranges and percentages of fine content. Since only the additional settlement due to water table rise up to the footing level was investigated in this test, it was not required to record settlements at different water table depths. This also allows using a small cylindrical mould, and the effort required to fill the mould was small in this test. A series of laboratory tests were conducted to obtain the properties of the test sand. The tests were carried out following the relevant Australian standards listed in Table 4.1.

Table 4.1: Laboratory test program for granular soils used in the tests

| Properties | Australian Standard used |
|---|---|
| Grain size distribution | AS1289.3.6.1-2009(Standard method of analysis by sieving) (Standards Australia 2009)<br><br>AS1289.3.6.3-2003(Standard method of fine analysis by using a hydrometer) (Standards Australia 2009) |
| Maximum and minimum dry density | AS1289.5.5.1-1998 (Standards Australia 1998a) |
| Specific gravity | AS1289.3.5.1-2006 (Standards Australia 2006) |
| Friction angle of sand | AS1289.6.2.1-2001(R2013) (Standards Australia 2013) |

### 4.2.1 Properties of soil used in settlement tank test

A locally available granular soil was used in the settlement tank test. In a model footing having smaller dimensions, the settlement might get affected by change in soil stiffness in a partially saturated area. From laboratory testing, it was observed that the capillary rise is higher in well graded soil. Hence, it is important to use a uniformly graded soil with soil grains large enough to significantly reduce the capillary height. Capillary effects were minimised by screening out the fines and very fine sands, using a 0.6 mm sieve, and removing any grains larger than 4.75 mm.

The soil properties of sieved out sand are summarised in Table 4.2. Two different relative densities (38% and 77%) of the sand were used. Since the model tests represent the larger footings with higher densities in the field, maximum relative density was limited to 77%.

### 4.2.1 Properties of soil used in small mould test

A total of nine soils were used in the small mould test, including the sand used in settlement tank test. The sands were chosen so that they represent wide range of variety in void ratio, uniformity, gradation and percentage of fine contents. Initially, tests were carried out on six soils which were termed as soil 1 to 6. Among them, soil 1 was the same soil used in the settlement tank test. Later on, silty fine grains (finer than 75 µm) were added with soil 5 in different quantities to make sands containing 10%, 15% and 20% fines and were termed as soil 5a, 5b and 5c respectively. Fig. 4.1 shows the photographs of the soils tested with millimetre scale. Fig. 4.2 shows the grain size distribution curves for all the soils. The basic soil properties of the sands are listed in Table 4.3.The soil property tests were carried out following Australian standards as in Table 4.1. Soils 1, 2 and 3 were basically uniformly graded soils having no fine contents. The other soils contained fine grains at different percentages to facilitate the study on effect of fines content on additional settlement due to submergence.

Table 4.2: Properties of sand used in settlement tank test

| Parameter | Value |
|---|---|
| Effective grain size $D_{10}$ (mm) | 0.67 |
| Coefficient of uniformity $C_u$ | 1.64 |
| Coefficient of curvature $C_c$ | 0.89 |
| Specific gravity of the grains | 2.61 |
| Maximum dry density (t/m$^3$) | 1.53 |
| Minimum void ratio | 0.706 |
| Minimum dry density (t/m$^3$) | 1.38 |
| Maximum void ratio | 0.891 |
| Relative densities ($D_r$) of the sands tested | 38% and 77% |
| USCS symbol | SP |

Table 4.3: Basic Soil Properties of the nine soils used in the model tests.

| Parameter | Soil 1 | Soil 2 | Soil 3 | Soil 4 | Soil 5 | Soil 6 | Soil 5a | Soil 5b | Soil 5c |
|---|---|---|---|---|---|---|---|---|---|
| Effective grain size $D_{10}$ (mm) | 0.67 | 0.70 | 2.37 | 0.036 | 0.13 | 0.03 | 0.075 | 0.032 | 0.013 |
| Coefficient of uniformity $C_u$ | 1.64 | 1.89 | 1.45 | 24.17 | 3.08 | 12.00 | 4.87 | 10.94 | 25.00 |
| Coefficient of curvature $C_c$ | 0.89 | 0.86 | 0.99 | 2.36 | 0.94 | 1.49 | 1.40 | 2.77 | 5.69 |
| Specific gravity of the grains | 2.61 | 2.65 | 2.68 | 2.66 | 2.64 | 2.66 | 2.67 | 2.67 | 2.67 |
| Maximum dry density ($t/m^3$) | 1.53 | 1.47 | 1.61 | 1.80 | 1.66 | 2.05 | 1.77 | 1.82 | 1.88 |
| Minimum void ratio, $e_{min}$ | 0.706 | 0.805 | 0.663 | 0.474 | 0.587 | 0.299 | 0.513 | 0.465 | 0.417 |
| Minimum dry density ($t/m^3$) | 1.38 | 1.44 | 1.53 | 1.37 | 1.44 | 1.42 | 1.46 | 1.46 | 1.45 |
| Maximum void ratio, $e_{max}$ | 0.889 | 0.838 | 0.749 | 0.949 | 0.835 | 0.875 | 0.828 | 0.831 | 0.840 |
| Void ratio range, $e_{max}$-$e_{min}$ | 0.183 | 0.033 | 0.086 | 0.475 | 0.248 | 0.576 | 0.315 | 0.366 | 0.423 |
| Fines Content (%) | 0 | 0 | 0 | 15.40 | 2.43 | 18.36 | 10.06 | 15.05 | 20.05 |
| USCS symbol | SP | SP | SP | SM | SP | SM | SP-SM | SM | SM |

(a)

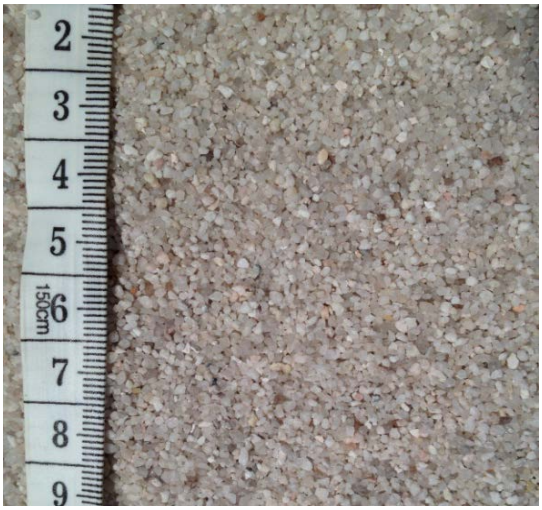

(b)

(c)

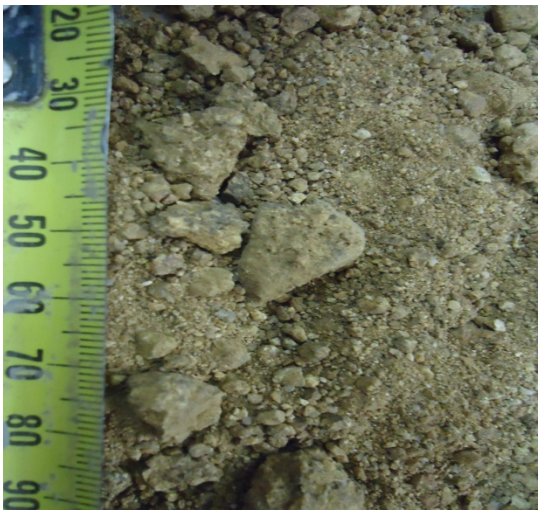

(d)

(e)

(f)

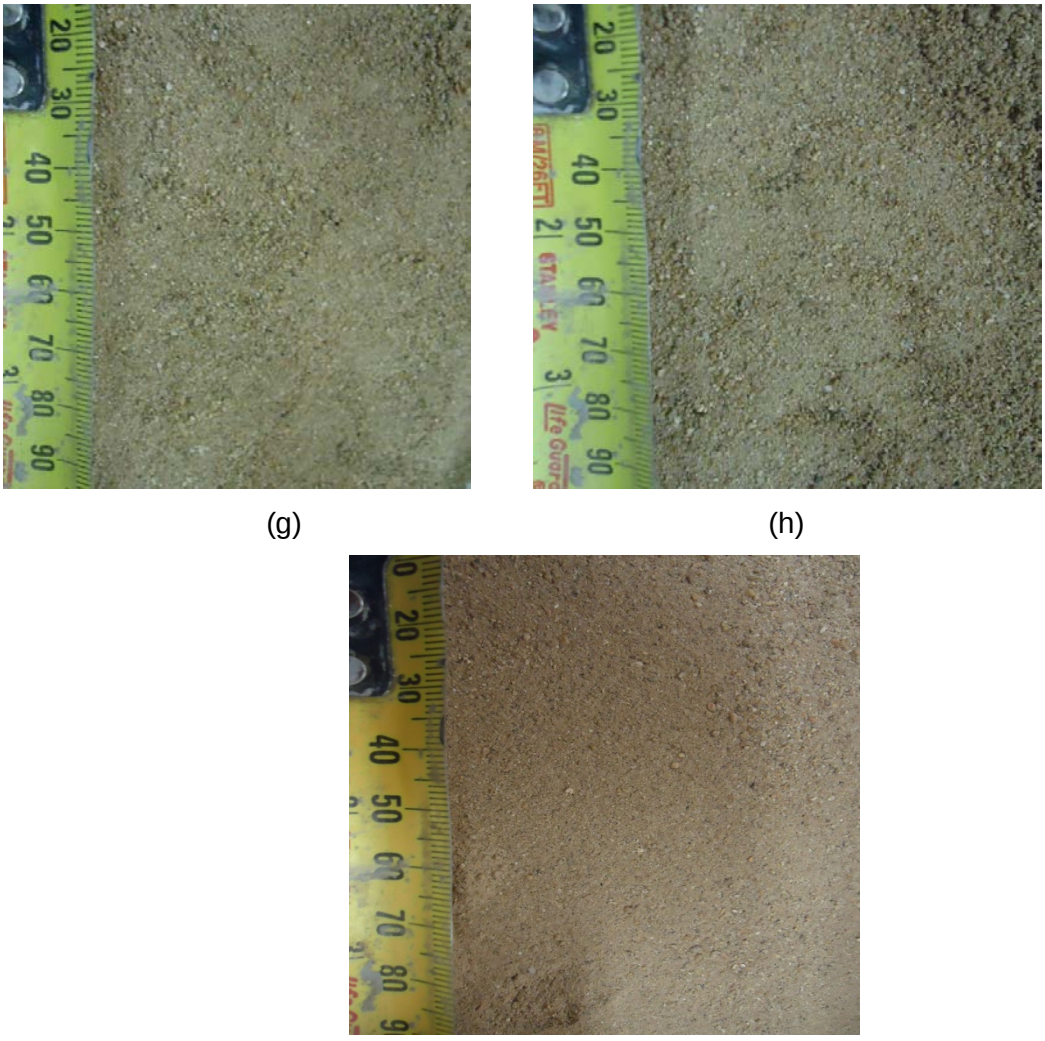

(g) (h)

(i)

**Figure 4. 1 : Photographs of the granular soils used in the test with mm scale, (a)soil 1,(b)soil 2,(c) soil 3, (d) soil 4,(e) soil 5,(f) soil 6,(g) soil 5a,(h) soil 5b, (i) soil 5c**

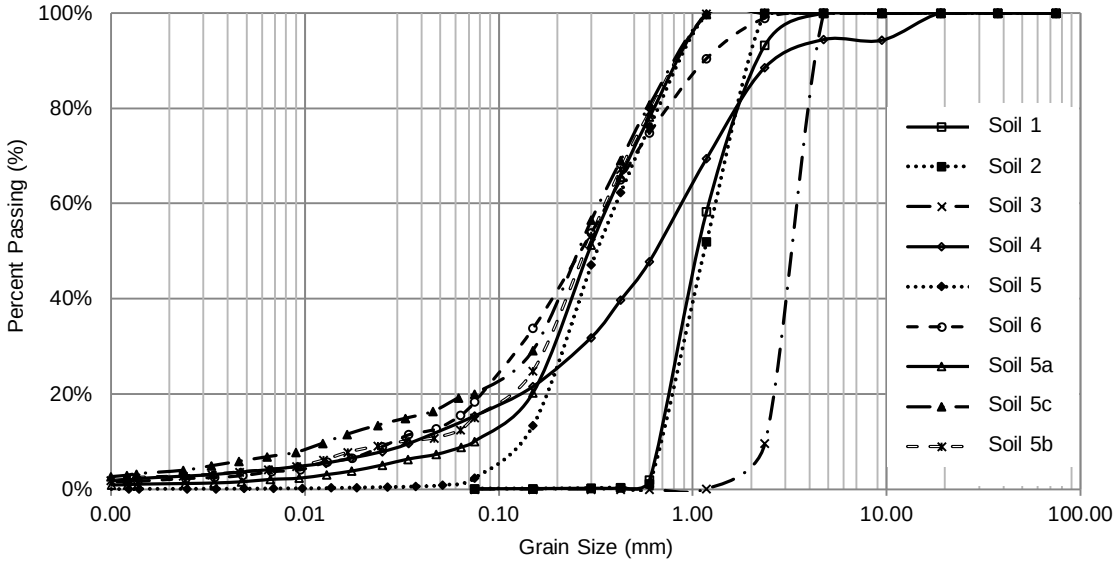


**Figure 4. 2 : Grain size distribution curves for the nine soils used in the model tests**

## 4.3 Settlement tank test

### 4.3.1 Experimental Program

The objective of the settlement tank test was to investigate the effect of footing shape and varying water table depth on additional settlement due to submergence, and propose a rational method for predicting water table correction factor. A series of laboratory model tests were carried out on rectangular tank (800 mm x 800 mm in plan and 600 mm high) containing same sand placed at constant relative densities throughout. Six footings of different shapes, including square, circle and rectangles ($B/L$ = 0.25, 0.50 and 0.75 where $B$ and $L$ are the width and length, respectively.), were used in the study. The tests were carried out on sand placed in loose ($D_r$ = 38%) and dense ($D_r$ = 77%) states. The water table was raised from bottom of the tank in increment, and additional settlement was measured with water at different depths below the footing, varying from 6$B$ to 0$B$.

### 4.3.2 Apparatus

#### *Rectangular Tank*

The settlement tank was made of Perspex with plan dimensions of 800 mm x 800 mm and height of 600 mm. All model footings had width of 100 mm, and placing them on the centre of the soil filled tank makes the horizontal and vertical boundaries 6.0 $B$ and 4.0 $B$ away from the footing centre. This was sufficient to eliminate the influence of the boundary distance on the test results. Water was allowed to enter the tank through the bottom. A vertical glass tube was attached to the tank wall to monitor the water level within the tank, which can also be seen through the Perspex wall. A ruler was fixed near the glass tube, to facilitate measurement of water table height throughout the test. Fig. 4.3 shows the rectangular tank used in the model tests.

**Figure 4. 3 : The Perspex tank used in the settlement tank test**

### *Model Footings*

A circular footing of 100 mm diameter and square and rectangular footings with width *B* =100 mm and width to length ratio = 1.0, 0.75, 0.50, 0.25 were used in the model tests. The footings were made of steel and were roughened at the bottom to simulate rough footings used in the field (as shown in Fig. 4.4). The width of 100 mm was taken so that the influence zone is well contained in the settlement tank. The strain influenced factor diagrams proposed in Chapter 3 extends to a greater depth than it was originally suggested by Schmertmann (1970). This indicates that water table rise can affect the settlement at greater depths. Testing with 100 mm wide model footings allows us to observe the effect of rising water level from a depth of 6.0 *B*.

### *Loading and Measurement Apparatus*

A hydraulic jack was used to apply the loading on the model footings. It was suspended from a frame that was fixed at the floor. A load cell was used to measure the applied load. The load cell was placed in between the hydraulic jack and the model footing and was equipped with a strain gauge that gives reading through a voltmeter when a load is applied. It was calibrated to determine the load in kilograms. Footing settlement was measured by two dial gauges accurate to 0.001 mm.

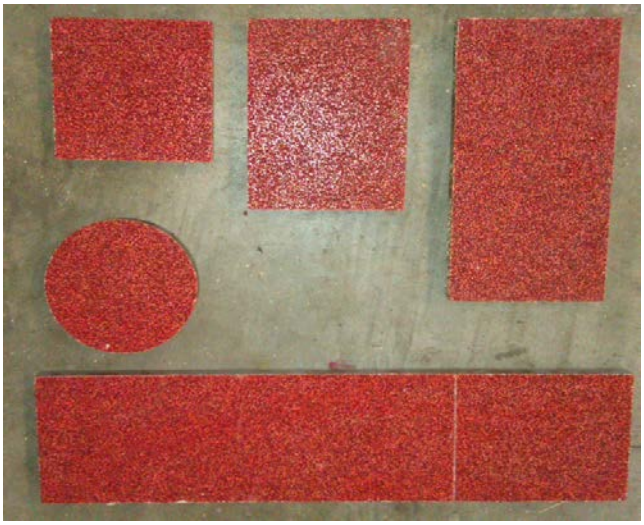

**Figure 4. 4 : Model footings used in the settlement tank test**

### 4.3.2 Testing Procedure

#### *Filling the tank*

The tank was filled with soil in six layers (100 mm each), maintaining the lift height equal to the footing width, *B*. The soil mass for each layer was calculated from the required relative density. To achieve uniform density in every layer, the soil was poured through a funnel held vertically and moved around the tank maintaining a specific height of fall. Each layer was compacted and levelled with a wooden float with same compacting effort. The tank was marked outside in every 100 mm to facilitate the sand placing in required density. Small square cans were placed at various levels to check the achieved density. The results showed that the achieved density was close to the expected density in all cases.

#### *Test Setup*

Once the tank is filled with sand, the surface was levelled carefully using spirit levels. The model footings were placed at the centre of the tank. These were then checked to ensure they were horizontal. A load cell was placed on top of the model footing to measure the load applied by the hydraulic jack. Two dial gauges were attached to the loading frame with the help of magnetic bases. A thin steel plate was placed in between the load cell and the hydraulic jack to hold the dial gauge pins. The experimental setup is shown in Fig. 4.5 along with the schematic diagram.

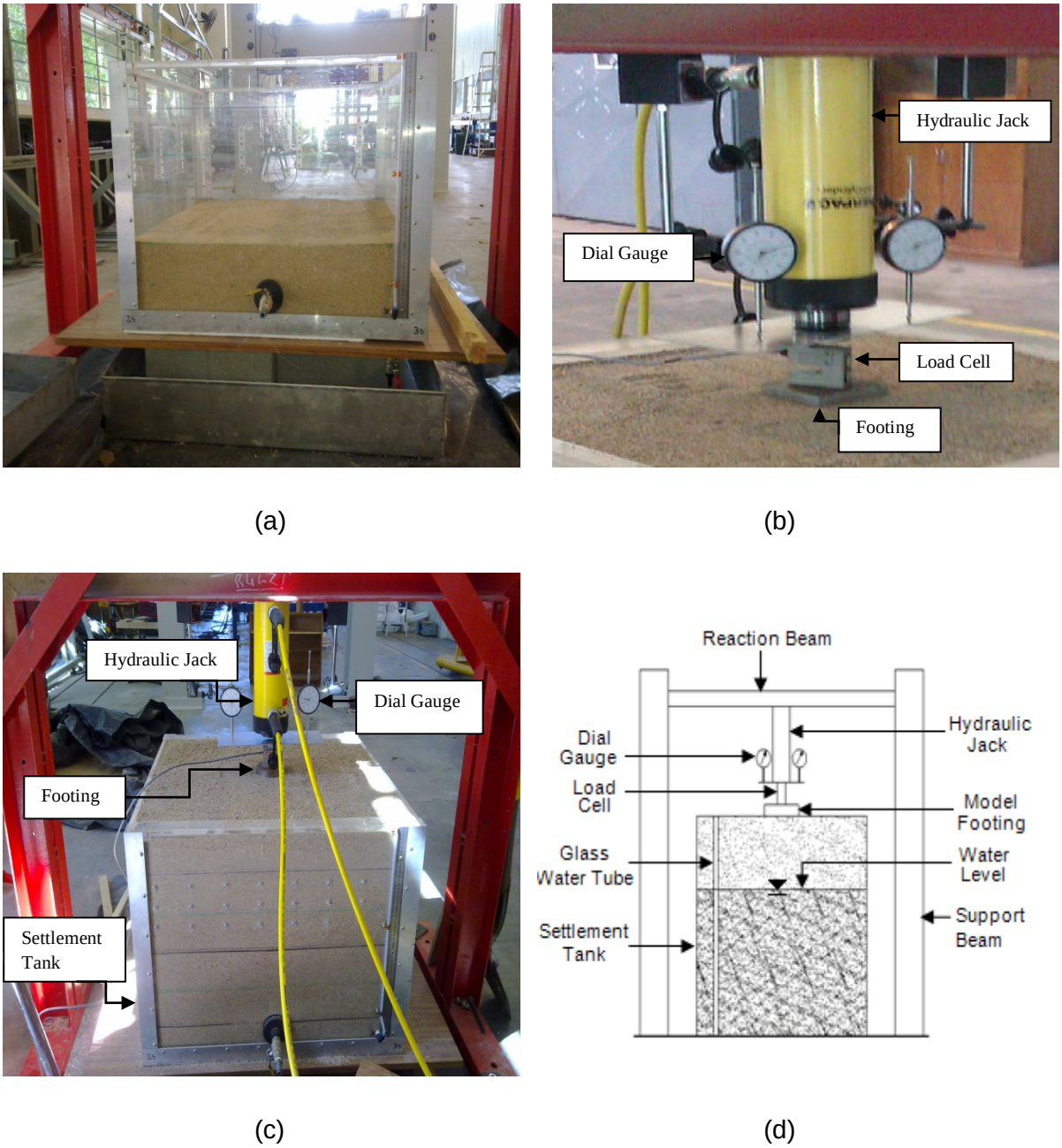


**Figure 4. 5 : Experimental setup for for settlement test in the laboratory: (a) filling the settlement tank in layers, (b) details of load and settlement measurement system, (c) experimental setup, (d) schematic diagram of the test setup.**

### *Determination of working load of model footings in dry state*

The objective of the test was to determine additional settlements of shallow footings due to water table rise and while they are subjected to working load. To determine the working load of footings in dry condition, tests were carried out on dry soils. Once the footings are placed on the sand bed and the test setup is ready, load was applied through the hydraulic jack in increments. After each loading, the voltmeter was allowed some time to stabilize and

settlement corresponding to the load was recorded. The average value of settlement reading of the two dial gauges was used in the study. Initially, an applied pressure-settlement curve was obtained by applying vertical pressure in increments and recording corresponding settlements of the footings placed on oven-dried sand. From the load-settlement plot, ultimate bearing capacity of the footings on loose sands were obtained by using double tangent method i.e. drawing tangents from two linear segments of the pressure-settlement curves and taking their intercept as the ultimate bearing capacity. The pressure-settlement curves of footings on dense sands clearly indicated the failure load and use of double tangent method was not required for these footings. The working loads of the footings were obtained by dividing the ultimate bearing capacity values by three, maintaining a safety factor of 3.

#### *Simulation of water table rise*

Once the working load of the model footings at a particular relative density is obtained, the next step is to subject the model footing to working load, raising the water level and recording additional settlement during the water table rise. The water table was raised from the bottom of the tank at 100 mm lifts (equal to footing width, $B$) until it reached up to 100 mm below the footing level. From there, a lift height of 20 mm (=$B$/5) was maintained until the water level reaches the base of the footing, and the additional settlements were recorded. The load on the footing was constantly adjusted to maintain the working load throughout the test. The duration between two successive increments of water level was generally about five minutes, where the capillary rise was about 50 mm. Fig. 4.6 shows the rise in water level during the test. The water table correction factor diagrams for all footings were then obtained by comparing the measured additional settlements under water table rise with the initial settlement under working load in dry condition.

## 4.4 Small Mould Test

### 4.4.1 Experimental Program

In the settlement tank test, effect of varying footing shapes and water table depths on additional settlement of footings due to submergence were investigated. Based on the test results, a rational method to predict water table correction factor due to water table rise was proposed which is discussed in the next Chapter. Also, the variation of water table correction factor with water table depth was established in the settlement tank test. In the small mould tests, a further attempt is made to understand the effect of difference in soil types on correction factor when the water table rises up to the footing level. Unlike the settlement tank test, it was not required to measure additional settlement at different water table depths. A

cylindrical mould was used instead of the settlement tank and laboratory model tests were carried out on nine different sands. Using a small cylindrical mould instead of large settlement tank reduced the effort required to run the tests, which allowed using more sands for the tests. Sands were placed in dense and loose states and a circular model footing was placed on top the sands. The footing was subjected to working load and was tested under dry and submerged conditions to get the water table correction factors.

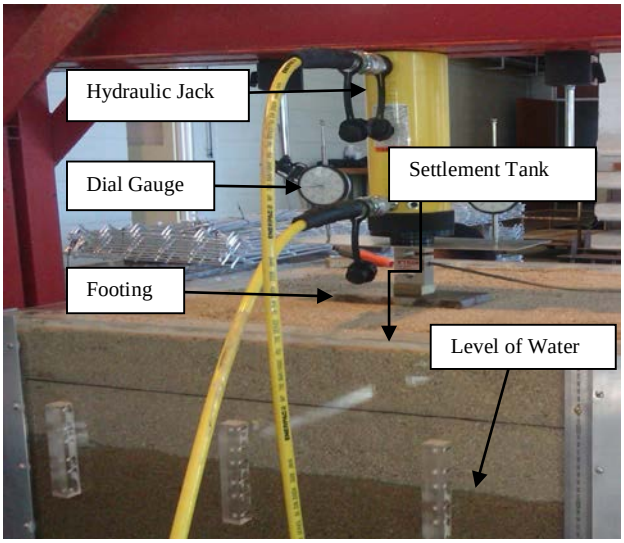


**Figure 4. 6 : Simulation of water level rise during the settlement tank test**

### 4.4.2 Apparatus

#### *Cylindrical Mould*

The metal mould used in the settlement test was cylindrical in shape having 152 mm diameter, 178.5 mm height and wall thickness of 5 mm. Considering the significant effort required in carrying out the model tests on nine sands, placed at two different densities, in dry and saturated conditions, the mould size for this set of tests was limited to the above values. The mould had a metal extension collar and a perforated metal extension base plate. It was identical to the moulds used in California Bearing Ratio Tests that follows Australian Standard 1289.6.1.1-1998. The perforated base plate allowed the water to get into the mould and wetting the soil in submerged tests.

#### *Model Footings*

Circular model footings were used and the footing width was carefully chosen with two main considerations- to minimize the particle size effect and to contain most of the stress bulb within the mould. Kusakabe (1995) recommended that footing width ($B$) to median grain size ($d_{50}$) ratio in model tests should be greater than 50-100 in order to avoid scale effect. Soil 1,2 and 3 have greater median grain size and footing diameter on these soils were selected to be

76 mm, other soils had considerably smaller $d_{50}$ value, and 53.2mm diameter footings were used on these soils. This makes the vertical and horizontal boundaries 1*B* and 2.35*B* away from the centre of 76 mm footing, and 1.43*B* and 3.35*B* away from 53.2 mm footing centre. Numerical modelling in FLAC (Itasca, 2008) shows that 92.5% and 93.4% of the stress bulb below the footing were contained within this zone for 76 mm and 53.2 mm diameter footing, respectively. The footings were made of steel and were roughened at the bottom to simulate rough footings used in the field.

#### *Loading Frame, Loading and Measurement Apparatus*

The cylindrical mould was placed on a loading frame and a hanger assembly was used for applying the load. The hanger was loaded directly by dead weights and if needed, it was loaded through a lever system. The hanger applied the normal load centrally on the model footing through a ball bearing in a spherical seating. Settlement was measured by a dial gauge placed on top of the footing.

### 4.4.3 Testing Procedure

#### *Filling the mould*

The mould was placed on the loading frame and a filter paper was put on top of the perforated base plate so that sand grains don't clog the pores. Each of the nine soils was tested at two different relative densities. For the uniformly graded soils (1, 2, 3 and 5), the relative densities used were 10% and 90%. For other soils $D_r$=38% and 77% were used. The mould was filled with soil in three layers (59.5 mm each). The soil mass for each layer was calculated from the required relative density. To achieve uniform density in every layer, the soil was poured through a funnel held vertically and moved around the mould maintaining a specific height of fall. Each layer was compacted and levelled with a wooden float with same compacting effort. The cylindrical mould was marked inside in three layers as guidance for placing the sand in required density.

#### *Test Setup*

After filling the mould in three layers, the sand surface was levelled carefully with spirit levels. Then the circular footing was placed concentrically with the centre of the mould and was checked for even level. A dial gauge was attached to the loading frame with the help of magnetic base and its pin was placed on top of the model footing. The hanger assembly was placed on top of the footing so that the load can be transferred through a ball bearing. The schematic diagram of the experimental setup and a photograph of the setup are shown in Fig. 4.7.

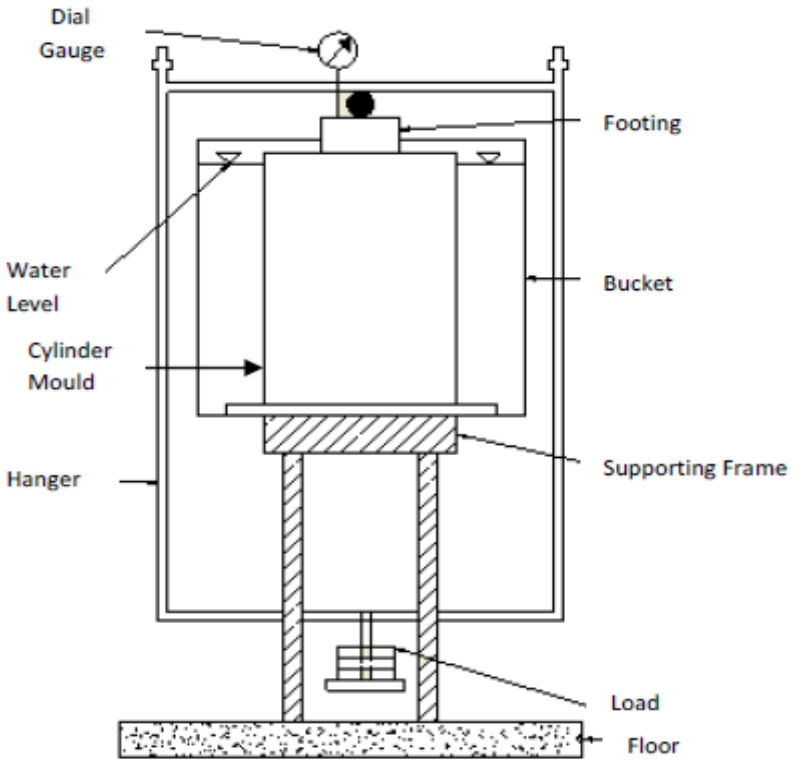


(a)

(b)

**Figure 4. 7 : Experimental setup for settlement test in the laboratory, (a) schematic diagram, (b) photograph.**

### *Determination of working load of model footings in dry state*

Initially, an applied pressure versus settlement curve was obtained by applying vertical pressure in increments and recording corresponding settlements of the footings placed on oven-dried sand. From the load-settlement plot, ultimate bearing capacity of the footings on loose sands was obtained by using double tangent method. This method involves drawing tangents from two linear segments of the pressure-settlement curves and taking their intercept as the ultimate bearing capacity. The working loads of the footings were obtained by dividing the ultimate bearing capacity values by three, maintaining a safety factor of three.

### *Settlement test on saturated soil*

The main objective of this test was to study the additional settlement when ground water table rises up to the footing level. This requires saturating the soil below the footing and measure additional settlement due to saturation. Similar setup was used for the wet test, but this time the mould was placed on a bucket. The footing was then subjected to a constant pressure representing the working load, and the bucket was filled with water up to the footing level. The additional settlements due to rise in the water table was then recorded. The correction factor for the water table at the footing level was then obtained by dividing settlement at submerged sand by settlement on dry sand. Fig. 4.8 shows the test setup for soil tested in dry and submerged condition. The same procedure was applied for all the nine soils at two different densities.

## 4.5 Scale effect

Fine grained soils (silts and clays) have very small particle size and are little affected by the foundation size. For the same footing size, there might be thousands of grains beneath the small model footing for a clayey soil, whereas there could be a few hundreds of sand grains under the model footing. This indicates that scale dependence of granular soils is much larger than that of cohesive soils. This is why it is important to account for the scale effect before using the small scale model footing test results for prototype footings.

Various researchers have addressed the scale effect phenomenon. Berry (1935) first presented results which indicated that the bearing capacity factor, $N_\gamma$ decreases with increasing footing size. This observation was termed as “scale effect” by De Beer (1963); Tatsuoka et al. (1991, 1994) suggested that two factors contribute to the footing size effect, namely, stress level dependency of mechanical properties of granular soils and the variation of footing width to

(a)

(b)

**Figure 4. 8 : Experimental setup for soil in (a) dry condition, (b) wet condition**

mean grain size ($B/d_{50}$) ratio. The second factor is also termed as "particle size effect". Based on modelling experiments, various researchers (Ovesen 1975; Yamaguchi et al. 1977; Bolton and Lau 1989) reported that there is a threshold value of $B/d_{50}$ ratio for small model tests above which the particle size effect is negligible. Kusakabe (1995) recommended that $B/d_{50}$ ratio should be greater than 50-100 in order to avoid scale effect.

The scale effect seen in model footings is partly dependent on the mean stress felt underneath the footing (Cerato and Lutenegger 2007). Larger footing causes higher mean stress and lower friction angle. From the curvature of Mohr-Coulomb failure envelope theory, it can be said that the friction angle decreases with increase in mean stress. Therefore, the decrease in $N_\gamma$ can be directly related to footing size- larger the footing, higher the mean stress, lower the friction angle and lower the bearing capacity factor.

The critical state concept can be used for explaining the scale effect observed in model footings. The critical state line is a unique line on a void ratio versus mean stress graph and it defines the state at which no volume change occurs. Fellenius and Altaee (1994) used Fuji river sand for footing tests and developed three different relationships with critical state line (shown in Fig. 4.9). The first study was conducted on three different sized footings resting on sand of same voids ratio i.e. same density (represented in line 1 of Fig. 4.9). The larger footing had higher mean stress and was closer to the critical state line. It behaved as if it was in a looser soil. The smaller footing was farthest from the critical state line and acted like resting on denser soil. Each footing size was tested at three different embedment depth- $D_f$= 0.0 $B$, 1.0 $B$ and 2.0 $B$ denoted as a, b, c respectively, in Fig. 4.9. The result shows that in spite of resting on the soil of same density, the footings exhibit scale effect due to difference in mean stress.

In the second study, a footing of a particular size and hence contact pressure was tested on soils of different densities (represented in line 2). The footing on densest soil was farthest from the critical state line and it showed the highest stress-settlement value. In the third study, different sized footings were used at void ratios parallel to the steady state line (represented in line 3) and the stress- settlement behaviour for these footings was found similar. This indicates that the foundations of different sizes will behave similarly if the distance from critical state line ($\Psi$) is same. This is an important finding which can be used for modelling small scale footings. The stress-settlement behaviour of model footings used in the laboratory emulates that behaviour of much larger prototype footings in the field resting

on granular soils having higher relative densities. This is why the settlement investigation using a model footing should be conducted on soils with lower densities (Cerato and Lutenegger 2007).

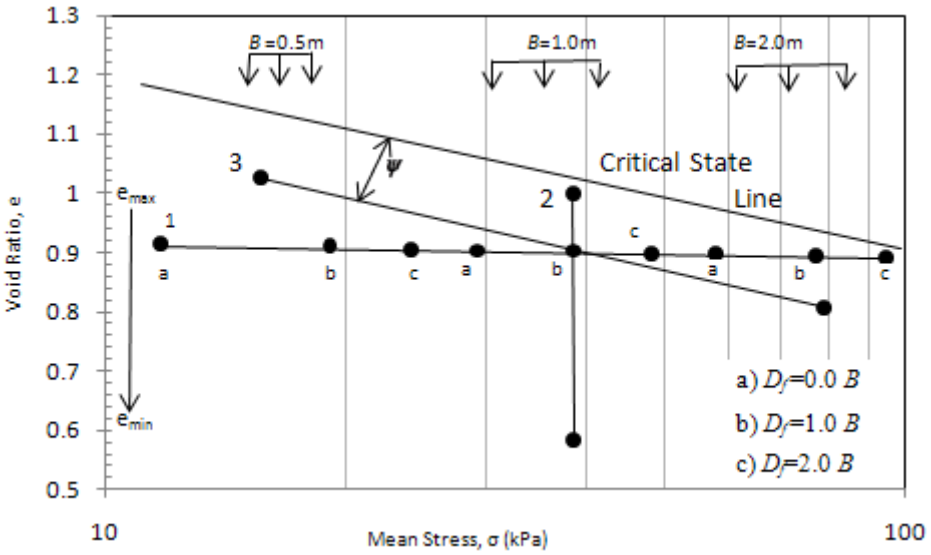


**Figure 4. 9 : Results of footing tests on Fuji river sand relating critical state line (adapted after Fellenius and Altaee(1994)**

In this study, scale effect was considered carefully based on the suggestions in the literature so that the model tests can successfully emulate the stress-settlement relationship of full scale test. To avoid the particle size effect, $B/d_{50}$ ratio should be greater than 50-100 as recommended by Kusakabe (1995). The footing width of settlement tank tests was 100 mm, large enough to eliminate particle size effect. In case of small mould test, soil 1, 2 and 3 have greater median grain size and footing diameter on these soils were selected to be 76 mm. Other soils had considerably smaller $d_{50}$ value, and 53.2mm diameter footings were used on these soils. Since the model tests performed in a smaller footing simulates the stress settlement behaviour of a larger footing resting on denser sand, the tests were conducted at a lower relative density. Maximum relative density used on the laboratory was restricted to 77.4% for the settlement tank test, and 90% for the small mould test.

## 4.6 Capillary Rise

Capillary rise of water through soils is a well known phenomenon. Rise of capillary water can vary from a few millimetres in gravels to several meters in clays. Capillary pressure is similar to suction and it increases effective stress. In case of clays, capillary suction is usually higher and it can significantly increase the effective stress. On the other hand, cohesionless soils have larger voids and capillary rise in this kind of soil is usually low. For prototype footings

on sands, the capillary rise is negligible considering the large footing dimensions. However, in the model tests on 100 mm wide footings, it is important to account for the capillary rise adequately. The soil stiffness varies in a partially saturated capillary zone, which can affect the settlement of a model footing. In the small mould tests, as all the readings were taken with the water table on the footing level, the capillary rise did not come into play in the model tests. However, in case of settlement tank test, settlement readings were taken at varying water table depths and it was important to ensure that capillary rise did not affect the test results.

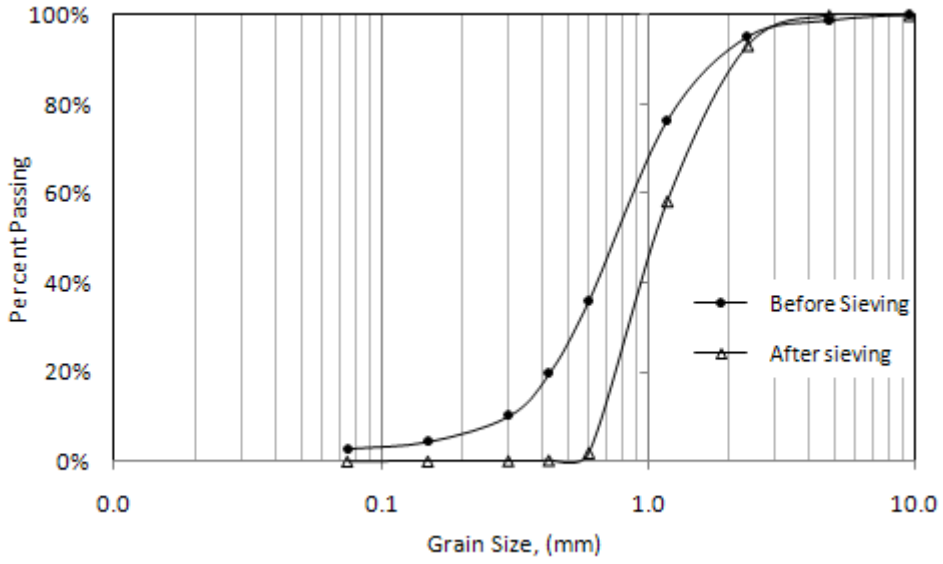


**Figure 4. 10 : Grain size distribution of the soil used in settlement tank before and after sieving**

From capillary tests carried out in soil filled Perspex tubes, using different types of granular soils, it was observed that the capillary height is more in well graded sands than in uniformly graded sands. The capillary height depends on the effective pore size, and the bigger pore size in a uniformly graded soil reduces the capillary rise. For this reason, the finer grains of the granular soil to be used in the settlement tank were sieved out to get a uniformly graded soil having larger pore size, and hence minimise the possible capillary rise. Two sieves, namely, 0.6 mm and 4.75 mm sieves were used to remove the grains smaller than the former sieve size and grains larger than the second sieve. This makes the soil fairly uniform with lower capillary height. Fig. 4.10 shows the soil grain size distribution before and after sieving. The capillary rise of the sieved soil sample was then tested using soil filled Perspex tubes protruding from water (as shown in Fig. 4.11). The height of capillary rise was

measured with time. Fig. 4.12 shows how the capillary height was minimized by increasing soil uniformity, by comparing the capillary rise of the soil before and after sieving both for loose and dense condition. Fig. 4.13 shows the capillary rise of the sieved soil of 10% and 80% relative densities with time. From Fig. 4.13, the capillary height observed at 5 minutes were 40 mm and 53 mm in loose sand and dense sand respectively. During the settlement tests, five minute was the maximum time required to get the settlement reading to stabilise between successive rises in water table. Therefore, the capillary rise is not expected to exceed 50 mm during each load increment applied over duration of five minutes in the settlement tank test.

**Figure 4. 11 : Capillary test of sieved soil using Perspex tubes protruding from water**

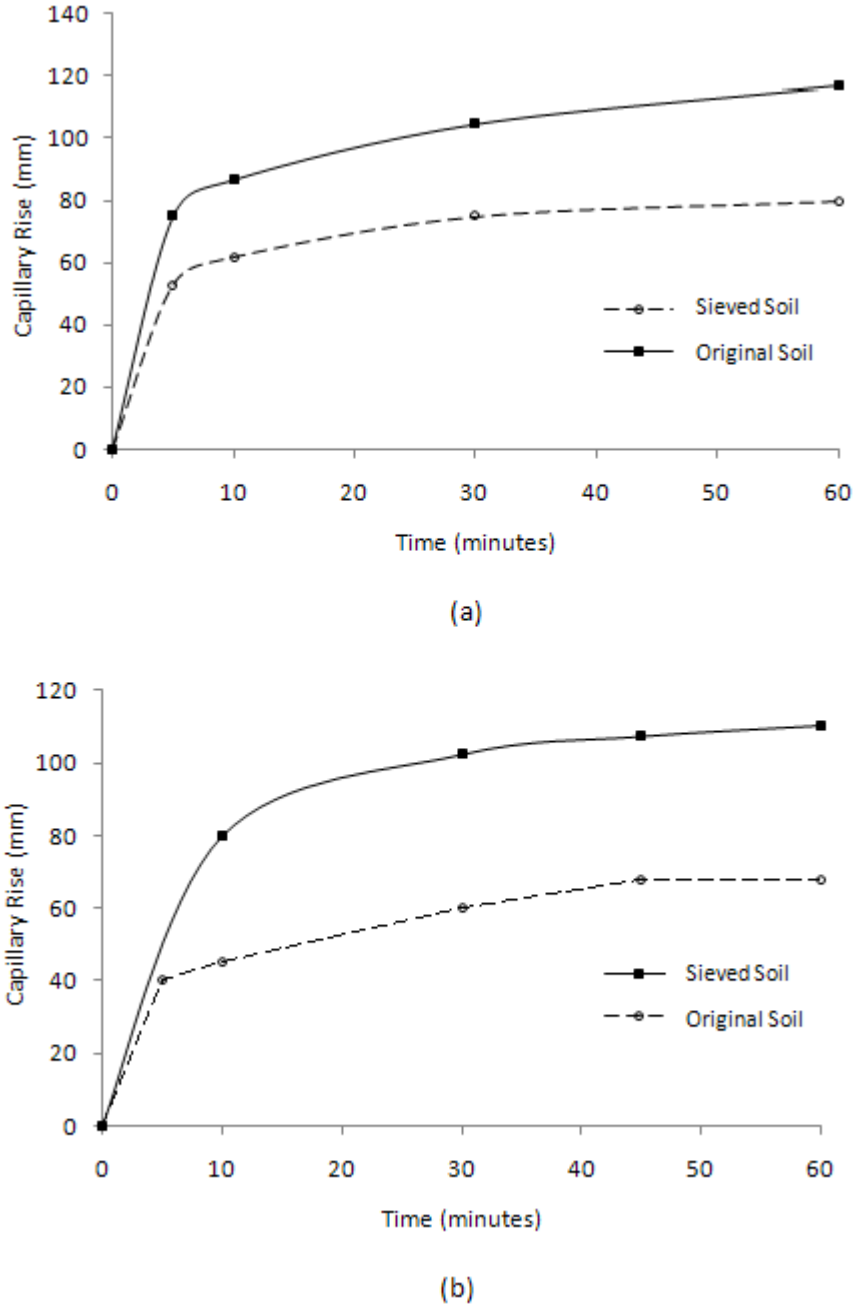


**Figure 4. 12 : Capillary rise comparison of the sieved soil and original soil at a) 10% relative density b) 80% relative density**

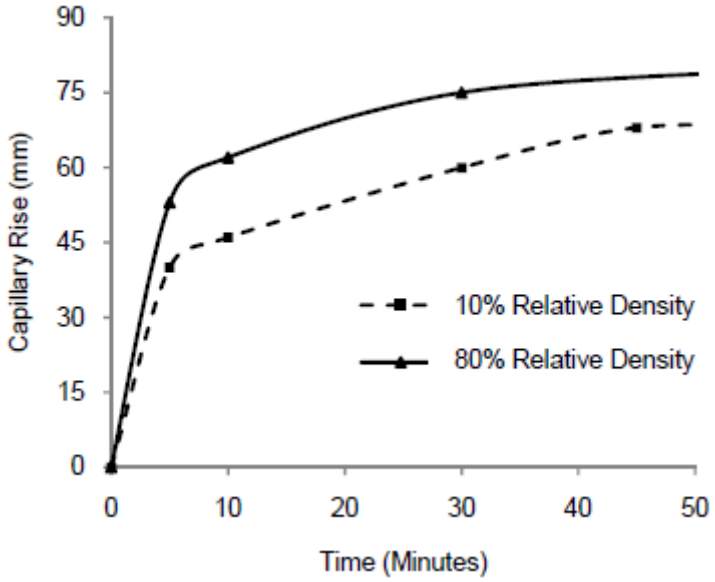


**Figure 4. 13 : Variation of capillary rise of the sieved sand with time**

Vanapalli and Mohamed (2007) showed that the elastic modulus of granular soil, which is a key parameter in shallow foundation settlement, can be significantly influenced by matric suction in unsaturated sand. However, the unsaturated zones of the model tests were kept quite small by limiting the capillary rise and hence the effect of matric suction on foundation settlement was negligible.

In a partially saturated zone, the effective stress increases due to negative pore water pressure, and hence the soil elastic modulus increases. Barnes (2010) proposed the following equation as a reasonable approximation of effective stress in unsaturated zone:

$$\sigma' = \sigma + \gamma_w z_a (S_r / 100) \tag{4.1}$$

where $\sigma'$ = effective stress

$\sigma$ = total stress

$\gamma_w$ = unit weight of water

$z_a$ = elevation above the water table in the unsaturated zone

$S_r$ = degree of saturation (%)

The elevation above water level ( $z_a$ ) was plotted against the degree of saturation ( $S_r$ ) curves for the test sand in loose and dense state after five minutes from capillary rise tests with soil

filled Perspex tubes that was separated into rings, and the increase in effective stresses due to capillary rise was calculated using Eq. 4.1. The result showed that the increase in effective stress is insignificant, which means that the change in soil elastic modulus due to matric suction was negligible. Fig. 4.14 shows the degree of saturation ($S_r$) and additional effective stress in dense sand due to capillary rise with elevation above water table ($z_a$) in unsaturated zone after five minutes. With increasing $z_a$, the degree of saturation decreases rapidly and the additional effective stress due to capillary rise peaks to 0.27 kPa at 36 mm above the water table in dense sand, where the degree of saturation is 77.1%. Compared to the initial overburden stress added to the stress applied through the footing, this increase in insignificant. More importantly, when the sand beneath the footing is fully submerged, with the water level coinciding with the footing level, there is no capillary effect to account for. This was the case with the second set of tests carried out in the small cylindrical mould.

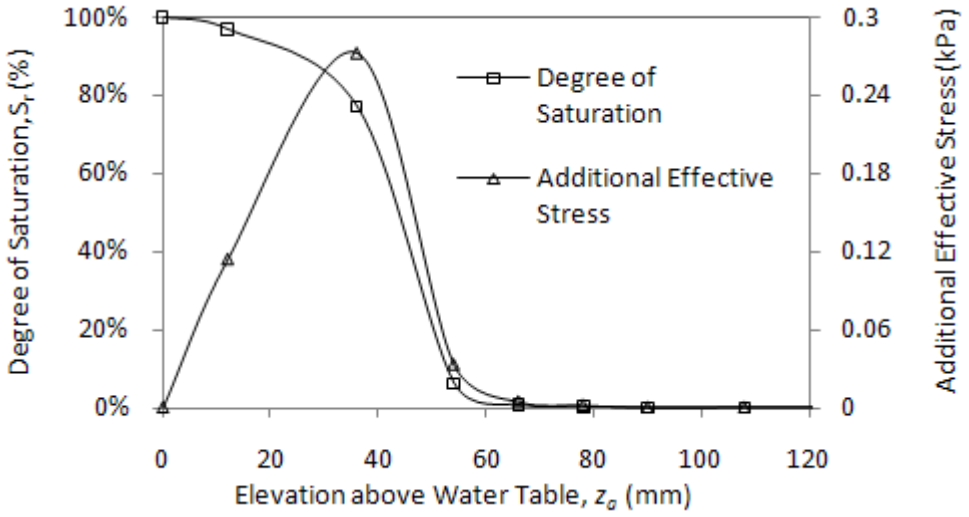


**Figure 4. 14 : Degree of saturation and additional effective stress with elevation above water table in unsaturated zone in dense sand after five minutes**

## 4.7 Conclusion

The details of comprehensive laboratory modelling of shallow footing settlement subjected to water level rise on granular soil is described in this Chapter. The objective of the model tests was to understand the effect of varying footing shape, water table depth, soil gradation, fines content on the additional settlement due to submergence. Properties of the granular soils used in the tests were obtained from basic laboratory tests following Australian Standards. Laboratory modelling was divided in two parts- settlement tank test and the small cylindrical mould tests. The apparatus used in the tests and the procedures adopted were discussed in

details. Effect of capillary rise and scale effect of modelling prototype footings were considered, and the experimental program was carefully designed to avoid these effects on laboratory modelling.

# Chapter 5 Interpretation of Laboratory Test Results

## 5.1 General

Although settlement in granular soil is almost instantaneous, there is a risk of additional settlement in future which may occur due to rise in water level below the footing. Floods, heavy rain falls or any other seasonal changes including high tides may raise the groundwater level, which reduce soil stiffness and cause additional settlement. Substantial additional settlement may occur due to rise in water level, which can threaten the integrity of the structure. Various researchers used the correction factor $C_w$ to account for the effect of rising ground water level on shallow foundation settlement (Terzaghi and Peck 1948; Teng 1962; Alpan 1964; Bazaraa 1967; Peck et al 1974; Bowles 1977; Department of the Navy 1982). Here, $C_w$ is the ratio of the settlement under the water table rise to the settlement in dry sand. It is always larger than one and increases with the water table rise. When water table reaches the ground level, $C_w$ takes the maximum value of $C_{w,max}$.These were reviewed in Chapter 2. According to the previous research, $C_{w,max}$ varies from 1 to 2 and the depth of water table that causes additional settlement varies between 0.4 $B$ and 2.0 $B$. However, laboratory experiments conducted by Murtaza et al. (1995); and Morgan et al. (2010) have suggested significantly higher values for $C_{w,max}$. Morgan et al. (2010) also observed that the depth at which the rise of water table induces additional settlement can be as much as 5$B$.

A comprehensive laboratory experimental program was described in Chapter 4 which was carried out to investigate the additional settlement induced by water table rise with varying footing shape, soil density, soil gradation and water table depth. The experimental program was divided into two parts: (a) settlement tank tests and (b) cylindrical mould tests. One objective of the settlement tank test was to study the additional settlements when the water table is at different depths below the footing and to develop the trend and hence plot variation of $C_w$ with normalized water table depth. The results show that the trend is similar for soils at different relative densities and the only thing that varies is $C_{w,max}$ at the top when the sand is submerged. Since the trend is developed from settlement tank test, it was not further required to obtain $C_w$ at different water table depths in the cylindrical mould tests. Therefore, a small cylindrical mould was used in the next set of tests which took much smaller efforts to conduct a test and hence enables to carry out tests on variety of soils at different relative densities. Here the only objective is to determine $C_{w,max}$ for different soils at different relative densities.

Based on the experimental results of settlement tank tests and strain influence factors proposed in Chapter 3, a rational method is proposed in this Chapter for estimating the additional settlement produced by the rise of water table. The method is independent of the different settlement prediction methods suggested in the literature, and relies only in the strain influence factors assumed. Repeated laboratory model tests using the settlement tank show that the water table correction factor equation proposed in this Chapter with strain influence factors proposed in Chapter 3 work well provided the right value of $C_{w,\max}$ is selected. This Chapter also describes the interpretations of cylindrical mould test data in an attempt to further evaluate $C_{w,\max}$ which is one of the key parameters in the proposed method. Based on the tests carried out on nine different sands, a method is proposed to estimate $C_{w,\max}$ from the standard penetration number $(N_1)_{60}$. The effect of fine content and the maximum-minimum void ratio range are investigated. The effect of soil particle shape on water table correction factor was also investigated by analysing the microscopic images of sand grains used in the tests.

## 5.2 Settlement tank test

The settlement tank test was carried out in a rectangular tank using 100 mm wide model footings of different shapes. The objective of this test was to quantify the effect of footing shape, soil density and varying water table depth on additional settlement of shallow footings due to rise of water level. A locally available sand was used and the test was carried out in two different densities, on five different footing shapes and at varying water table depths. The detail of the test setup was given in Chapter 4. This section describes the test results obtained from the settlement tank test. Based on the interpretation of test data, a rational method is proposed to quantify the effect of water table rise on shallow foundation settlement.

### 5.2.1 Settlement Tank Test Results

Initially, settlement tank tests were carried out on dry sand. The rectangular tank was filled with dry sands and the model footing was placed on the soil surface. Pressure was applied using hydraulic jack and settlement was measured using dial gauges. From the experimental data, applied pressure versus settlement curves were obtained for various footing shapes in loose and dense conditions. Fig. 5.1 shows the applied pressure versus settlement curve for model footings resting on dry loose sand (38% relative density). Fig. 5.1 shows that the failure load is not well defined in the applied pressure-settlement curves and local shear failure occurred as the tests were carried out on relatively loose sand. Only a slight heave occurred at the ground level near the model footings.

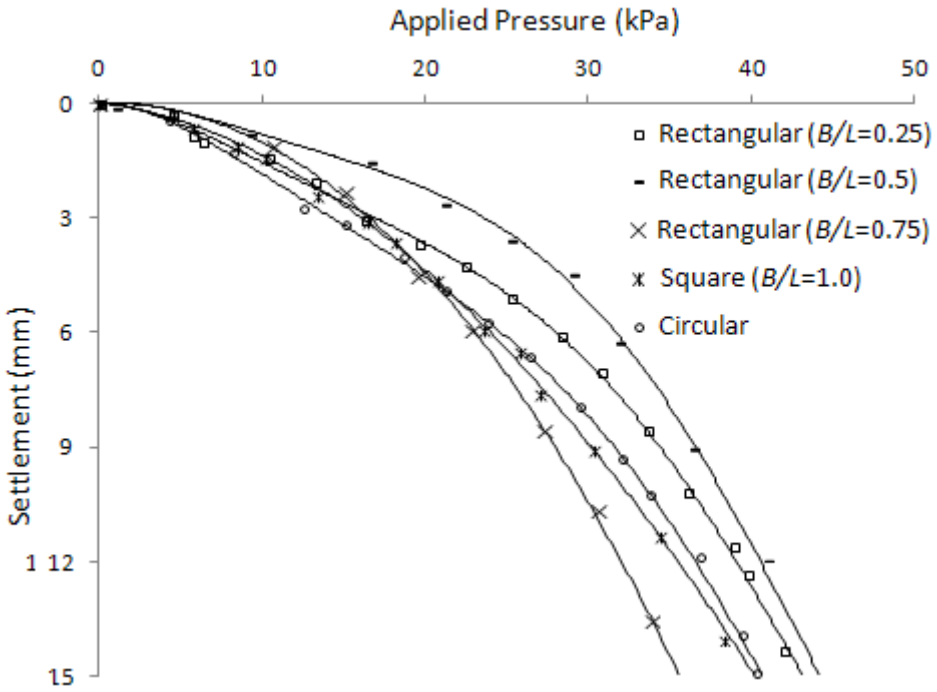


**Figure 5. 1 : Applied pressure vs. settlement curve for model footings resting on dry loose sand**

Unlike the general shear failure, the failure load cannot be defined straightaway from the pressure-settlement curves in local and punching shear failure mode. In this case, the bearing capacity of footing can be determined indirectly. Murtaza et al. (1995) used double tangent method to determine the bearing capacity of footings in their study. Same technique was used in this study to get the failure load of footings resting on loose sands. The method requires drawing tangents from the two relatively straight segments of the pressure-settlement curve and taking the point of interception of the two tangents as the bearing capacity of the footing on that sand. Fig. 5.2 shows the application of double tangent method for a rectangular footing ($B/L$=0.25). From the interception of the two tangents, the failure load obtained for the footing is 21.0kPa.

Fig. 5.3 shows the applied pressure-settlement curve for footings resting on dense sands (77% relative density) in dry states. Unlike the loose sands, the failure load can be defined easily from the pressure-settlement curve as general shear failure occurred in the dense soil condition. The figure shows that the ultimate bearing capacity is lower in circular footing compared to the square footing and in case of rectangular footing; the bearing capacity tends to increase as the foundation width to length ratio ($B/L$ ratio) decreases. This phenomenon matches well with the previous research findings and prevailing bearing capacity equations.

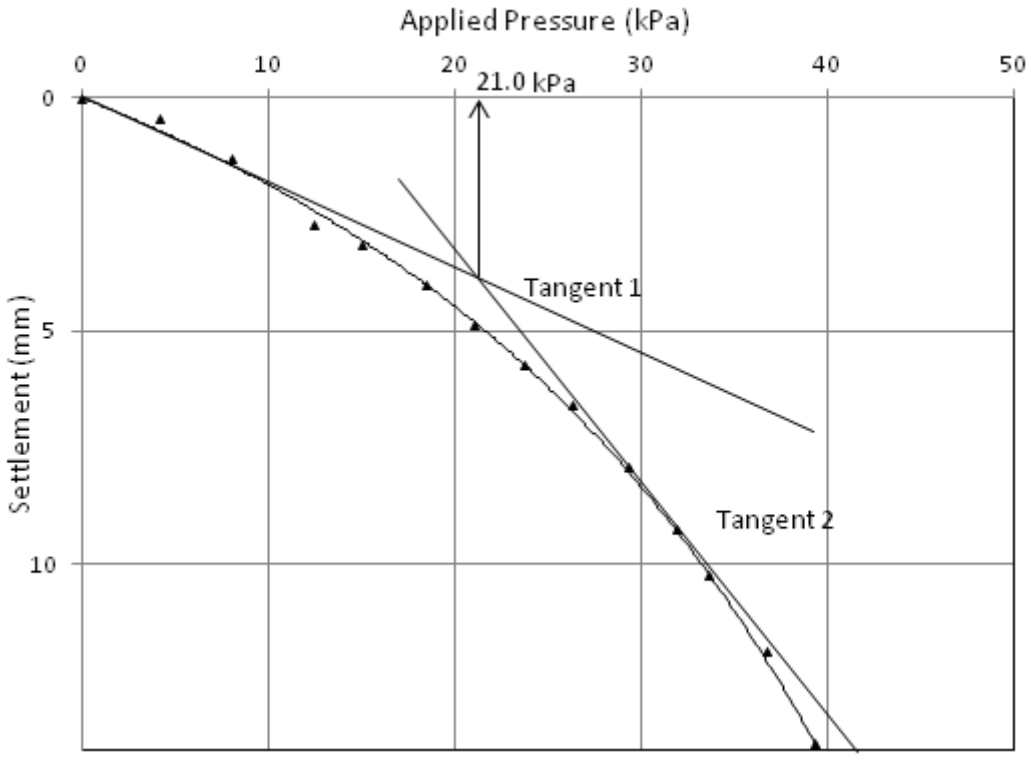


**Figure 5. 2 : Bearing capacity determination using double tangent method for rectangular footing (B/L=0.25) resting on dry loose sand.**

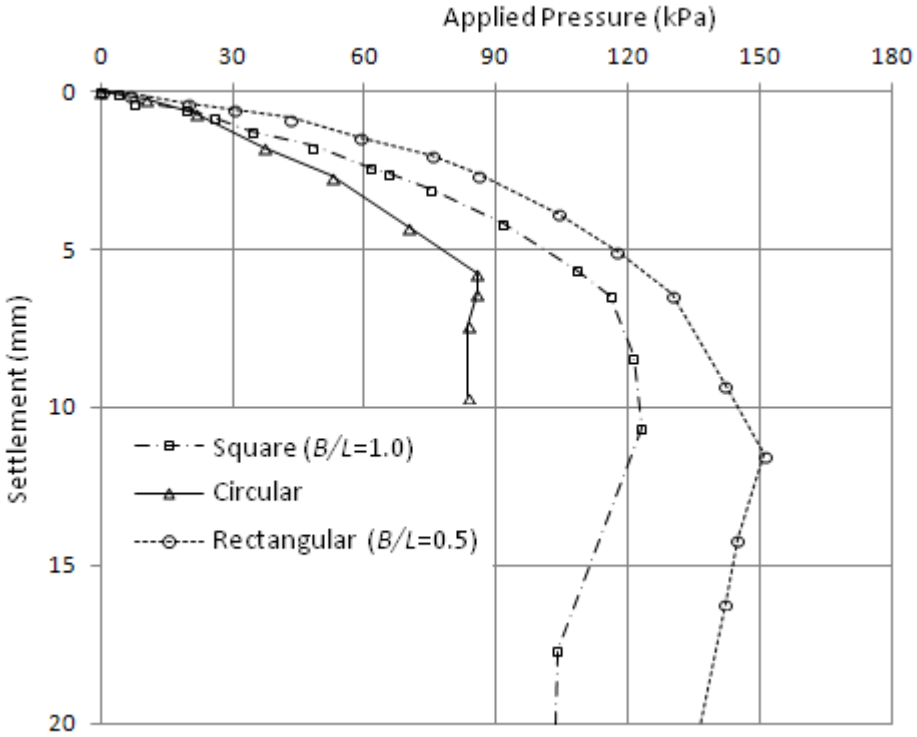


**Figure 5. 3 : Pressure-settlement plot for model footings resting on dense sand (77% relative density) in dry condition**

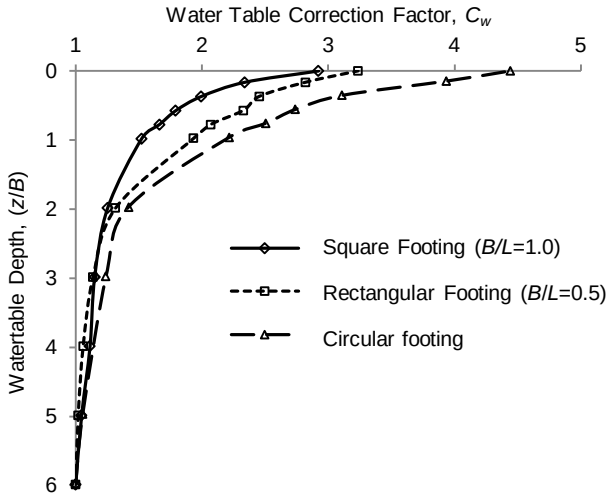


(a)

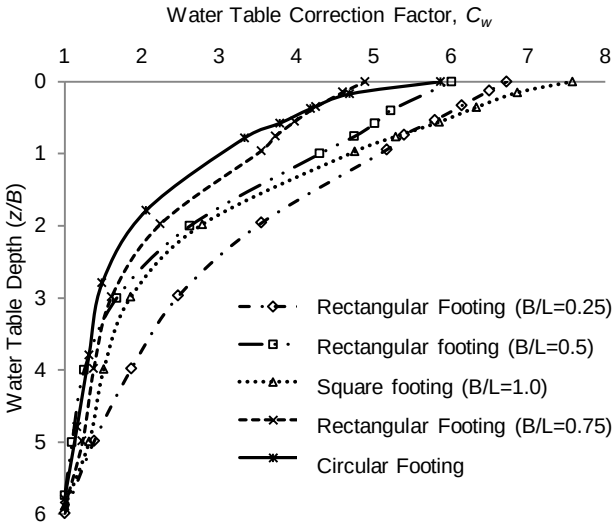


(b)

**Figure 5. 4 : Cw-z/B variation for dense and loose sands: from the model tests on (a) dense sand, (b) loose sand**

The designers usually use a safety factor of three to provide sufficient safety against bearing capacity failure, i.e., they divide the soil bearing capacity by three and take that as allowable working load. This study also used the same safety factor of three. Bearing capacity of soils obtained from the pressure-settlement curves in loose and dense sands in dry condition was divided by three to get the working load. In the next step of the settlement tank test, the footing was subjected to the working load in dry condition and settlement was measured. Then water level was allowed to rise from the bottom and the additional settlements were observed. The water table correction factor $C_w$ for each depth of water level was obtained by dividing the observed settlement at that water level by the settlement in dry condition. Fig.

5.4 shows the variation of the correction factor $C_w$ with normalized water table depth $z/B$ for all the tests.

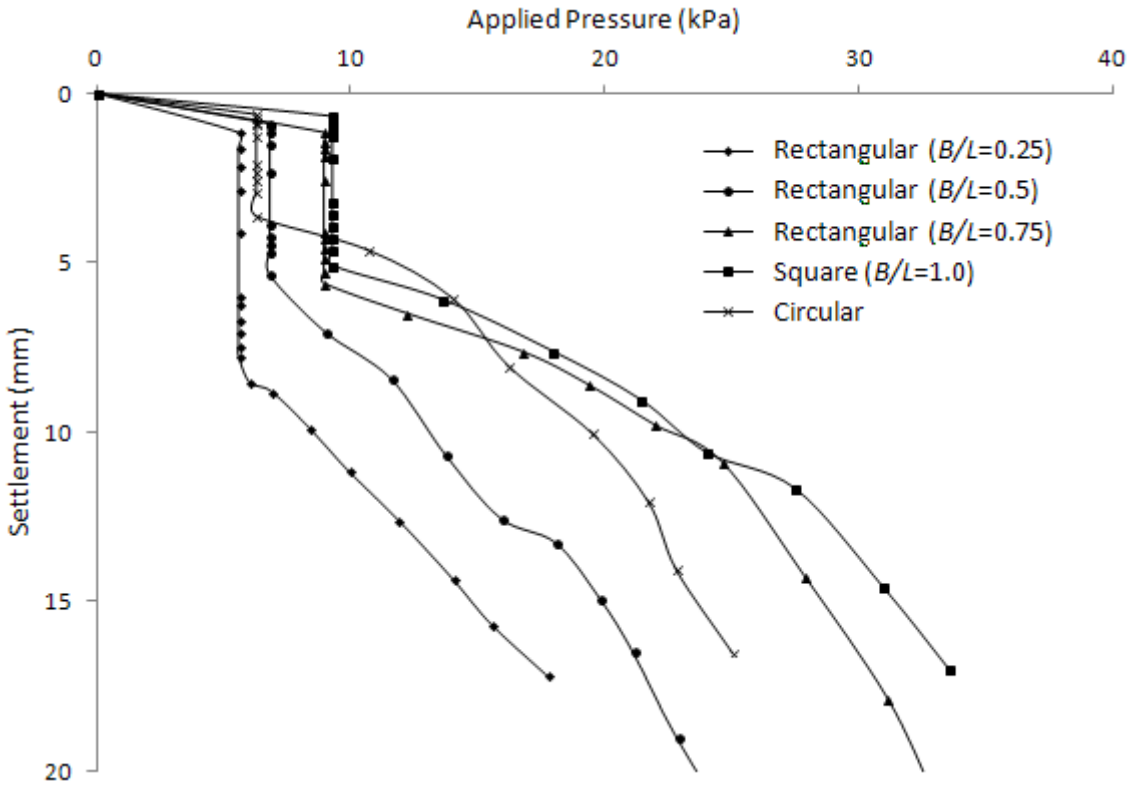


(a)

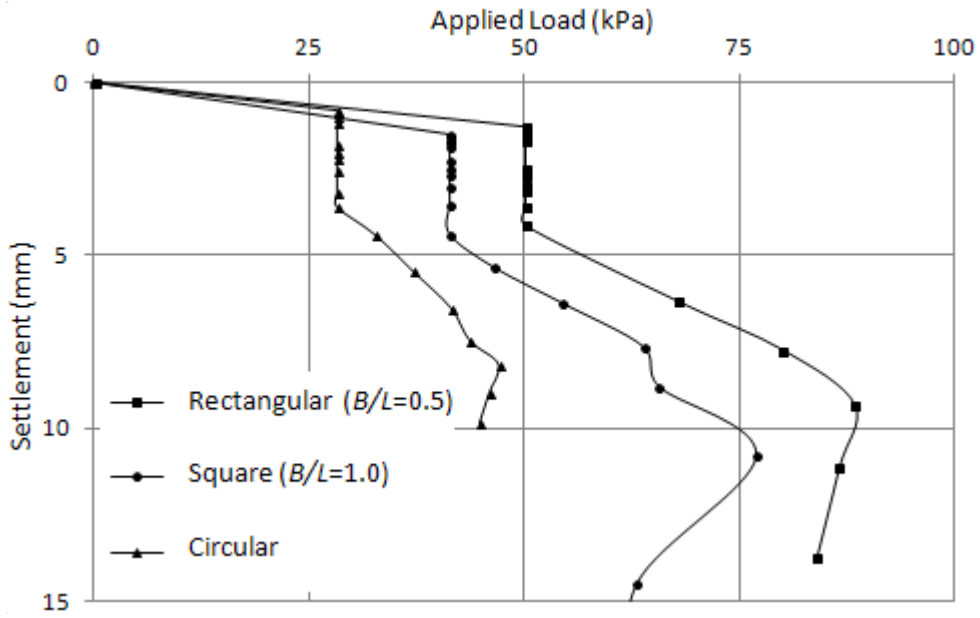


(b)

**Figure 5. 5 : Applied pressure-settlement test in wet tests for footings resting on a) loose sands, b) dense sands**

After the water level rose up to the footing level, the test was carried out further by increasing the applied pressure until the footing failed under bearing capacity. Fig. 5.5 shows the pressure-settlement curve obtained from the wet tests. Here, the initial straight line portion shows the settlement of the footing at working load in dry condition. Then a sharp increase in settlement was observed as the water level rises from the bottom and reaches the footing level while the applied pressure remained constant. The last segment of the load-settlement curve was obtained by increasing the pressure in submerged condition.

### 5.2.2 Water table rise in granular soils

Fig. 5.6(a) shows the schematic diagram of a footing in sands where the water table is well below the footing level initially, when the settlement is computed. When the water table rises into the influence zone, it reduces the soil stiffness and induces additional settlement. Fig. 5.6(b) shows the variation of the strain influence factor $I_z$ with depth $z$. The strain influence factor was originally proposed by Schmertmann (1970), and can be seen as an entity that reflects the vertical normal strain at a specific depth due to the footing load. The depth at which the strain influence becomes zero varies with the shape of the footing. Schmertmann et al. (1978) suggested that this depth can be taken as $2B$ for square and $4B$ for strip footings, and modified the strain influence factor proposed by Schmertmann (1970). The strain influence factors proposed in Chapter 3 suggested slightly different influence factors that vary with the footing shape, and extending to depths below $5B$. The experimental work conducted in this study also support that the settlements can be influenced when the water table rises from a depth significantly greater than that proposed by Schmertmann et al. (1978). Schmertmann et al. (1978) strain influence factors and influence factors proposed in Chapter 3 are shown in Fig. 5.7.

The water table correction factor $C_w$ is defined as the ratio of the settlement when the water table rises to a specific depth to the settlement in the dry sand where the water table is below the zone of influence. Therefore, $C_w$ is always greater than unity and increases with the water table rise, to the maximum value of $C_{w,max}$ when the water table reaches the footing level (Fig. 5.6 c).

When the water table rises, it can be seen in Fig. 5.6(b) that a portion of the strain influence diagram is submerged, where the soil stiffness is reduced substantially. Terzaghi (1943) suggested that the reduction in soil stiffness due to saturation is about 50% and proposed that the settlement doubles when the water table rises to the footing level. That makes the $C_{w,max}$ as two.

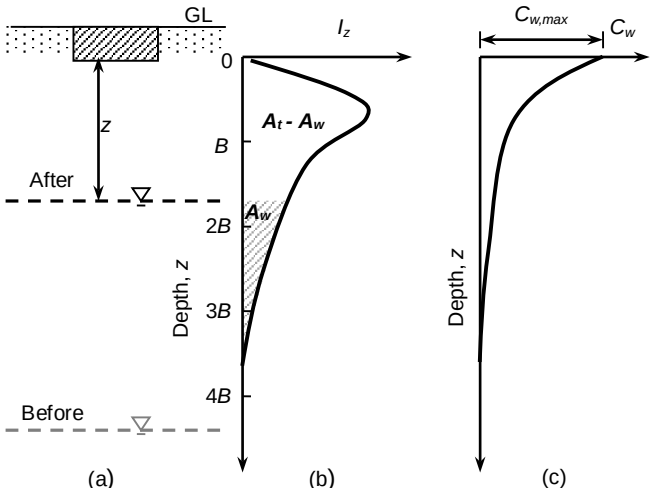


**Figure 5. 6 : (a) Schematic diagram, (b) Strain influence factor, and(c) Water table correction factor Cw**

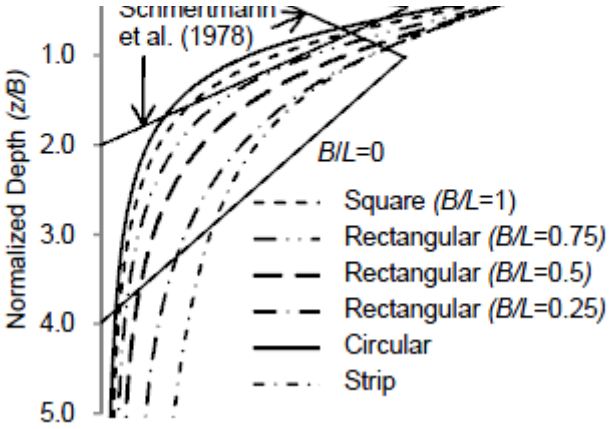


**Figure 5. 7 : Comparison of strain influence factor diagrams proposed in Chapter 3 to those proposed by Schmertmann et al. (1978)**

Water table correction factors were also proposed by Teng (1962); Alpan (1964); Bazaraa (1967); Terzaghi and Peck (1967); Peck et al. (1974); Bowles (1977); and NAVFAC (1982). These were discussed in detail in Chapter 2. The general trend is that the variation of $C_w$ with depth was linear or convex upwards, similar in shape to the one in Fig. 5.6(c). The main differences were in: (a) $C_{w,max}$, the maximum value of $C_w$ which occurs when the water table rises to the footing level, and (b) the depth at which the water table rise starts to induce additional settlements. The $C_{w,max}$ varies from 1 to 2 in all the cases. The depth at which the water table starts inducing additional settlements varies between 0.4 $B$ and 2.0 $B$, where $B$ is the width of the footing.

A few laboratory experiments have been conducted so far to investigate the effect of rising water table on settlement, and contradictory results were reported. Agarwal and Rana (1987) used three square model footings in their experiments and the results suggested $C_{w,max}$ of 2.0, which support Terzaghi's (1943) proposition. Murtaza et al. (1995) carried out model tests in the laboratory on sands at three different relative densities, and reported $C_{w,max}$ values in the range of 8-12. Morgan et al. (2010) carried out some model tests on two different sands and showed that the additional settlements are greater in loose sands than in dense sands, and $C_{w,max}$ varied in the range of 2.3-6.5. The shape of the $C_w$-$z$ plot was convex upwards, similar to Fig. 5.6(c). Additional settlements were induced when water table was at 5$B$ below the footing levels. Numerical modelling conducted in Chapter 6 also shows that the $C_w$-$z$ plot is convex upwards, implying that additional settlements increase at a faster rate when the water table approaches the footing level.

### 5.2.3 Proposed model for determining $C_w$

It can be seen intuitively that when the water table is below the strain influence zone, $C_w = 1$ (i.e. no additional settlement occurs). When the water table rises to the footing level, where $A_w = A_t$, the water table correction factor reaches its maximum value of $C_{w,max}$. Based on settlement tank tests and the influence factor diagram proposed in Chapter 3, the following equation is proposed for the water table correction factor $C_w$ as a function of $A_w/A_t$, which varies with depth of $z$ of the water table below the footing level.

$$C_w = 1 + \left(C_{w,\max} - 1\right)\left(\frac{A_w}{A_t}\right)^n \qquad (5.1)$$

$A_w$ is the area of the influence factor diagram that is submerged and $A_t$ is the total area of the influence factor diagram (see Fig. 5.6b). $C_{w,max}$ is the maximum value of $C_w$ that occurs when the water table rises to the footing level. $n$ is a curve-fitting parameter that controls the shape of the $C_w$-$z$ plot which depends on the relative density of the sand. Fig. 5.8 shows the variation of $C_w$ with depth of water table for a square footing, for different values of $n$, assuming strain influence factors proposed in Chapter 3, and $C_{w,max}$ of 2.0 suggested by Terzaghi (1943). It can be seen that the curves are convex upwards for all values of $n$ assumed in the plot and for $n$ = 0.85-1.10, and the curves fall within a narrow band.

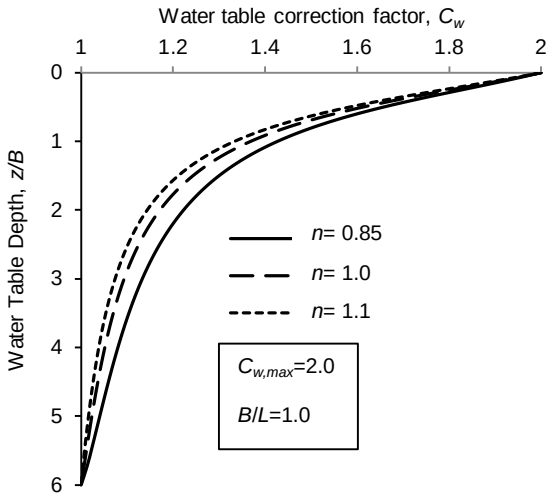


**Figure 5. 8 : Effects of n on Cw – z variation based on proposed strain influence factors for square footings (Cw,max = 2).**

Fig. 5.9 shows the variation of $C_w$ with depth of water table $z$ for a square footing based on the influence factors proposed by Schmertmann (1970), with the modification suggested by Terzaghi et al. (1996), and the suggested modification in Chapter 3. Here $n$ is assumed as 1.0, and $C_{w,max}$ is assumed as 2.0. Unlike the model proposed by Alpan (1964); Bazaraa (1967); Terzaghi and Peck (1967); Bowles (1977); and NAVFAC (1982); the proposed variation of $C_w$ with depth is convex upwards. This compares with the shape proposed by Teng (1962); Peck et al. (1974) and the numerical predictions shown in Chapter 6.

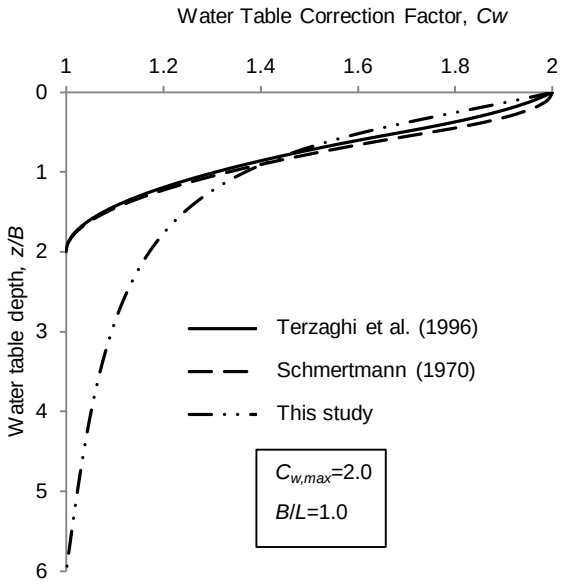


**Figure 5. 9 : Cw – z variation for different strain influence factors for square footings (Cw,max = 2, n = 1)**

The value of $A_w/A_t$ obtained by using strain influence factors of Chapter 3 for various footing shapes at different depths are shown in Fig. 5.10 and summarized in Table 5.1. This will help practising engineers to use Eq. 5.1 by simply substituting $A_w/A_t$ value from the table or from Fig. 5.10.

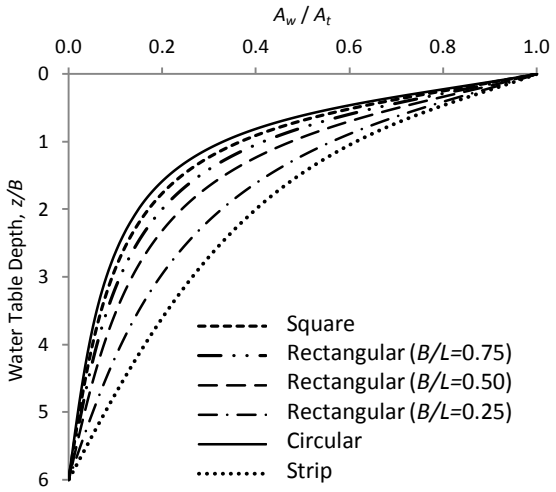


**Figure 5. 10 : Variation of Aw//At of various footings with water table depth**

Table 5.1: $A_w/A_t$ values at different depths for various footing shapes

| Water table depth ($D_w/B$) | Footing Shape | | | | | |
|---|---|---|---|---|---|---|
| | Circular Footing | Square Footing ($B/L$=1) | Rectangular Footing ($B/L$=0.75) | Rectangular Footing ($B/L$=0.50) | Rectangular Footing ($B/L$=0.25) | Strip Footing ($B/L$=0) |
| 0 | 1 | 1 | 1 | 1 | 1 | 1 |
| 0.5 | 0.573 | 0.612 | 0.658 | 0.703 | 0.757 | 0.785 |
| 1 | 0.33 | 0.368 | 0.416 | 0.475 | 0.562 | 0.614 |
| 2 | 0.149 | 0.171 | 0.2 | 0.241 | 0.327 | 0.399 |
| 3 | 0.08 | 0.094 | 0.11 | 0.135 | 0.196 | 0.264 |
| 4 | 0.044 | 0.051 | 0.06 | 0.075 | 0.113 | 0.163 |
| 5 | 0.019 | 0.023 | 0.027 | 0.034 | 0.051 | 0.078 |
| 6 | 0 | 0 | 0 | 0 | 0 | 0 |

### 5.2.4 Interpretation of settlement tank test data

For all levels of the water table, the correction factor $C_w$ was determined as the ratio of the settlement with the raised water table to the settlement when the sand was dry. Fig. 5.11 shows the variation of $C_w$ with normalised depth $z/B$, for the dense and loose sands, derived from the model tests. The following observations are made from these tests.

1. The additional settlements due to rise of water table are more pronounced in loose sands than in dense sands. This is true for all six footing shapes, with the $C_w$ being larger for loose sands at all water levels.
2. The values for $C_{w,max}$ for loose sands lie in the range of 4.9-7.6 for the different footing shapes, and for dense sands it lies in the range of 2.9-4.4.
3. Additional settlements are induced when water table is at 6$B$ below the footing level. A careful observation of the correction factor diagrams obtained from the experimental results show that the rise of water table produce significant additional settlement even at depths as high as 5$B$ and the settlement due to submergence is further influenced by the soil density and footing shape.
4. The rate of increment in additional settlement with rising water level is not linear; rather, the increase is faster when the water table is at the vicinity of the foundation level. The $C_w$-$z$ variation is convex upwards for all footing shapes and both densities. This was evident in Fig. 5.6(c). This trend suggests that when the water table rises, the rate of increase in $C_w$ increases throughout.
5. $C_{w,max}$ values were determined when the entire sand bed is saturated and hence there is no capillary effect to account for. The very slight influence of capillary was only present when water level was below the footing level, which has been neglected in the analysis.

After several curve fitting trials, it was decided to take $C_{w,max}$ and $n$ in Eq. 5.1 as 6.3 and 0.85 for loose sands, and 3.4 and 1.1 for dense sands. Thus, Eq. 5.1 can be written as:

$$C_w = 1 + 5.3\left(\frac{A_w}{A_t}\right)^{0.85} \quad \text{for loose sands} \tag{5.2}$$

$$C_w = 1 + 2.4\left(\frac{A_w}{A_t}\right)^{1.1} \quad \text{for dense sands} \tag{5.3}$$

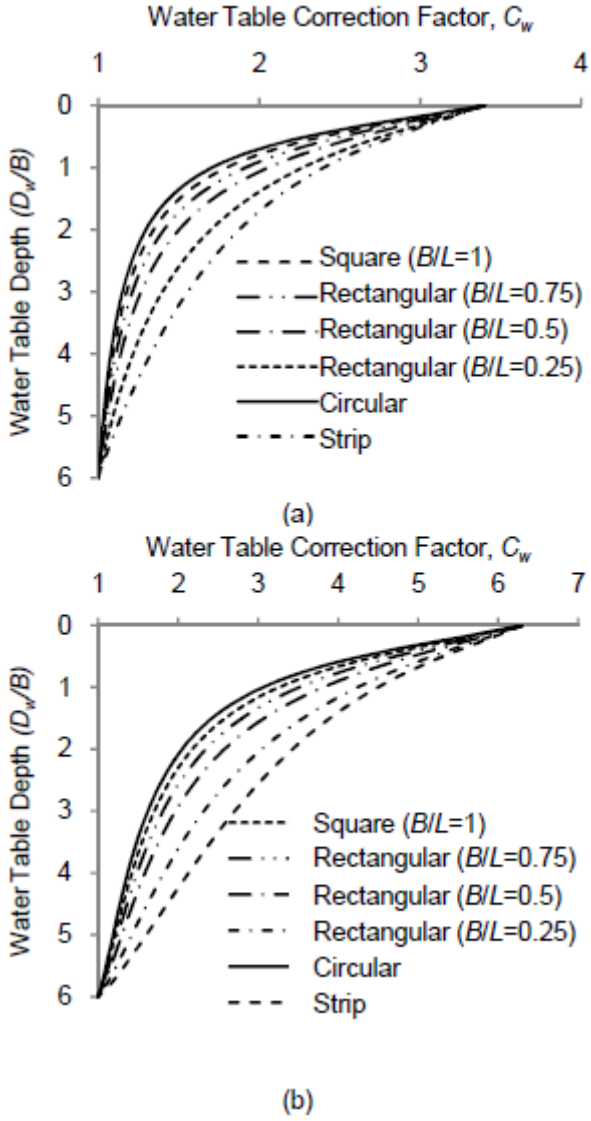


**Figure 5. 11 : Water table correction factor diagrams based on proposed semi-empirical equation for (a) dense sand, and (b) loose sand**

Eqs. 5.2 and 5.3 incorporate the relative density and the footing shape into the water table correction factor $C_w$. Fig. 5.11(a) shows the variation of $C_w$ with the water table rise, for different footing shapes, in dense sands assuming n = 1.1 (Eq. 5.3). This is reproduced for loose sands in Fig. 5.11(b) for n = 0.85. These are derived from the two equations 5.2 & 5.3 and the strain influence factors proposed in Chapter two. While the rate of increase in $C_w$ becomes larger at shallower depths, this is more pronounced for square or circular footings than strip footings.

### 5.2.5 Model validation

Fig. 5.12 shows the variation of $C_w$ with $z/B$, for circular and rectangular ($B/L$=0.5) footings as determined from the model tests for dense and loose sands. Also shown in the figure are

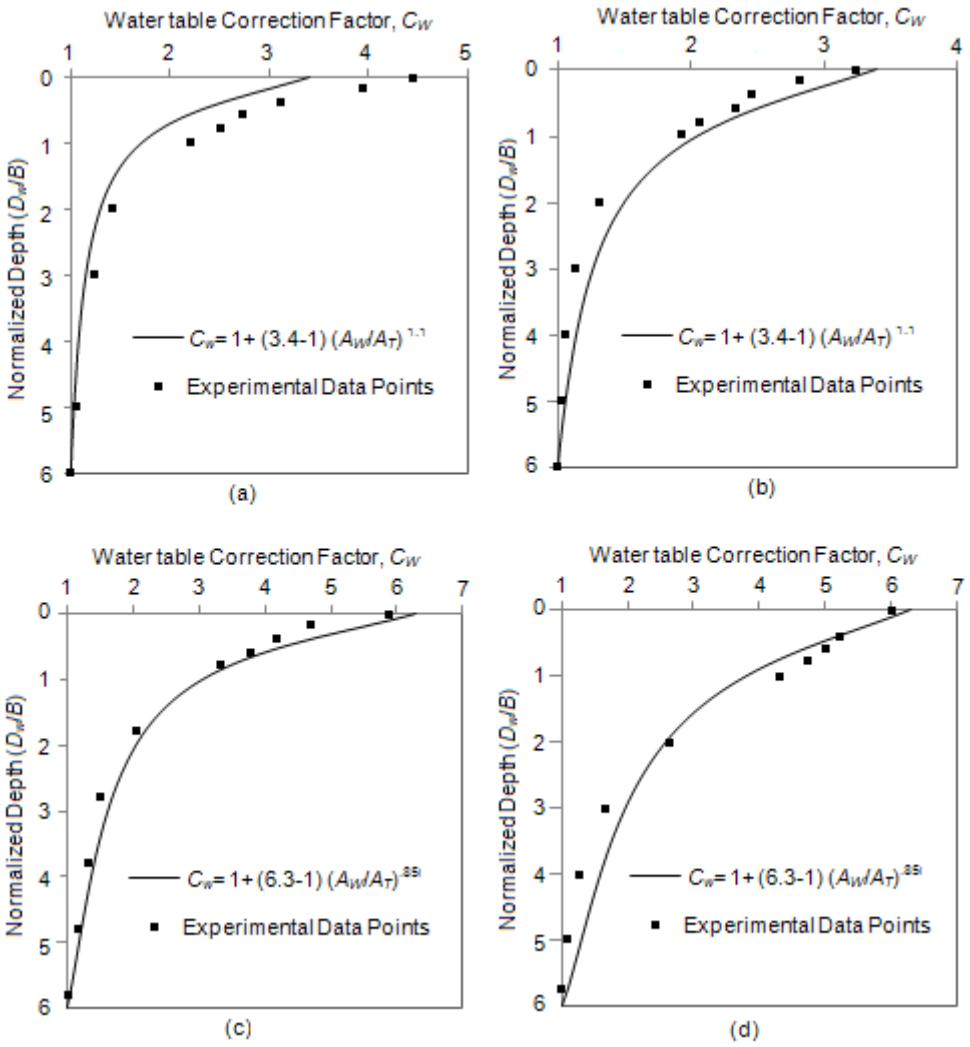


**Figure 5. 12 : Cw-z/B variation from the model tests: (a) circular footing in dense sand, (b) rectangular (B/L = 0.5) footing in dense sand, (c) circular footing in loose sand, and (d) rectangular (B/L = 0.5) footing in loose sand.**

the theoretical variations determined using Eq. 5.2 and 5.3. There is very good agreement between the theoretical and experimental plots, suggesting that Eq. 5.2 and 5.3 would give reasonable estimates for the water table correction factor for this sand used in the model tests. It also suggests that assuming the same $C_{w,max}$ for various footing shapes resting on the same soil at same relative density gives good agreement between the theoretical and experimental plots. Noting that $n$ is very close to unity for the loose and dense sands tested here, as a first approximation, $n$ can be taken as unity for all relative densities. It can also be seen from Fig. 5.8 that taking $n$ as 1 has very little influence on $C_w$. Thus, Eq. 5.1 becomes,

$$C_w = 1 + \left(C_{w,\max} - 1\right)\frac{A_w}{A_t} \tag{5.4}$$

where, $C_{w,max}$ has to be determined for the specific sand by measuring the additional settlement by inundating the entire sand. This exercise can be carried out in a smaller tank and using smaller footings since the capillary effects do not come into play when the sand bed is fully saturated.

The work reported herein is based on strain influence factors proposed in Chapter 3 that extend to 6*B* below the footing. The original and modified strain influence factor diagrams proposed by Schmertmann (1970); Schmertmann et al. (1978) and Terzaghi et al. (1996) extend to shallower depths (e.g. 2*B* below the footing level for circular and square footing) and hence cannot explain the increase in foundation settlement with rising water table at a greater depth as observed in the model tests. The modified strain influence factor diagrams proposed in Chapter 3 extend to a greater depth as shown in Fig. 5.7 and can be effectively used for predicting water table correction factor diagram. For designers still wanting to use Schmertmann et al. (1978) influence factors, Eq. 5.4 is still applicable, with appropriate value for $C_{w,max}$.

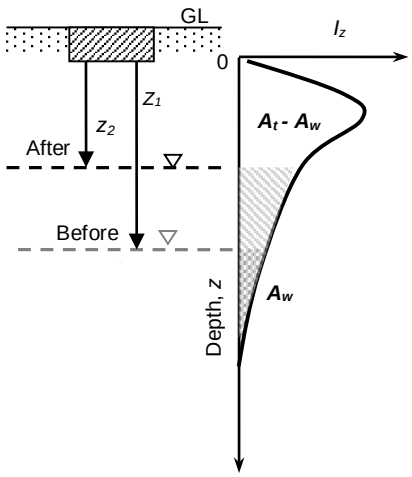


**Figure 5. 13 : Change in water level within the depth of influence**

### 5.2.6 Additional settlement due to change in water level within the influence zone

The method can also be used to compute the additional settlement in situations where the water table is already within the depth of influence (i.e. less than 5*B*) and rises subsequently, by employing the principle of superposition. As shown in Fig. 5.13, if the water level rises from a depth of $z_1$ to $z_2$, the submerged area of influence factor diagram also increases from $A_{w1}$ (dark hatched area) to $A_{w2}$ (entire hatched area). The water table correction factor at water

table depth $z_1$ and $z_2$ can be termed as $C_{w1}$ and $C_{w2}$ respectively, and the correction factor equation can be written as,

$$C_{w1} = 1 + \left(C_{w,\max} - 1\right)\frac{A_{w1}}{A_t} \tag{5.5}$$

$$C_{w2} = 1 + \left(C_{w,\max} - 1\right)\frac{A_{w2}}{A_t} \tag{5.6}$$

The settlement at water table depth $z_1$ and $z_2$ can be termed as $S_{z1}$ and $S_{z2}$, and can be obtained by multiplying the water table correction factor with settlement at dry condition $S_d$,

$$S_{z1} = C_{w1} * S_d \tag{5.7}$$

$$S_{z2} = C_{w2} * S_d \tag{5.8}$$

Dividing Eq. 5.8 by Eq. 5.7 and rearranging, we get

$$S_{z2} = \frac{C_{w2}}{C_{w1}} * S_{z1} \tag{5.9}$$

$$\text{or, } S_{z2} = \frac{A_t + (C_{w,\max} - 1) * A_{w1}}{A_t + (C_{w,\max} - 1) * A_{w2}} * S_{z1} \tag{5.10}$$

So, if the settlement at water table depth $z_1$ is known, settlement due to further change in water level can be obtained using Eq. 5.9 or Eq. 5.10.

## 5.3 Cylindrical Mould Test

In the previous section, a rational method for predicting the water table correction factor is proposed from data analysis of the settlement tank tests. The small cylindrical mould tests were carried out as a continuation of the settlement tank tests in an attempt to further understand the water table correction factor when the water level rises up to the footing level. Effect of fine grains and soil gradation on additional settlement due to water level rise is also investigated in the small mould tests. Instead of the large settlement tank, a small cylindrical mould was used. Nine different soils were used in the tests in dense and loose states and in dry and saturated conditions.

The test setup was prepared as detailed in Chapter 4. Initially, the test was run on dry soils. After filling the mould with soil of required density, the model footing was placed at the centre and load was applied through the loading arrangement. The applied pressure-settlement plots were obtained from dry tests of all nine soils in loose and dense condition.

The bearing capacity of the model footing was then obtained from the pressure-settlement diagram using double tangent method. Fig. 5.14 shows the applied pressure-settlement diagram and the application of double tangent method for Soil 3 in dense and dry state.

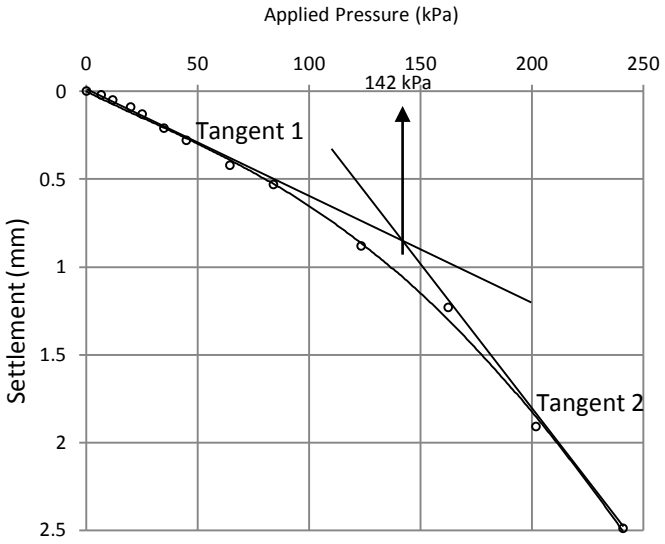


**Figure 5. 14 : Applied pressure-settlement diagram and the application of double tangent method for Soil 3 in dense and dry state**

Using a safety factor of three, the working load was obtained by dividing the bearing capacity by three. For the wet test, the footing was initially subjected to the working load at dry condition and the settlement corresponding to the applied pressure was recorded. Then water was allowed to rise up to the footing level and final settlement was recorded. $C_{w,max}$ for each of the soil was obtained by diving the settlement of footing when water table reaches the footing level with the settlement of footing when the soil is dry. $C_{w,max}$ obtained this way was then used to correlate with various soil parameters.

### 5.3.1 Interpretation of small mould test data

From laboratory model tests, $C_{w,max}$ for the nine soils in different densities were obtained which were then used in correlating various soil parameters including standard penetration number $(N_1)_{60}$ corrected for overburden & energy ratio, void ratio range, fines content $F_c$, volumetric strain potential $\epsilon_v$ etc. $C_{w,max}$ values of the soils are given in Table 5.2 along with the relative densities of the sands tested. The uniformly graded soils (soil 1, 2, 3 and 5) were tested at $D_r$=10% and 90% and others at $D_r$=38% and 77%. For uniformly graded soils, the void ratio ranges ($e_{max}$-$e_{min}$) were too small. Since, small amount of soil was required to fill the small cylindrical mould, smaller relative density difference in uniform soils would result in only a few grams of difference between loose and dense soils. This is why; the relative

density difference for uniformly graded soils was increased. However, for consistency in analysis, $C_{w,max}$ of all the soils should be measured at same densities. $C_{w,max}$ of soil 1 was determined in a significantly larger settlement tank as discussed in the previous section at $D_r$= 38 and 77%, whereas it was tested at 10% and 90% $D_r$ in this study. Fig. 5.15 shows the variation of $C_{w,max}$ with $D_r$ obtained from the settlement tank test and small mould test. It shows that $C_{w,max}$ linearly decreases with increasing $D_r$. This finding was useful to interpolate $C_{w,max}$ of the other uniform sands (soil 4, 5a, 5b, 5c and 6) at $D_r$= 38% and 77%. These two relative densities were then used in analysis in this study. $C_{w,max}$ at $D_r$= 38 and 77% of all the soils are noted in Table 5.2.

Table 5.2: $C_{w,max}$ and $D_r$ of the sands tested.

| Soil No. | $C_{w,max}$ and $D_r$ of the sands tested | | | | $C_{w,max}$ at $D_r$=38% | $C_{w,max}$ at $D_r$=77% |
|---|---|---|---|---|---|---|
| | $D_r$ | $C_{w,max}$ | $D_r$ | $C_{w,max}$ | $D_r$ | $C_{w,max}$ |
| 1 | 10% | 7.25 | 90% | 2.44 | 6.3 | 3.4 |
| 2 | 10% | 7 | 90% | 3.67 | 4.2 | 5.85 |
| 3 | 10% | 2.1 | 90% | 1.81 | 1.83 | 2.07 |
| 4 | 38% | 7.06 | 77% | 2.25 | 7.06 | 2.25 |
| 5 | 10% | 5.19 | 90% | 1.53 | 3.93 | 2.11 |
| 6 | 38% | 29.88 | 77% | 4.48 | 29.88 | 4.48 |
| 5a | 38% | 6.76 | 77% | 2.03 | 6.76 | 2.03 |
| 5b | 38% | 7.75 | 77% | 2.07 | 7.75 | 2.07 |
| 5c | 38% | 37.83 | 77% | 3.76 | 37.83 | 3.76 |

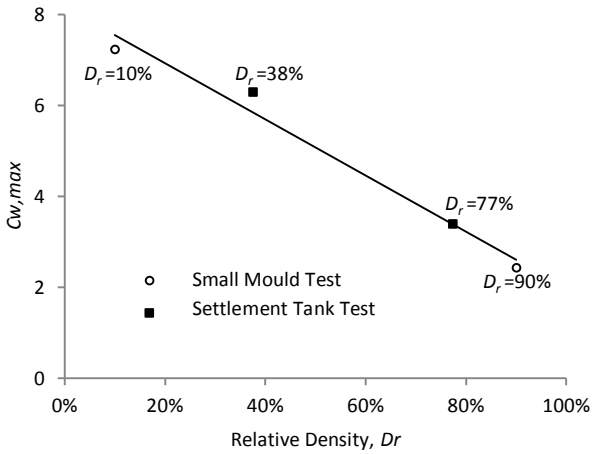


**Figure 5. 15 : Variation of Cw,max of soil 1 with relative density obtained from settlement tank test and small mould test**

### 5.3.2 Relationship between Standard Penetration Number (*N*) and $C_{w,max}$

The deformation and strength characteristics of granular soils are mainly influenced by two parameters- the material properties and the physical state of the soil. The conventional parameters used in identifying sand behaviour are the mean grain size and the fine content $F_c$. However, Cubrinovski and Ishihara (1999, 2002) pointed that soils having identical fines content can show remarkably different stress-strain characteristics. They proposed that the void ratio range ($e_{max}$-$e_{min}$) i.e., the difference between the void ratio of sand in loosest and densest packing, is more indicative of the overall grain size distribution and deformation behaviour of granular soil as it allows for the effects of relevant material properties. Das and Sivakugan (2011) also suggested that void ratio range can be used as a controlling parameter for predicting strength and compressibility of cohesionless soils.

The field standard penetration (SPT) number in granular soils ($N_{60}$) is dependent on effective overburden pressure ($\sigma'_0$) and it can be normalized with an overburden pressure of 98 kPa by the following (Liao and Whitman, 1986):

$$(N_1)_{60} = N_{60}\left[\frac{98}{\sigma'_0(\text{kPa})}\right]^{0.5} \tag{5.11}$$

where, $(N_1)_{60}$= SPT number, corrected for overburden pressure and hammer efficiency

Cubrinovski and Ishihara (1999) proposed an empirical correlation between $(N_1)_{60}$, relative density $D_r$, and void ratio range ($e_{max}$-$e_{min}$) which is applicable to granular soils including clean sands, sands with silts and gravelly sands. The expression is:

$$\frac{(N_1)_{60}}{D_r^2} = \frac{9}{(e_{\max} - e_{\min})^{1.7}} \tag{5.12}$$

Using Eq. 5.12, $(N_1)_{60}$ for the test conditions of the nine soils at different densities were obtained. The results were then plotted against $C_{w,max}$ as shown in Fig. 5.16. Soil 1,2,3 are very uniform with small $e_{max}$-$e_{min}$ values that results in very high and unrealistic values of $(N_1)_{60}$ derived from Eq. 5.12. For this reason, data points from these soils were excluded from Fig. 5.16. The figure clearly indicates that correction factor drops with higher SPT number. Based on the best fit curve in Fig. 5.16, the relation between $C_{w,max}$ and $(N_1)_{60}$ can be proposed as :

$$C_{w,\max} = 20.67 * (N_1)_{60}^{-0.57} \tag{5.13}$$

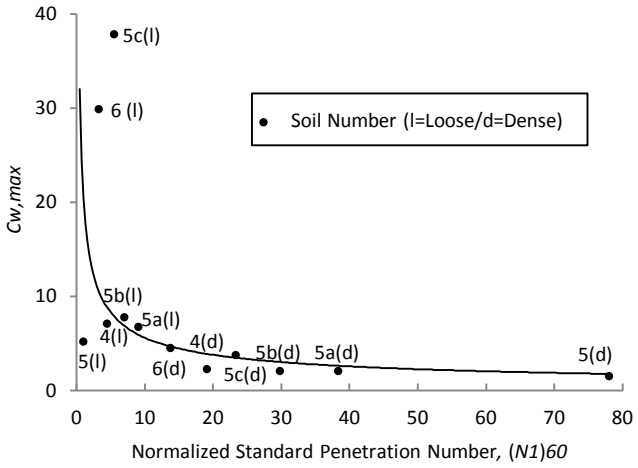


**Figure 5. 16 : Variation of Cw,max with normalized standard penetration number $(N_1)_{60}$ obtained from Eq. 5.12**

Field SPT value for dense sand usually ranges within 25-42. Substituting these in Eq. 5.13 shows that the maximum correction factor should range between 2.5 to 3.3 in dense sand. If the void ratio range for a particular granular soil is known, $C_{w,max}$ for that soil at a given relative density can be obtained using Eq. 5.12 and 5.13. Alternately, the field SPT number can be used to obtain maximum correction factor by using Eq. 5.13. It is also possible to find the correction factor at any water level by substituting $C_{w,max}$ value in Eq. 5.4.

### 5.3.3 Effect of fines content on $C_{w,max}$

Another objective of the study was to investigate the effect of fines content on the additional settlement due to rise in water level. To investigate that, fine grains were added to soil 5 to make soils containing 10%, 15% and 20% fines and were named as soil 5a, 5b and5c

respectively. Fig. 5.17 shows variation of $C_{w,max}$ with increasing fines contents in soil 5 in both loose and dense conditions. As structures are usually built on dense soil, characteristics of dense soil are of particular interest for practicing engineers. Therefore, the variation of $C_{w,max}$ with dense soils is shown in the inset.

Fig. 5.18 shows the $C_{w,max}$ against percentage fines curve for all nine soils with dense soils curve in the inset. Both the figures indicate the same trend that compressibility of submerged granular soil significantly increases when fine content is more than 15% of the soil mass. The rate of settlement increase with increase in percentage of fines is much higher in loose state. Additional settlement in dense state is less significant up to a fine content of 15% but beyond that, it increases considerably. The ratio of $C_{w,max}$ in loose sand to that in dense sand also increases with presence of fines, as shown in Fig. 5.19. It means that soils having high percentage of fines become more compressible in loose state at submerged condition. The increase in fines contents increase the void ratio range of the soil and makes the soil more compressible.

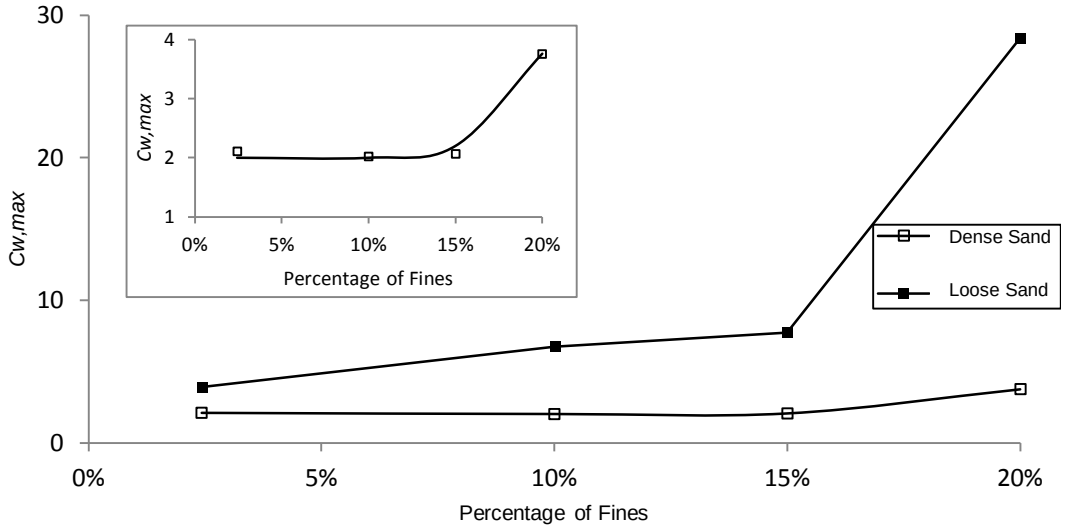


**Figure 5. 17 : Effect of fine contents on Cw,max of soil 5 in loose and dense state. Inset: Cw,max vs. fines content for dense state.**

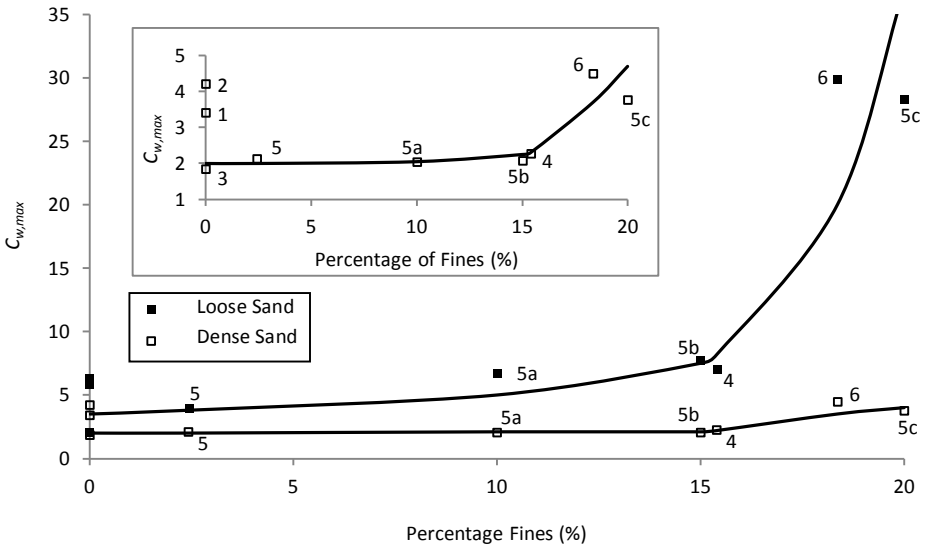


**Figure 5. 18 : Variation of Cw,max with fine contents for all soils in loose and dense state. Inset: Cw,max vs. fines content for dense state. (Soil number given alongside corresponding data point)**

### 5.3.4 Effect of void ratio range on $C_{w,max}$

$C_{w,max}$ ratio in loose to dense state was also investigated against void ratio range of the granular soils. Fig. 5.20 shows that $C_{w,max}$ ratio increases exponentially with increasing void

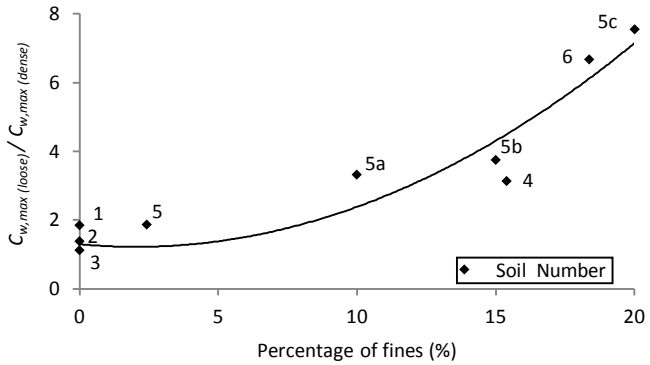


**Figure 5. 19 : Variation of Cw,max ratio in loose sand to dense sand with fine contents**

ratio range of the soil. The void ratio range is usually low for uniformly graded sands and gravels (<0.3), medium for clean sands (0.3-0.5) and higher for sands with fines (>0.5) (Cubrinovski and Ishihara 1999). This means that loose sands with fines are more compressible in submerged conditions than loose uniform sands.

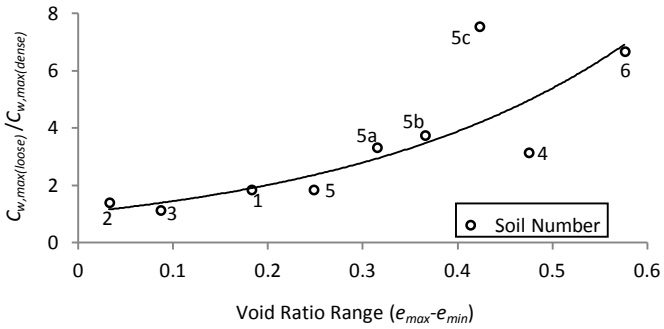


**Figure 5. 20 : Change in Cw,max ratio with void ratio range**

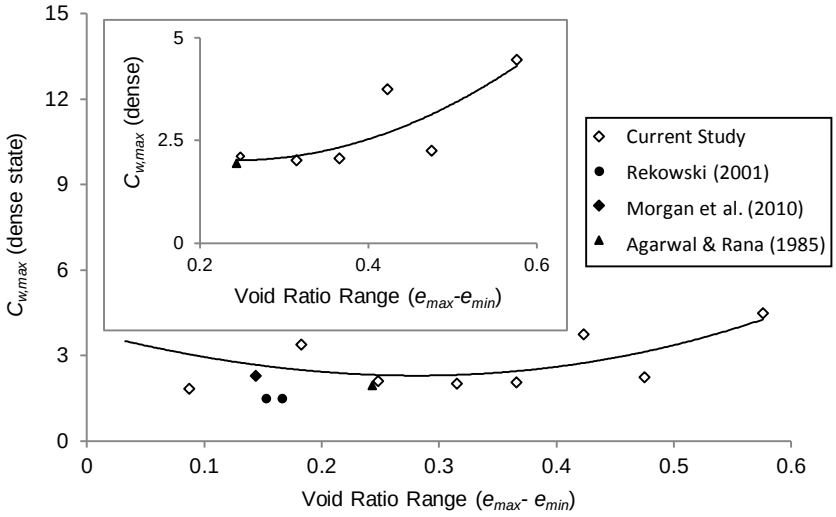


**Figure 5. 21 : Variation of Cw,max in dense sands with void ratio range. Inset: Cw,max vs. void ratio range for $e_{max}$-$e_{min}$>0.2**

$C_{w,max}$ of dense sands were also investigated with the void ratio range, as shown in Fig. 5.21. Results from previous laboratory investigations of Agarwal and Rana (1985); Rekowski (2001); and Morgan et al. (2010) are also included in the figure. The figure shows that there is no observable correlation between void ratio range and $C_{w,max}$ for dense uniform soils and gravel ($e_{max}$-$e_{min}$<0.2). However, for soils having void ratio range greater than 0.2, $C_{w,max}$ of dense sands increases with $e_{max}$-$e_{min}$, as shown in the inset of Fig. 5.21.

### 5.3.5 Effect of Volumetric Strain Potential on $C_{w,max}$

Another measure of soil compressibility is volumetric strain potential $\epsilon_v$, which is the strain that a soil undergoes as the soil turns into densest possible state from loosest state i.e., void ratio changes to $e_{min}$ from $e_{max}$. The expression for $\epsilon_v$ is:

$$\varepsilon_v = \frac{e_{max} - e_{min}}{1 + e_{min}} \tag{5.14}$$

Das and Sivakugan (2011) proposed and empirical equation for $\epsilon_v$ based on the results of Cubrinovski and Ishihara (2002) and Patra et al. (2010), which is:

$$\varepsilon_v(\%) = 22(e_{max} - e_{min}) + 11 \tag{5.15}$$

$C_{w,max}$ ratio of loose to dense soil was plotted against volumetric strain potential for both the expressions in Eq. 5.14 and 5.15 as shown in Fig. 5.22. The figure shows that $C_{w,max}$ ratio increases exponentially with volumetric strain indicating that soils having higher potential for volumetric strain are likely to experience more submergence induced settlement in loose condition than in dense condition.

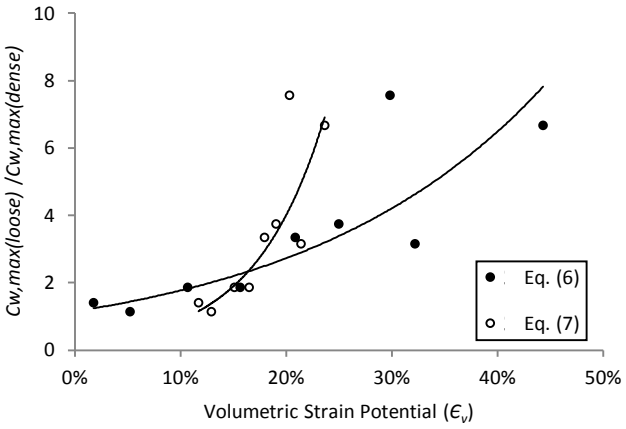


**Figure 5. 22 : Change in Cw,max ratio on loose sand to dense sand with volumetric strain potential.**

### 5.3.6 Soil Gradation and Water Table Correction Factor

Schultze and Moussa (1961) and Oda (1972) suggested that at the same initial void ratio, a well graded soil is more compressible than a uniformly graded soil. Among the nine soils tested in the small mould test, three soils are well graded (soil 4, 6 and 5b) i.e. coefficient of uniformity $C_u$>6 and coefficient of curvature $C_c$=1-3. Soil 1, 2, 3 and 5 were fairly uniform. Fig. 5.23 shows the $C_{w,max}$ ratio for well graded and uniform soils. The soils are divided by the $C_u$=6 line. The figure clearly shows that $C_{w,max}$ ratios for uniformly graded sands tend to be much less than that of well graded sands. This means loose well graded sands are more compressible than loose uniform soils when submerged.

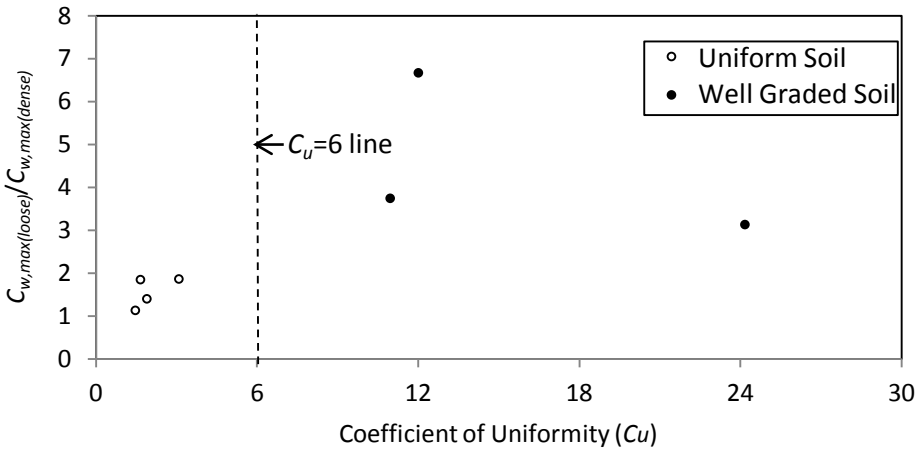


**Figure 5. 23 : Change in Cw,max ratio with coefficient of uniformity in uniform and well graded soils**

## 5.4 Effect of particle shape on water table correction factor

Another objective of this study was to study the effect of particle shape on additional settlement of shallow footings due to water level rise. Soil grain size distribution and particle shape plays an important role in determining soil behaviour and this is widely recognized. The stress-strain behaviour of soil mass results from interaction of grains which is affected by grain size and shape. Soil particle shape can be characterized by different parameters including sphericity ($S$), roundness($R$), regularity ($\xi$) and elongation index ($EI$) all less than unity. For a perfectly spherical grain, they become one. The definitions of these parameters are given below (Wadell 1932; Krumbein 1941; Powers 1953; Krumbein and Sloss 1963; Barrett 1980):

Sphericity – sphericity reflects the similarity of a grains length, width and height. It can be quantified as the square root of the diameter ratio of maximum inscribed circle and the minimum circumscribed circle, as shown in Fig. 5.24.

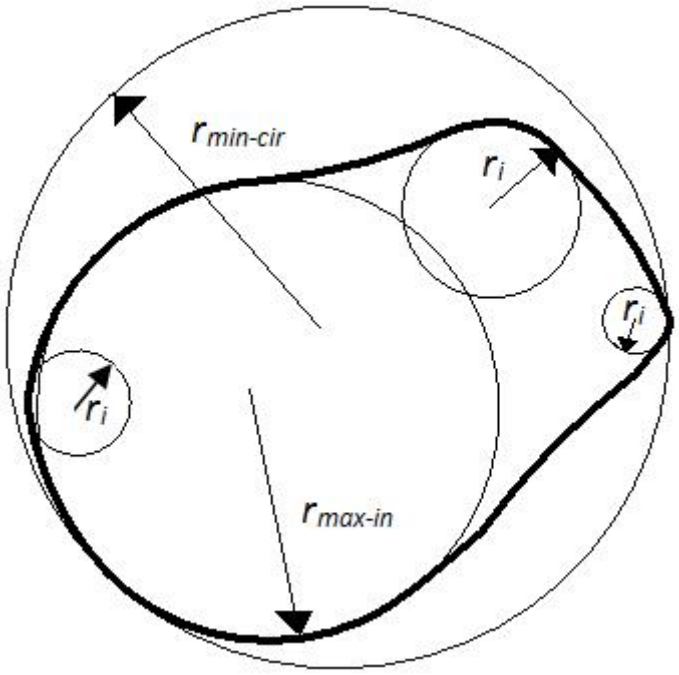


**Figure 5. 24 : Particle shape determination.**

$$\text{Sphericity, } S = \sqrt{\frac{d_{max-in}}{d_{min-cir}}} \tag{5.16}$$

where, $d_{max-in}$ = maximum /largest inscribed circle within a sand particle

$d_{max-in}$ = minimum /smallest circumscribed circle of a sand particle

Roundness- Roundness is a measure of angularity of particle corners. Roundness can be obtained by averaging the radius of corners of the particle relative to the radius of maximum inscribed circle and employing the following equation-

$$\text{Roundness, } R = \frac{\sum_{i=1}^{N} \frac{r_i}{N}}{r_{max-in}} \tag{5.17}$$

Here, $r_i$ is the radius of curvature of the of the particle corners and $N$ is the total number of inscribed circles.

Regularity is average of roundness and sphericity and is obtained by the following equation-

$$\xi = (R+S)/2 \tag{5.18}$$

Elongation index is ratio between the length of intermediate axis ($l_2$) and major axis ($l_1$) of the particle. It reflects the relationship between the two principal axes of the particle in a two dimensional image.

In this study, the particle shape parameters were determined using the definitions stated above. Images of nine sands were obtained using optical microscope. For each soil, 30 soil grains were analysed using Autodesk Inventor 2002 and *S*, *R*, $\xi$ and *EI* were obtained. Fig. 5.25 shows a photograph of the optical microscope and Fig. 5.26 shows the method of determining particle shape parameters. The particle shape parameters for the nine soils are summarized in Table 5.3.

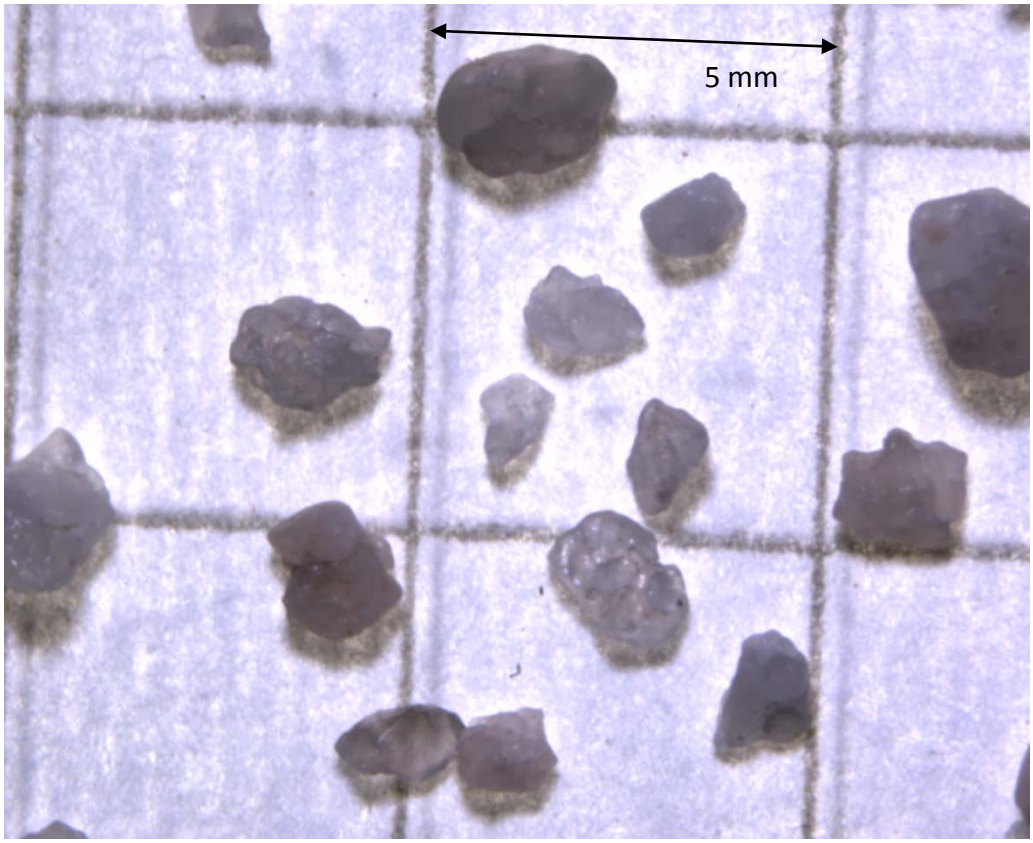


**Figure 5. 25 : Optical micro-photograph of soil 2**

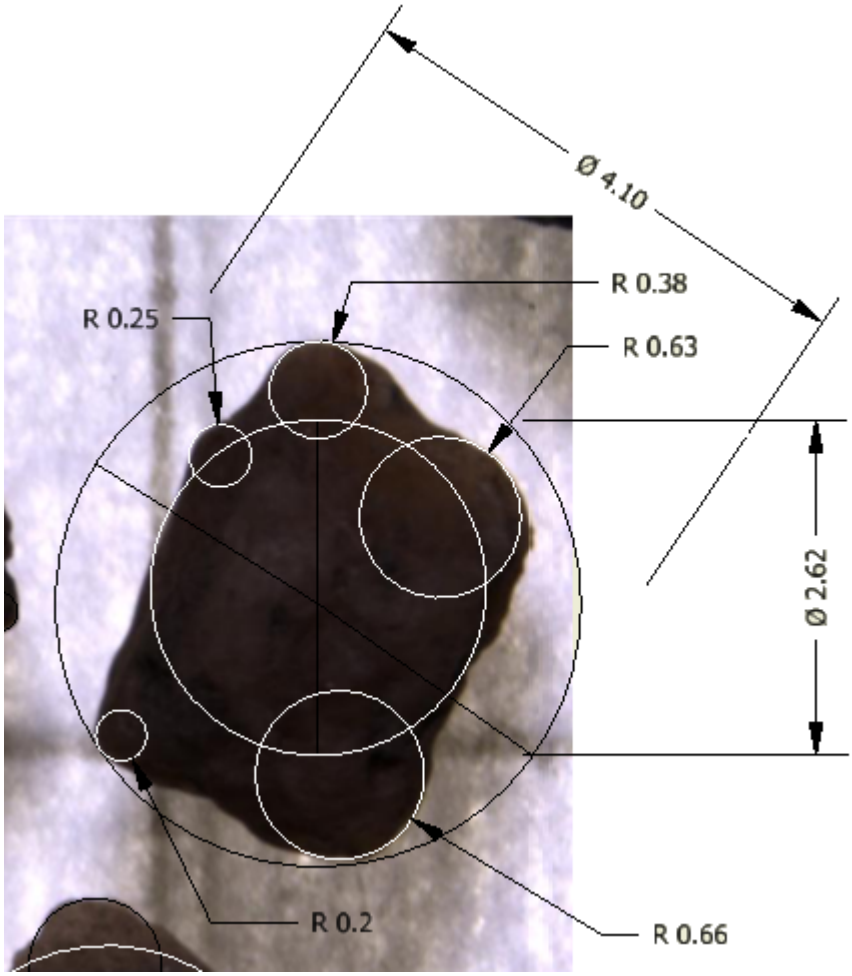


**Figure 5. 26 : Particle shape parameter determination method using Autodesk Inventor 2012**

Roundness and sphericity are important parameters in determining soil behaviour of cohesionless soils (Fatt 1958; Meady 1966; Ridgway and Rupp 1969). The physical properties which are influenced by particle sphericity and roundness are void ratio, pore size distribution, compressibility, strength and cohesion (Morris 1959; Meade 1966; Ingles and grant 1975). Effect of sphericity and roundness on angle of internal friction is well documented in the literature. Zelasko et al. (1975) suggested that decrease in sphericity increases soil angle of friction. Richards and Green (1986) and Holubec and D'Appolonia (1973) found that friction angle of spherical glass beads are much less than sands of similar particle size. Decrease in roundness also increases soil angle of friction (Zelasko et al. 1975; Norris 1977). Since decrease in sphericity and roundness increases soil friction angle, decrease in regularity also increases friction angle, as it is the average of roundness and sphericity. Increase friction angle is associated with higher soil stiffness, which means reduction in roundness and sphericity results in higher soil elastic modulus.

Table 5.3: Particle shape parameters of the nine soils used in the test

| Soil | Sphericity, $S$ | Roundness, $R$ | Regularity, $\xi$ | Elongation Index ($EI$) | | | |
|---|---|---|---|---|---|---|---|
| | | | | Maximum | Minimum | Average | Standard Deviation |
| 1 | 0.80 | 0.36 | 0.58 | 0.54 | 0.99 | 0.74 | 0.13 |
| 2 | 0.81 | 0.33 | 0.57 | 0.52 | 0.98 | 0.78 | 0.12 |
| 3 | 0.82 | 0.33 | 0.57 | 0.63 | 1.00 | 0.81 | 0.12 |
| 4 | 0.80 | 0.36 | 0.58 | 0.42 | 0.96 | 0.72 | 0.15 |
| 5 | 0.82 | 0.40 | 0.61 | 0.53 | 0.98 | 0.80 | 0.10 |
| 6 | 0.86 | 0.44 | 0.65 | 0.45 | 0.99 | 0.76 | 0.14 |
| 5a | 0.82 | 0.42 | 0.62 | 0.48 | 0.93 | 0.74 | 0.13 |
| 5b | 0.82 | 0.37 | 0.59 | 0.48 | 1.00 | 0.75 | 0.13 |
| 5c | 0.85 | 0.42 | 0.64 | 0.47 | 0.97 | 0.72 | 0.11 |

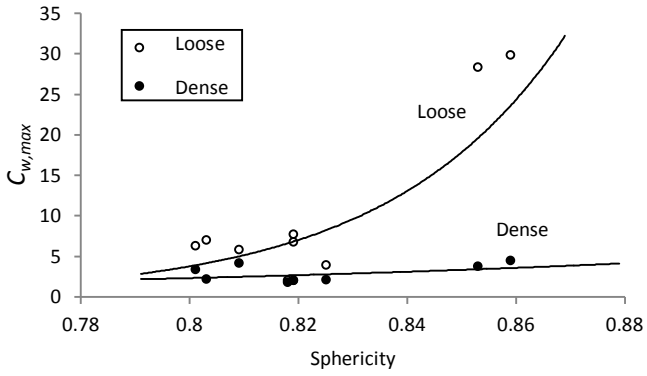


(a)

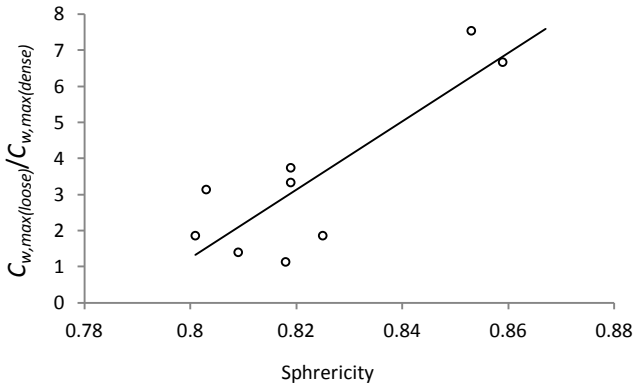


(b)

**Figure 5. 27 : Effect of sphericity on a) Cw,max in loose and dense state, b) Cw,max ratio in loose state to dense state**

The soil particle shape parameters were compared with water table correction factors obtained from small mould tests. The variation of $C_{w,max}$ in loose and dense soils with sphericity, roundness and regularity are shown in Figs. 5.27, 5.28 and 5.29, respectively. The ratio of correction factors in loose and dense sands was also compared with these parameters. The figures show that $C_{w,max}$ decreases with decreasing sphericity, roundness and regularity and rate of decline in loose sands is higher than that of dense sands. This indicates that additional settlement due to submergence is higher for soils having higher sphericity, roundness and regularity. This matches well with previous findings that lower roundness and sphericity is associated with denser and stiffer soils. Rate of increase in $C_{w,max}$ of loose sands with increasing sphericity, roundness and regularity is higher than that of dense sands, which is reflected in the plots of $C_{w,max}$ ratio verses shape parameters, as in Figs. 5.27, 5.28 and 5.29. This means that loose soils with round spherical shapes are more compressible in submerged condition.

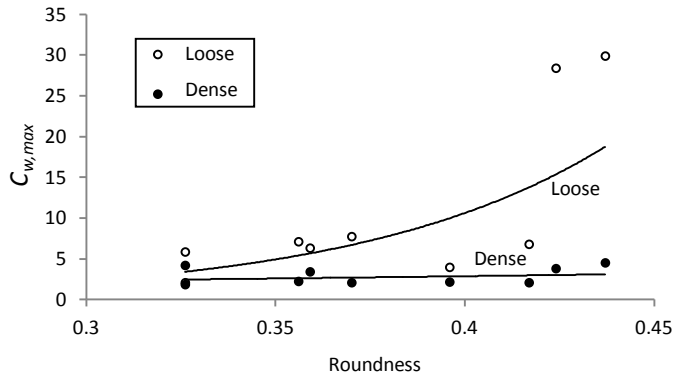


(a)

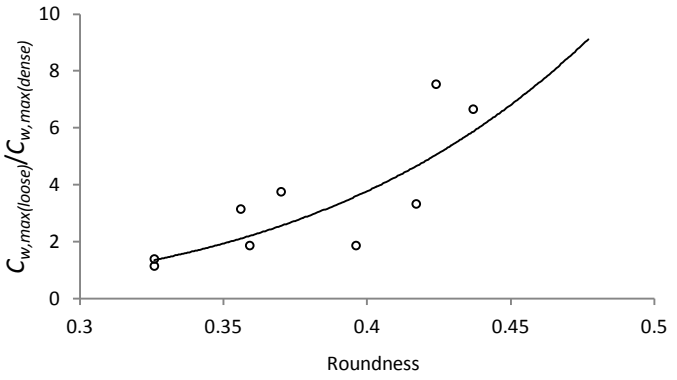


(b)

**Figure 5. 28 : Effect of roundness on a) Cw,max in loose and dense state, b) Cw,max ratio in loose state to dense state**

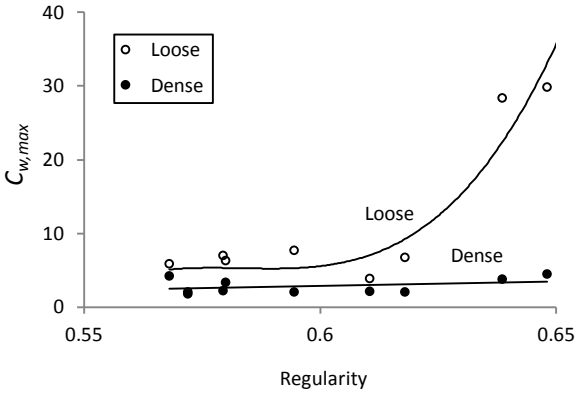


(a)

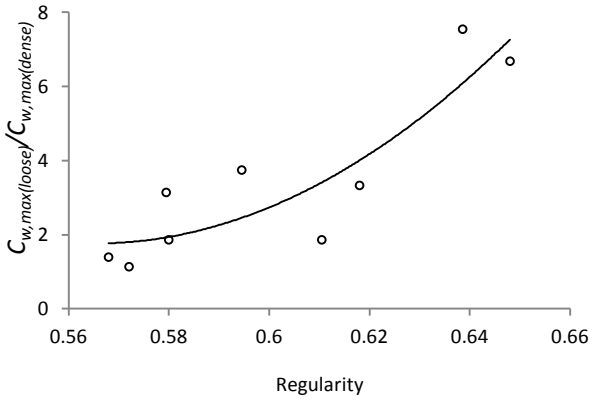


(b)

**Figure 5. 29 : Effect of regularity on a) Cw,max in loose and dense state, b) Cw,max ratio in loose state to dense state**

## 5.5 Summary and Conclusion

There are significant uncertainties associated with the predictions of settlements of shallow foundations in granular soils. This is well documented in the literature. The additional settlements produced by the rise of water table below the footing can bring in further uncertainties. Therefore, it is desirable to have some rational method for determining the additional settlements induced by the water table rise that can occur due to floods, rain fall or rise in sea level.

Model tests on a rectangular tank were carried out on square, circular and rectangular footings on sands placed at loose and dense states subjected to allowable loads. Water table was raised from the bottom of the tank to the footing level, and the additional settlements were recorded at water table depths of 0, 0.2*B*, 0.4*B*, 0.6*B*, 0.8*B*, *B*, 2*B*, 3*B*, 4*B*, 5*B* and 6*B* below the footings. It was shown that the Eq. 5.1 can effectively model the water table rise in

sands and can be used for determining the water table correction factor $C_w$ at all water table depths.

$$C_w = 1 + (C_{w,\max} - 1)\left(\frac{A_w}{A_t}\right)^n \tag{5.1}$$

It was shown that $n$ varies in a narrow range of 0.85-1.10 for loose and dense sands, and can be assumed as unity for all practical purposes, and especially as a first estimate. $C_{w,max}$ has to be determined for a specific sand. This can be determined in a smaller model since the entire sand is inundated during the test and the capillary effects do not come into play when determining $C_{w,max}$. It is also suggested that for designers wanting to use Schmertmann et al. (1978) strain influence factors can continue to use them in Eq. 5.1.

Model tests were also carried out with small moulds on nine soil samples to investigate effect of various relevant soil properties on settlement increase due to submergence. The results suggests an expression for $C_{w,max}$ in Eq. 5.13, which shows that maximum value of correction factor of any soil can be determined simply from field SPT value or from relative density and void ratio range of the soil. $C_{w,max}$ can also be used to predict correction factor for any depth of water table, by using in Eq. 5.1. Also, effect of fines content on water table correction factor was investigated which shows that $C_{w,max}$ increases significantly for granular soils containing more than 15% fines contents. Ratio of $C_{w,max}$ in loose sand to dense sand was investigated against void ratio range and volumetric strain potential which shows that the ratio increases exponentially with rising $e_{max}$-$e_{min}$ and $\epsilon_v$ value. The rational method developed from small mould tests to predict $C_{w,max}$ can be used in conjunction with the method based on settlement tank test results and will assist designers to account for future water table rise while predicting settlement of shallow footings in cohesinless soils.

# Chapter 6 Numerical Modelling of Water Table Rise in Granular Soil

## 6.1 General

Numerical modelling has become a useful tool in most branches of science and engineering. It is routinely used to solve complex problems that are difficult to model in the laboratory or to solve analytically. Numerical modelling is now widely used in geotechnical problems including ground condition analysis, seismic studies, slope stability analysis, foundation design etc. In geomechanics, numerical modelling provides the benefit of using more realistic non-linear material behaviour, fast and systematic solutions and fast parametric studies. These features result in cost reduction and optimization of geotechnical engineering problems. Various finite element and finite difference codes are being used to simulate geotechnical problems. The most commonly used software in geotechnical applications are FLAC, FLAC$^{3D}$, PLAXIS, ANSYS and ABAQUS. Usually, the selection of a geotechnical modelling software depends on factors like availability, solution approach, time and cost considerations and industry application.

There has been very little work reported in the literature on the effects of water table rise on the settlements of footings in sands. None of these considered the effect of foundation shape on additional settlement due to water table rise. There has been suggestions on the use of a water table correction factor, in the range of 1-2, that can used as a multiplier on the settlement computed for the footing on dry sands. In this Chapter, explicit finite difference code FLAC 7.0 (Itasca, 2011) and FLAC$^{3D}$ 5.0 (2012) were used to simulate the rise of ground water table in granular soil and the resulting additional settlement was studied. The numerical results were compared with the laboratory test data and the semi empirical equation developed in Chapter 5. Elastic, nonlinear elastic and elasto-plastic constitutive models were used to investigate the variation of water table correction factor with water table depth. Effect of various parameters (footing embedment depth, Poisson's ratio, finite layer thickness and layered soil system, etc.) on additional settlement due to water level rise is also discussed in this Chapter.

Characterization of stress-strain relationship and failure behaviour of granular soils are complex due to their particulate nature. This is why a number of constitutive models have been proposed in the literature to predict the behaviour of granular soils. Bathurst and

Rothenberg (1988) and Jenkins and Strack (1993) proposed constitutive relations to address the discrete particle to particle description of granular soils. On the other hand, a continuum approach that consists of macroscopic constitutive model based on plasticity theory, along with some stress dilatancy rules, is most commonly used by researchers. Some of the earlier constitutive models were proposed by Drucker et al. (1957), Roscoe et al. (1963), Poorooshasb et al. (1967), Roscoe and Burland (1968) and Lade and Kim (1988). There have been recent developments in developing constitutive models those address more complicated issues such as cyclic loading and strain localization (Vermeer, 1984; Darve,1984; Dafalias,1986).

## 6.2 Review of FLAC and FLAC$^{3D}$

Nowadays, various finite element and finite difference codes are being used to simulate geotechnical problems. FLAC, FLAC$^{3D}$, PLAXIS, ANSYS and ABAQUS are the most commonly used software in geotechnical applications. Usually, the selection of a geotechnical modelling software depends on various factors including solution approach, availability, time and cost considerations etc. In this study, FLAC and FLAC$^{3D}$ were used considering the above factors and their suitability to the research problem. FLAC (Fast Lagrangian Analysis of Continua) and FLAC$^{3D}$ are widely used explicit finite difference codes. Though they were developed originally for modelling geotechnical and mining problems, they can be also used for various civil and mechanical engineering applications. FLAC and FLAC$^{3D}$ simulate the behaviour of soil, rock or other materials where the materials are represented by a grid system. FLAC is normally used to simulate two dimensional and axisymetric problems whereas FLAC$^{3D}$ is used for modelling three dimensional cases.

It is important in geotechnical modelling to define the material behaviour when subjected to loading. It can be defined by using appropriate constitutive models. There are various built-in constitutive models in FLAC and FLAC$^{3D}$. These include linear elastic model as well as plastic models such as Mohr-Coulomb, Drucker-Prager, Modified Cam-Clay, Strain Hardening, Strain Softening etc. An important feature of FLAC and FLAC$^{3D}$ is FISH, a built-in programming language, which is used to write users own functions and to implement user-defined constitutive models.

FLAC uses the finite difference method for solving geotechnical problems. The difference between finite difference method (FDM) and finite element method (FEM) lies in the

solution scheme. An explicit, time marching solution scheme is adopted in FDM and FEM uses implicit, matrix-oriented solution scheme. An explicit solution scheme is used by FLAC for solving equations (Coetzee et al., 1998), which is achieved by time stepping. Time stepping is an iterative process where adjustments are made in each node in the mesh through a series of steps. In the explicit method, calculation of wave speed is always kept ahead of the physical wave speed that allows the equations to always function on known values fixed for the duration of calculations.

## 6.3 Numerical Modelling of water table rise in settlement tank in the laboratory

A settlement tank and a small cylindrical mould were used in laboratory modelling of shallow footings as described in Chapter 4 and 5. In this section, the model tests using settlement tank is simulated in FLAC and FLAC$^{3D}$. The schematic diagram of the settlement tank is given in Fig. 6.1. Circular, square and rectangular model footings were used in the settlement tank tests in the laboratory. Square and rectangular footings were modelled in FLAC$^{3D}$. Only a quarter of the tank was modelled in FLAC$^{3D}$ since there is symmetry between each quarter. Circular footing was modelled as an axi-symmetric problem and the strip footing was modelled as a plane strain problem using FLAC.

The vertical boundaries were assumed to be rollers that allow vertical deformation only, and restrict any horizontal deformations. The bottom boundary was fixed in both horizontal and vertical directions. Three different constitutive models, namely, linear elastic, non-linear elastic and elasto-plastic models were considered in modelling the sand behaviour. The mesh density was determined by sensitivity analysis as discussed in section 6.3.1. The FLAC code of the model is given in Appendix A1.

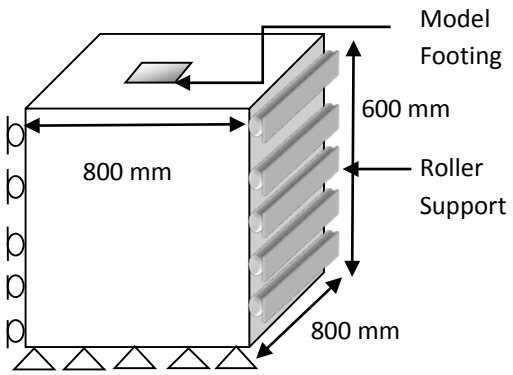


**Figure 6. 1 : Schematic diagram of the settlement tank used in laboratory test and in numerical modelling**

### 6.3.1 Sensitivity Analysis

For sensitivity analysis, the constitutive model, initial condition and boundary conditions were selected in such a way that they effectively represent the laboratory testing condition. Linear elastic model was used and the following parameters were assumed: The Young's modulus of the dry sand $E$ = 20 MPa, Poisson's ratio $\nu$ = 0.2, dry unit weight of the sand = 14.64 kN/m$^3$ (this represents dense sand). Gravitational stresses were not considered since the in situ stress has no effect on elastic settlement. Following the settlement tank test conditions, the vertical boundary was placed horizontally 4$B$ away from the centreline of the footing and the horizontal boundary was placed vertically 6$B$ away from the footing centre. Numerical modelling in FLAC with boundaries far away from the centre of footing (30$B$ away vertically and 20$B$ away horizontally from the centre) shows that 99% of the stress bulb can be contained in a boundary condition similar to the laboratory model (i.e., vertical and horizontal boundaries 4$B$ and 6$B$ away respectively from the centreline of the footing). Roller supports have been used in plane of symmetry and in vertical boundary, and pin support was used in the horizontal boundary.

To eliminate the uncertainties associated in numerical modelling, comprehensive sensitivity analysis was conducted on all important parameters. This helped to increase accuracy of the model and made it more representative to the field condition. The pressure distribution below a flexible footing due to a uniform load is assumed to be uniform if the load is concentric. Change in vertical stress due to applied pressure is high immediately below the footing, and lower stresses are observed at greater depths. It is important to take this into consideration while modelling, and stress elements (or zones) need to be smaller at the zone of higher stress concentration and vice versa. This means the mesh should be finer immediately below the footing and coarser at the far end where the stress change is negligible.

#### FLAC

While modelling circular and strip footing using FLAC, the mesh density below the footing was divided into three zones, as shown in Fig. 6.2. Each zone had different mesh density depending on the stress concentration in that zone. Zone 1 extends laterally 1$B$ away from the centre of the footing, and to a depth of 1$B$ below the footing. This is the zone with higher stress concentration and hence, the mesh size is finer in this zone. Zone 2 starts from 1$B$ away from the centre of the footing and extends to a distance of 2$B$, both vertically and

horizontally. The soil located at distance is greater than 2*B* away laterally and vertically downwards falls in zone 3 where coarser mesh is used due to relatively small stress concentration in that area.

The mesh density was established by gradually refining the grid and comparing the results. Five different sets of mesh density combination were used, namely, 16x4x1, 100x25x1, 400x100x4, 1600x400x25, and 6400x1600x100. Here, each number indicates the number of elements within a square area of 1*B* side length in the respective zone. A mesh density of 100x25x1 indicates that there are 100 elements within zone 1, 25 elements in a 1*B* x 1*B* square area of zone 2 and 1 element within a 1*B* x 1*B* square area of zone 3. Distribution of elements in mesh density combination 100x25x1is shown in Fig. 6.3

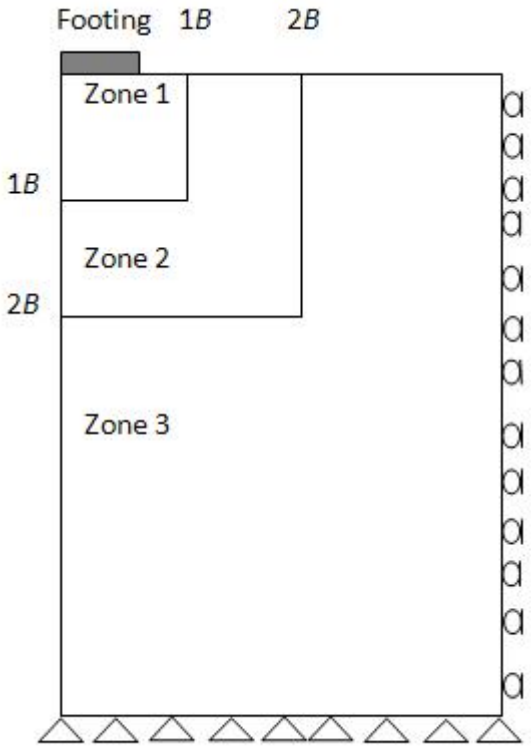


**Figure 6. 2 : Distribution of mesh density zones in FLAC**

0 0 1*B* 2*B* 3*B* 4*B*



1*B*

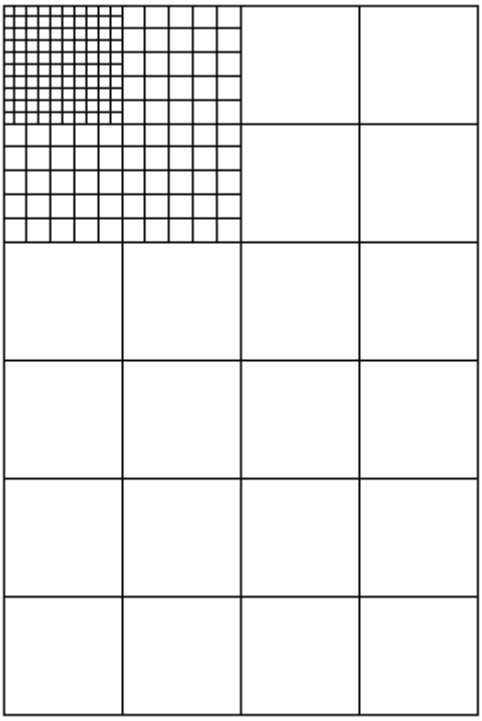

**Figure 6. 3 : Distribution of elements in 100x25x1mesh density combination**

The settlement immediately below the centre of a circular footing due to 50 kPa applied uniform pressure was investigated for various mesh density combinations and plotted in Fig. 6.4. Also, variation of vertical stresses at a depth 0.5*B* below the centreline of the footings were plotted against various mesh densities in Fig. 6.5. The results are also given in tabular form in Table 6.1. Since higher number of elements requires longer computation time and higher computer specification, optimum grid size should be selected that will have lesser elements and higher accuracy. Based on the results shown in Fig. 6.4 and Fig. 6.5, mesh combination 1600x400x25 was selected that has 3300 elements.

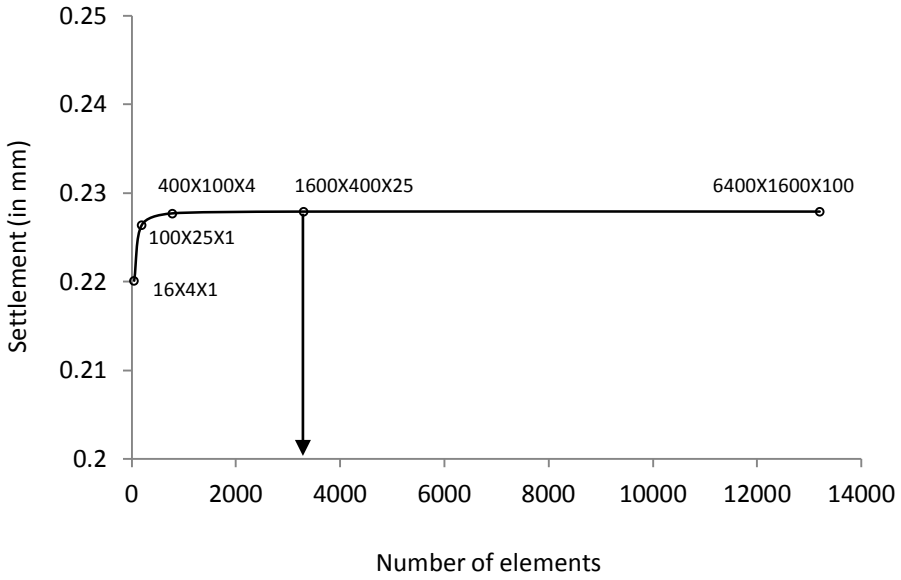


**Figure 6. 4 : Settlement at various mesh combinations**

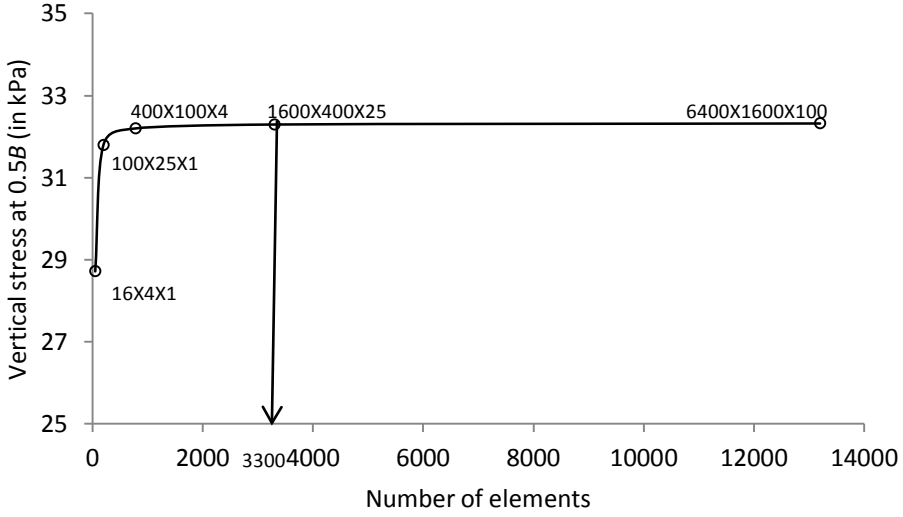


**Figure 6. 5 : Variation of vertical stress at a depth 0.5*B* below the centreline of the footing at various mesh densities.**

Table 6.1: Grid size, number of elements, vertical displacements and vertical stresses at 0.5*B* below the centre of footing in FLAC

| Grid Size | Number of Elements | Vertical Displacement (mm) | Vertical Stress at 0.5 *B* below the footing (kPa) |
|---|---|---|---|
| 16x4x1 | 48 | 0.2201 | 28.715 |

| | | | |
|---|---|---|---|
| 100x25x1 | 195 | 0.2264 | 31.79 |
| 400x100x4 | 780 | 0.2277 | 32.2 |
| **1600x400x25** | **3300** | **0.2279** | **32.295** |
| 6400x1600x100 | 13200 | 0.2279 | 32.32 |

### FLAC$^{3D}$

While modelling square and rectangular footings, the problem becomes three dimensional and FLAC$^{3D}$ was used. There are two planes of symmetry for square and rectangular footings. For ease of computation and reducing the overall computation time, only a quarter of the footing and the surrounding soil were modelled. The stress distribution pattern of shallow footings shows that most of the stress is concentrated within the depth of 2*B* below the footing base. Beyond the depth of 2*B*, the stress due to the applied load is little, and greater the depth, lower is the stress. This should be reflected properly when selecting the mesh densities for the different locations. Among the regular mesh shapes in FLAC$^{3D}$, the radially graded mesh around brick elements can be used effectively to model the shallow footing resting on ground surface and subjected to an applied pressure. There are two parts in radially graded mesh around brick shape; the brick shape will represent the higher stress concentration zone immediately below the footing, and the radially graded mesh that will represent the outer area that has lower stress concentration. The shape is shown in Fig. 6.6. The brick mesh extended to a distance of 2*B* laterally and vertically downward from the centre of the footing. A denser mesh was used in this region to account for the higher stress concentration. The radially graded mesh was made of coarser mesh size and greater the distance, the mesh size got larger.

For mesh sensitivity analysis, four different mesh densities were used and results were compared to get the optimum mesh size. The mesh sizes used were 20x10, 24x12, 32x16 and 40x20. Here, 20x10 means that there were 20 elements along the length 2*B* of the brick mesh in x, y and z direction, and 10 elements in the radially graded mesh in each direction. The vertical displacement of a rectangular footing (*B*/*L*=0.5) due an applied uniform pressure of 50 kPa was obtained for each mesh density and plotted in Fig. 6.7. The results are also tabulated in Table 6.2. It can be noted from Fig. 6.6 that the mesh combination of 32x16 gives fairly accurate result and will save computation time. This mesh size was chosen for

further analysis using FLAC$^{3D}$. Fig. 6.8 shows the stress distribution below the footing due an applied load of 10 kPA for circular and rectangular footing, obtained from FLAC and FLAC$^{3D}$.

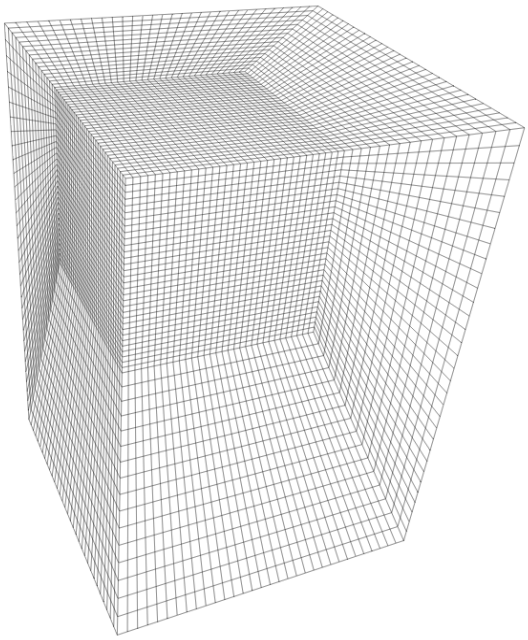

**Figure 6. 6 : Radially graded mesh around brick shape used in modelling square and rectangular footings on FLAC$^{3D}$**

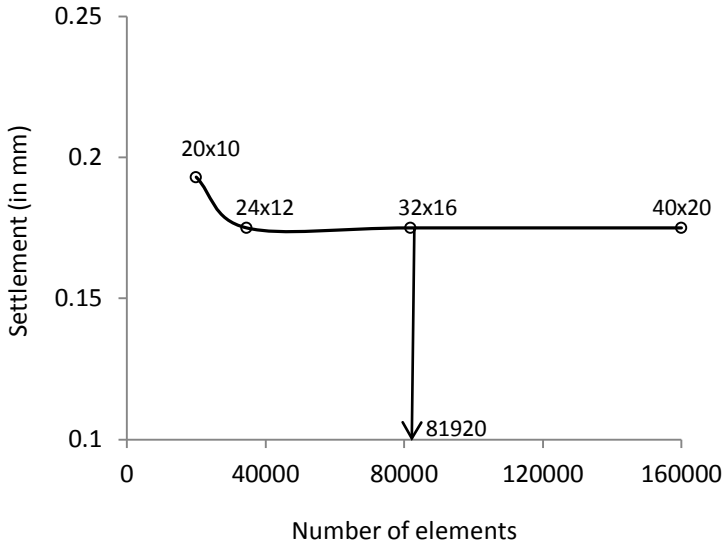


**Figure 6. 7 : Settlement at various mesh combinations**

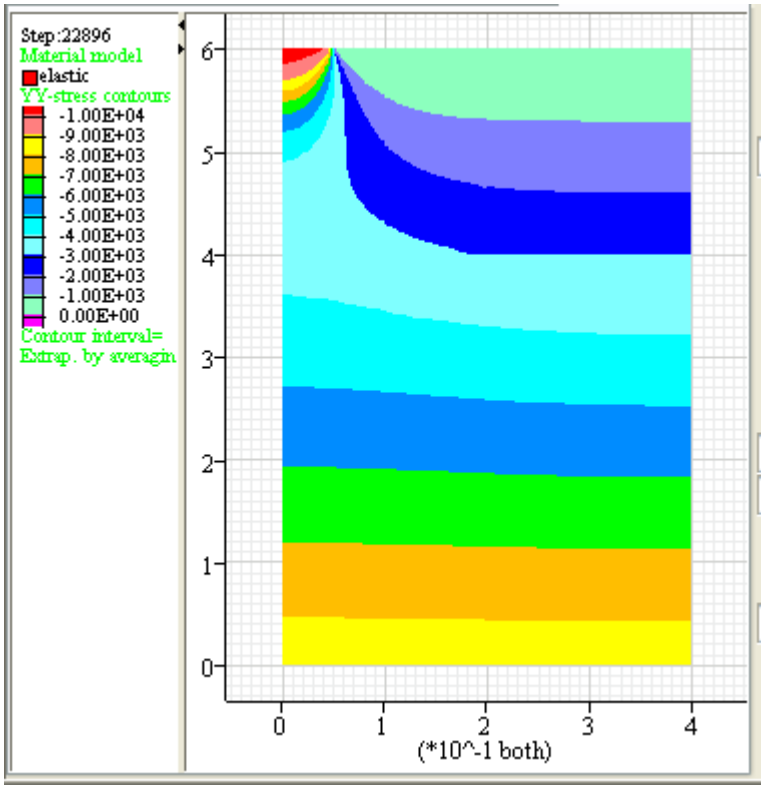


(a)

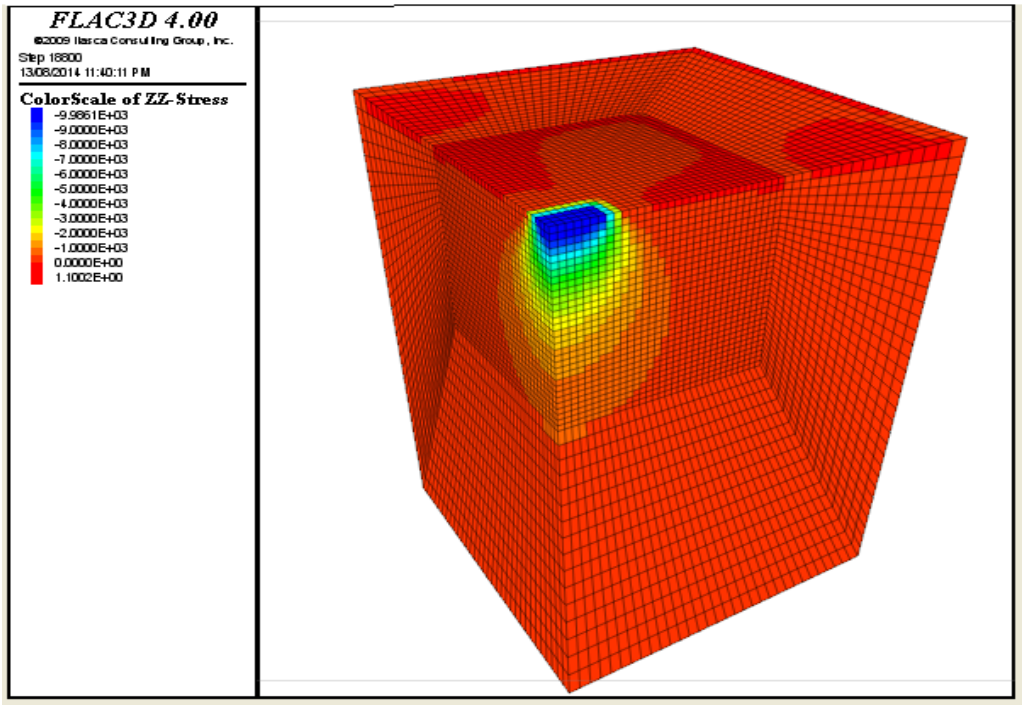


(b) for quarter of the footing

**Figure 6. 8 : Stress distribution below the footing due an applied load of 10 kPa for a) circular footing and b) rectangular footing, obtained from FLAC and FLAC3D, respectively.**

Table 6.2: Grid size, number of elements and vertical displacements of the centre of footing (footing width, $B$= 0.1m, Young's modulus = 20 MPa, Poisson's ratio, $\nu$ =0.2)

| Grid Size | Number of Elements | Vertical Displacement (mm) |
|---|---|---|
| 20x10 | 20000 | 0.193 |
| 24x12 | 34560 | 0.175 |
| **32x16** | **81920** | **0.175** |
| 40x20 | 160000 | 0.175 |

## 6.4 Comparison of Numerical and Experimental Results

The laboratory model tests using the settlement tank were modelled in FLAC and FLAC$^{3D}$ as described in the previous section. In this section, the results of numerical and experimental models are compared. Linear elastic model is used in simulation. The model relies on Hook's law of stress strain relationship. While modelling, the Young's modulus was assumed to be 5 MPa considering the lower soil stiffness in small scale footings. Terzaghi (1943) suggested that soils stiffness reduces to half in submerged sand. Hence the Young's modulus of submerged sand was taken as half of the dry sand. The Poisson's ratio for elastic continuum solutions ranges from 0.1 to 0.2 in sands, as suggested by Tatsuoka et al. (1994). Therefore, the Poisson's ratio was taken as 0.2 for the dense sands. The dry unit weight of dense soil 1 was 14.64 kN/m$^3$ in the settlement tank test and the same value was used in simulation. Fig. 6.9 (a) shows the comparison of numerical modelling results and experimental results of settlement tank test using circular footing resting on dense sand, and Fig. 6.9 (b) shows the comparison for the same footing resting on loose sand. Percentage of total additional settlement at various water level depths obtained from numerical and experimental results are plotted in the figure for loose and dense conditions. Fig. 6.10 shows the comparison of experimental and numerical results using FLAC$^{3D}$ for a rectangular footing with width to length ratio of 0.5 ($B$/$L$=0.5) resting on dense sand.

Figs. 6.9 and 6.10 show that the experimental and numerical curves are similar in shape, both in loose and dense conditions. A careful observation of the curves in Figs. 6.9 and 6.10 shows that both the experimental and numerical results indicate that rate of increment in additional

settlement with rising water level is not linear; rather, the increase is faster when the water table is in the vicinity of the foundation level. This indicates that the water table correction factor diagram should be convex upwards, which contradicts with the suggestions of some previous researchers suggesting linear variation. This also supports the experimental findings by Rekowski (2001) and Morgan et al. (2010) at James Cook University who used different settlement tank and sands for their model tests.

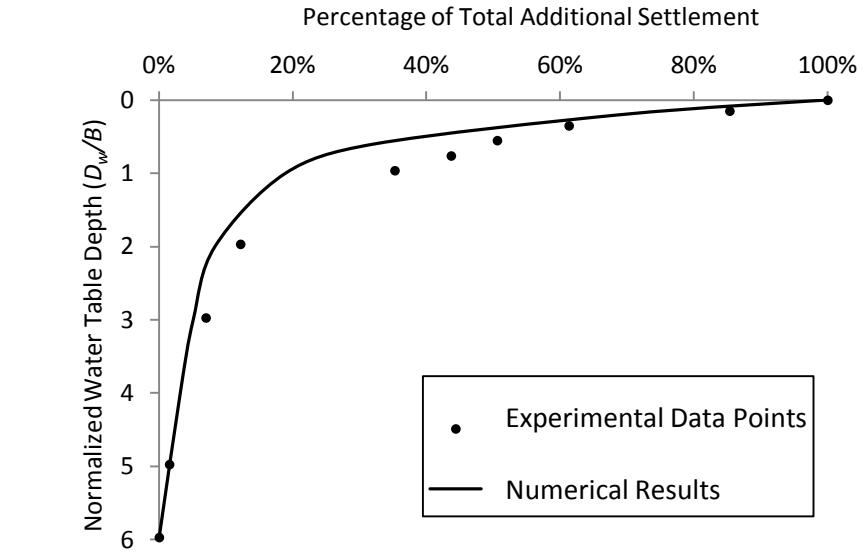


(a)

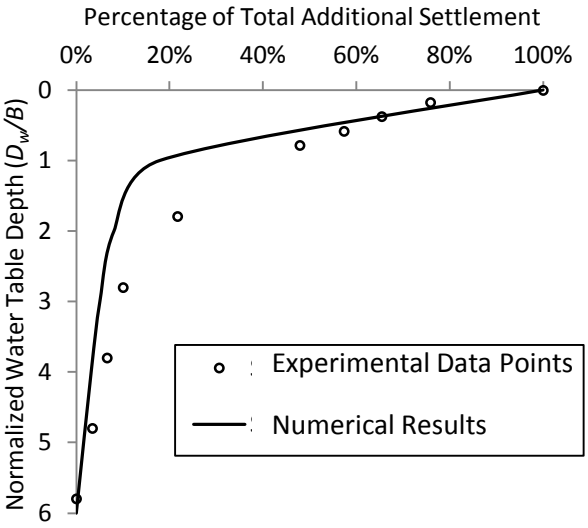


(b)

**Figure 6. 9 : : Comparison of percentage of additional settlement of circular footing at various water table depths obtained from numerical and experimental results on, a) dense sand, b) loose sand**

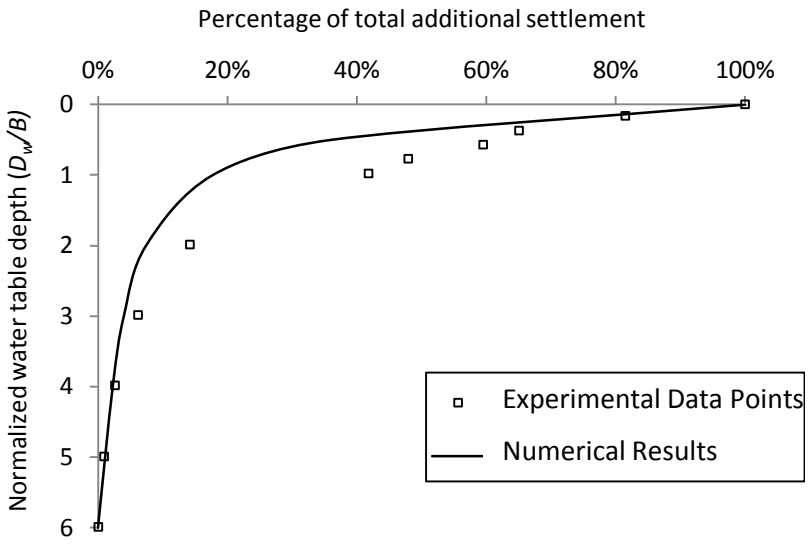


**Figure 6. 10 : Comparison of percentage of additional settlement of rectangular footing resting on dense sand at various water table depths obtained from numerical and experimental results**

The comparison of experimental and numerical results shown in Figure 6.9 and 6.10 shows that there are noticeable differences in certain zones, which might be contributed by lack of accuracy in experimental data collection, or by using less advanced constitutive soil models in numerical simulation.

## 6.5 Comparison of the numerical and experimental results with $C_w$ prediction method proposed in Chapter 5

A rational method for estimating additional settlement due to water table rise in granular soils was proposed in Chapter 5, based on the strain influence factors proposed in Chapter 3 and the experimental results obtained from settlement tank test. The method relies on a semi empirical equation of water table correction factor Cw,

$$C_w = 1 + \left(C_{w,\max} - 1\right)\left(\frac{A_w}{A_t}\right)^n \qquad \textbf{(6.1)}$$

where, $C_{w,max}$ is the maximum value of $C_w$, $A_w$ is the area of the influence factor diagram that is submerged, $A_t$ is the total area of the influence factor diagram and $n$ is a curve-fitting parameter. It was shown in section 5.2.5 that there is a good agreement between the experimental results and the proposed method. Section 6.4 Shows that numerical modelling of shallow footings subjected to water level rise using FLAC and FLAC$^{3D}$ validates the experimental results obtained from settlement tank test. It is also important to validate the

proposed method for predicting additional settlement due to water level rise with numerical results. Fig. 6.11 Shows the variation of percentage of total additional settlement with varying water table depth in circular and a rectangular footing ($B/L$=0.5), obtained from numerical modelling and by using Eq. 6.1. The experimental results from settlement tank test were also incorporated in the figure for comparison. The figure shows that the proposed water table correction factor equation is in good agreement with both the numerical modelling results and the experimental data points. A few differences between numerical, experimental results and proposed method could be resulted from less accurate data collection and use of less advanced soil models.

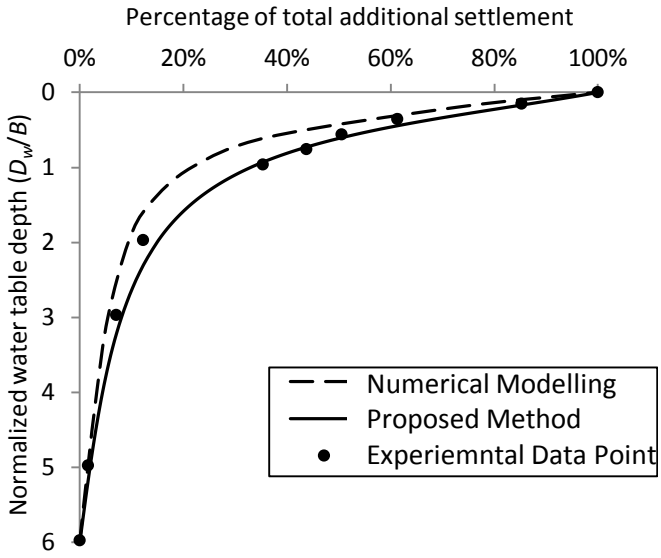


(a)

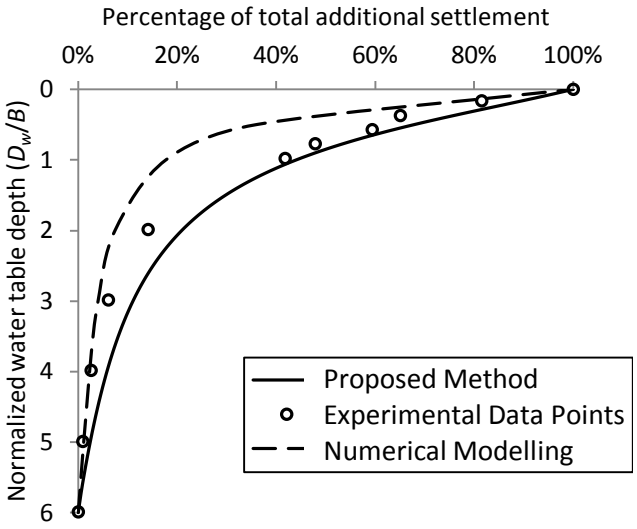


(b)

**Figure 6. 11 : Comparison of proposed method and experimental results with numerical results using FLAC and FLAC$^{3D}$ for a) circular footing, b) rectangular footing ($B/L$=0.5)**

## 6.6 Use of various constitutive models in determining $C_w$

In this study, various constitutive models were used to investigate the variation of water table correction factor with water table depth. The entire modelling was carried out using finite difference code FLAC and the following constitutive models were used to describe the soil behaviour;

a) Linear elastic
b) Hyperbolic non-linear elastic
c) Mohr-Coulomb elasto-plastic

The following parameters were assumed: The Young's modulus of the dry sand $E$ = 30 MPa, Poisson's ratio $\nu$ = 0.2, dry unit weight of the sand = 17.2 kN/m$^3$, saturated unit weight = 20.1 kN/m$^3$, and submerged unit weight of the sand = 10.3 kN/m$^3$. Based on Terzaghi's (1943) suggestion, it was assumed that the soil stiffness halves when the soil is submerged. Therefore, the modulus of the soil below the water table was reduced by 50% to 15 MPa.

Circular footing was modelled as an axi-symmetric problem and the strip footing was modelled as a plane strain problem. Footing width of 1.0 m was considered in the analysis. The vertical boundaries were assumed to be rollers that allow vertical deformation only, and

restrict any horizontal deformations. The bottom boundary was fixed in both horizontal and vertical directions.

### 6.6.1 Linear Elastic Model

Fig. 6.12 shows the variation of additional settlement when the water table rises from a depth of 8*B* below the base of a circular and strip footings. Here, the soil is assumed to be linear elastic. Additional settlements are induced when the water level reaches 4*B* below the circular footing, and 8*B* below the strip footing. The additional settlements increase at a faster rate when the water table approaches the footing level. In other words, the additional settlement produced when the water table rises from depth of 1.0*B* to 0.5*B* is significantly greater than that for the rise from 2*B* to 1.5*B*, irrespective of the shape of the footing. This is also supported by the experimental results in this study as described in Chapter 5 and also by the experimental results by Rekowski (2001) and Morgan et al. (2010). It can be seen in Fig. 2.2 that most of the current correction factors are increasing linearly with the rise of water table, and do not recognise this fact.

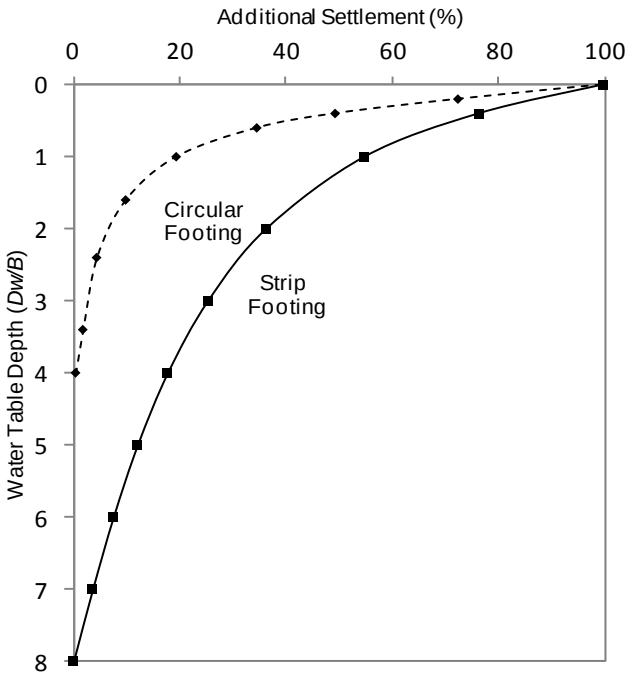


**Figure 6. 12 : Additional Settlements due to rise in water table, based on linear elastic constitutive model**

### 6.6.2 Hyperbolic Non-linear Elastic Model

In the case of linear elastic model, the soil stiffness is the same at any stress and hence the current stress level has no influence on the water table correction factor $C_w$. This is not the case with a non-linear elastic stress-strain model, where the stiffness decreases with the

increase in stresses. The hyperbolic nonlinear elastic soil model in FLAC is used to predict two important aspects of soil behaviour- nonlinearity and stress dependency. This model is based on the stress-strain relationship proposed by Kondner and Zelaska (1963):

$$(\sigma_1 - \sigma_3) = \frac{\varepsilon}{\frac{1}{E_i} + \frac{\varepsilon}{(\sigma_1 - \sigma_3)_{\max}}} \tag{6.2}$$

where: $(\sigma_1 - \sigma_3)_{\max}$ = asymptotic value of stress difference

$\varepsilon$ = axial strain

$E_i$ = initial tangent modulus which is also the slope of $\sigma - \varepsilon$ curve

While modelling, the initial tangent modulus was assumed to be 30 MPa which was reduced to half in submerged condition. The asymptotic value of stress difference is closely related to the strength of the soils and was taken as the bearing capacity of the soil. Fig. 6.13(a) shows the variation of $C_w$ against the normalised depth of water table $D_w/B$ assuming hyperbolic non-linear elastic model for a circular footing on sand with friction angle $\phi$ of $40^0$. Here, it is clear that the stress level at the base of the footing has some influence on the additional settlement, especially when the water table is in the vicinity of the footing base. With increasing stress levels, there is a slight increase in $C_w$, with the maximum value of 2.5 when the stress at the footing interface is two-third of the bearing capacity.

Fig. 3(b) shows that friction angle has some effect on the additional settlement produced by the water table rise, especially when the water table rises closer to the footing base. Denser sands give lower water table correction factors, implying that the effects of the water table rise is more pronounced in loose sands than in dense sands. At all stress levels, and for all friction angles, the water table correction factors are greater with a hyperbolic non-linear model than the linear elastic model.

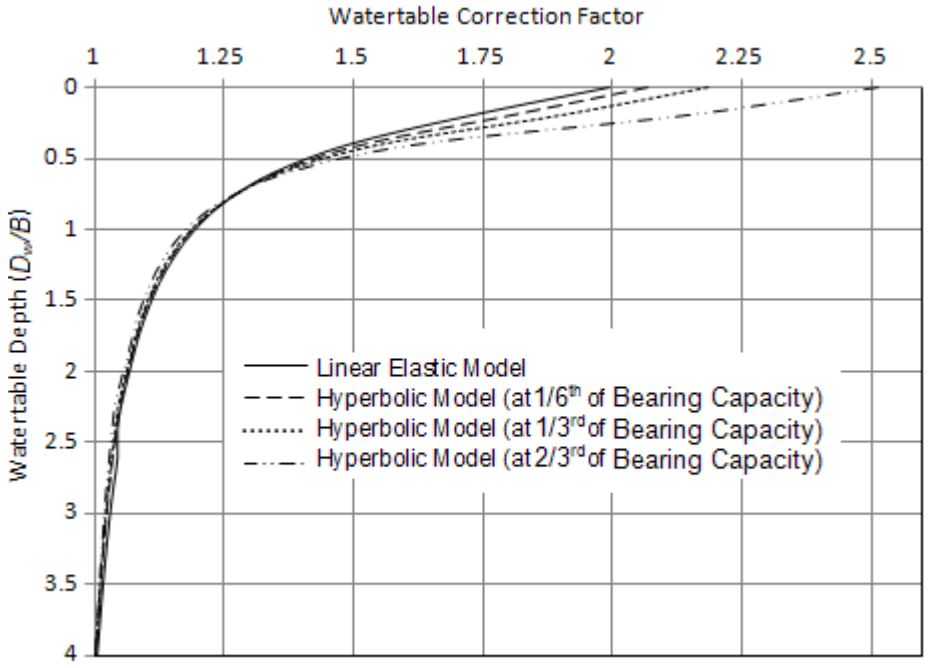


(a)

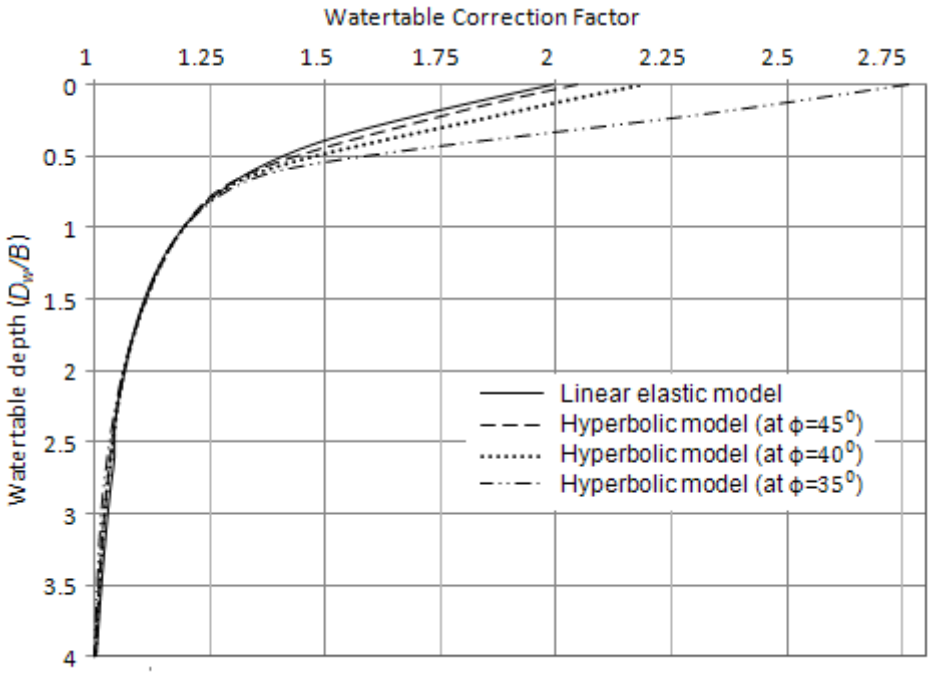


(b)

**Figure 6. 13 : $C_w$ versus $D_w$ /$B$ for a circular footing on a hyperbolic non-linear elastic medium: (a) For Φ = 40˚and different stress levels, and (b) At same applied load (150 kPa) and different friction angles**

### 6.6.3 Mohr-Coulomb Elasto-plastic Model

Along with linear elastic and non-linear elastic models, the Mohr-Coulomb elasto-plastic model was used to simulate the rise of water table below the footing and the additional settlement was observed. Fig. 6.14 shows the settlement correction for water table obtained

from three different models. A fixed set of parameters were used: The Young's modulus of the sand $E$ = 30 MPa for dry sand and 15 MPa for submerged sand, Poisson's ratio $\nu$ = 0.3, friction angle $\phi = 35^0$ , initial tangent modulus $E_i$ = 30 MPa and 15 MPa for dry and submerged sand respectively. The footing was subjected to working load for all three models. The working load is defined as the one which gives factor of safety of 3 against bearing capacity failure, which was estimated through FLAC runs. The linear elastic model gives two times settlement in saturated soil, agreeing with Terzaghi's (1943) statement. The hyperbolic soil model gives higher additional settlement than the linear elastic model. When the Mohr-Coulomb model is used, the additional settlement due to submergence is much larger, which may explain the high additional settlement found in the literature.

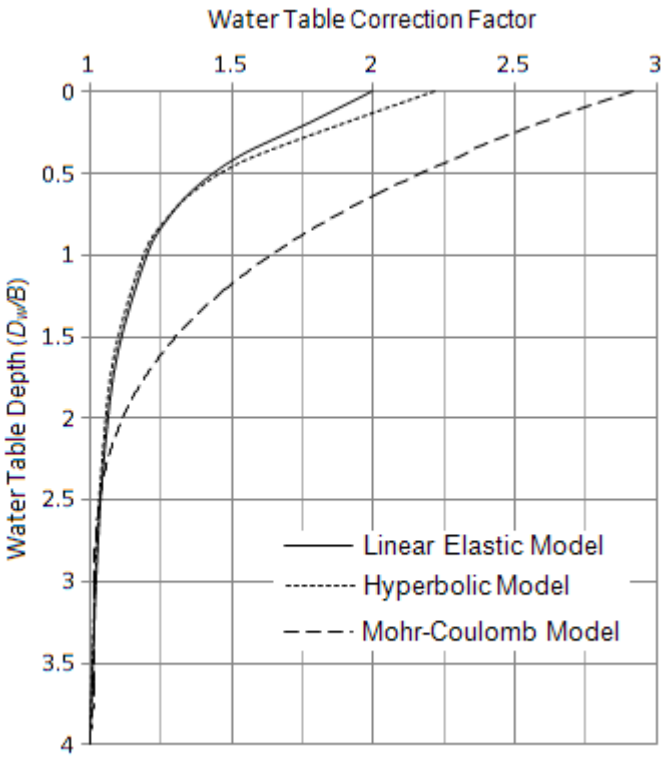


**Figure 6. 14 : Settlement corrections in circular footings for water table rise based on the three different soil models under working loads.**

### 6.6.4 Comparison of different constitutive models

Limited laboratory test data on model footings suggest that the additional settlement due to water table rise can be significantly more than what was suggested by Terzaghi. In this study, increase in the foundation settlement due to the water table rise in granular soil is investigated using various constitutive models in FLAC. Using linear elastic model shows that the settlement gets doubled in saturated soil when the water table rises to the bottom of the

foundation, irrespective of the applied pressure, agreeing with Terzaghi's suggestion [Fig. 6.15(a)]. Using hyperbolic nonlinear elastic model gives much larger additional settlements at higher stress level, agreeing better with the laboratory test data as shown in Fig. 6.15(b).

Fig. 6.16 combines the results obtained using the two elastic models and Mohr-Coulomb elasto-plastic model. The load-settlement plots for dry soil are shown in solid lines and the ones for submerged soil are shown in dashed lines. Results show that Terzaghi's intuitive reasoning is supported by linear elastic model, whereas the Mohr-Coulomb plasticity model and the hyperbolic model better describe the additional settlement value observed in laboratory tests. In reality, the stress-strain behaviour of soil is not linear elastic over the complete range of loading. At higher stress, the nonlinear models can be more suitable to explain the high additional settlement due to submergence found in the literature. The nonlinear elastic soil model accounts for the effects of stress level, soil strength and stiffness on the watertable correction factor, so it can be more suitable to be used for practical design. For all models, significant additional settlement due to water table rise was observed when the water level is closer to the footing.

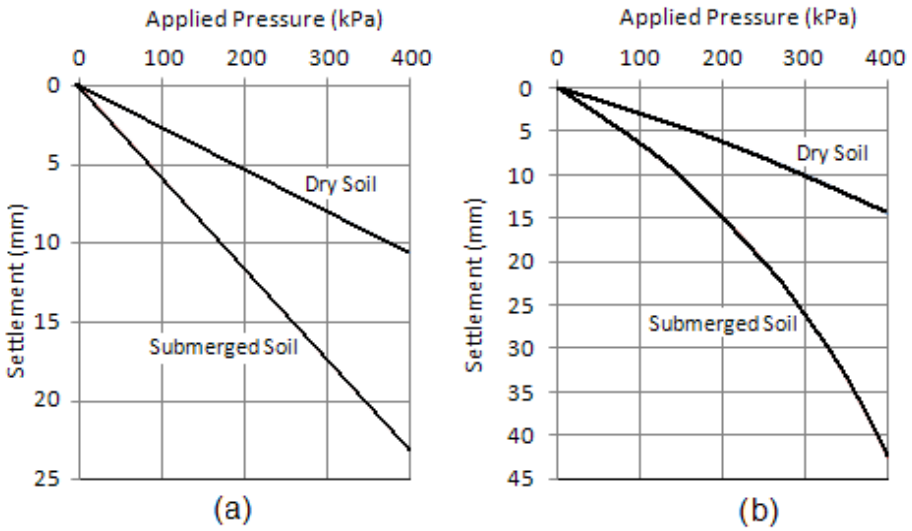


**Figure 6. 15 : Settlement in dry and submerged soil in (a) elastic medium, and (b) hyperbolic soil model (Young's modulus of the dry sand *E* = 20 MPa, Poisson's ratio = 0.2, dry unit weight of the sand = 17.2 kN/m$^3$, saturated unit weight = 20.1 kN/m$^3$, and submerged unit weight of the sand = 10.3 kN/m$^3$)**

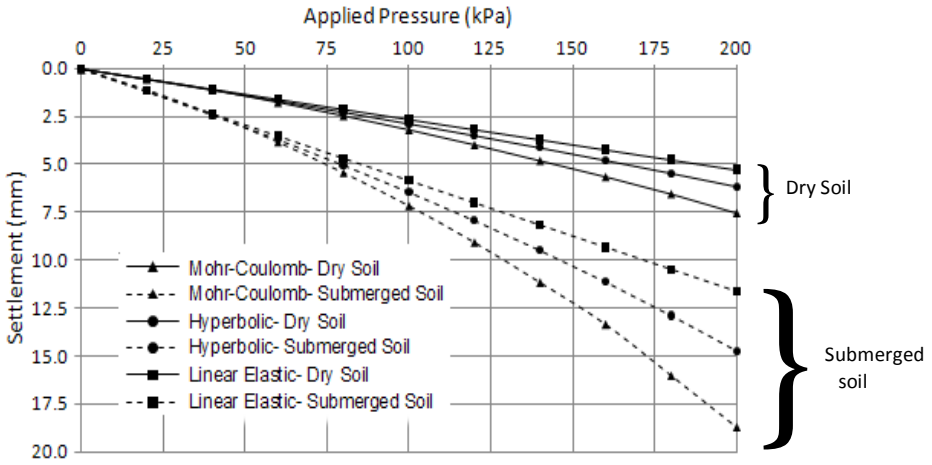


**Figure 6. 16 : Applied pressure vs. settlement curve for different models in dry and submerged condition based on three different constitutive models**

## 6.7 Effect of various parameters on water table correction factor

Settlement of a shallow footing resting on granular soil depends on various contributing factors. These factors also might affect the additional settlement due to water level rise. It is difficult to investigate all these factors and their effect on additional settlement in the laboratory. Numerical modelling can be a useful tool in studying the effect of these factors on water table correction factor. In this study, various parameters i.e., embedment depth, Poisson's ratio, finite layer thickness, layered soil profile, Gibson soil profile were investigated to quantify their effect on additional settlement due to submergence.

### 6.7.1 Effect of embedment depth

Depth of embedment ($D_f$) of a foundation can affect the additional settlement due to water table rise and it has been addressed by various researchers (Teng 1962; Bazaraa 1967; Peck et al. 1974; Bowles 1977; NAVFAC 1982). The variation of water table correction factor with varying embedment depth proposed by various researchers has been discussed in Chapter 2. In this study, effect of $D_f$ on additional settlement due to water level rise is investigated using numerical modelling in FLAC. Burland (1970) proposed a technique for numerical modelling of embedded foundations. He suggested that the actual loading situation of an embedded circular footing can be represented by applying uniform circular load at base of unlined shaft. This provides more realistic evaluation of the loading condition (Mayne and Poulos, 1999). This study used Burland's (1970) modelling principle and an unlined shaft was modelled where the load was applied at the base of the footing.

In this study, water table rise was simulated at three different embedment depths, $D_f$=0, 0.6$B$ and $B$. To be considered as shallow foundation, $D_f$ should be less than foundation width $B$

(Das and Sivakugan, 2010). Hence, the study was limited for maximum value of embedment depth equal to *B*. A circular footing was modelled using linear elastic model in FLAC. The footing diameter was taken as 1.0 meter and the horizontal and vertical boundaries were kept 6*B* and 4*B* away from the centre of the footing. For consistency, parameters used in the modelling were kept the same as previous models (i.e., Young's modulus of the dry sand $E$ = 20 MPa, Poisson's ratio $\nu$ = 0.2, dry unit weight of the sand = 17.2 kN/m$^3$, saturated unit weight = 20.1 kN/m$^3$, and submerged unit weight of the sand = 10.3 kN/m$^3$). 100 kPa uniform pressure was applied at the base of the footing and water level rise was simulated by reducing the Young's modulus of submerged soil as half of that of the dry soil. Water table correction factor at varying water table depth was obtained by comparing the additional settlement with settlement in dry conditions and the results are plotted in Fig. 6.17. For footings resting on the ground surface (i.e., $D_f$ = 0), $C_w$ for water level at the base of the footing is two, if linear elastic model is used. Numerical results suggest that $C_w$ for water level at the base of the footing is 1.92 if $D_f$=0.6*B*, and 1.85 if $D_f$=*B*. As the water level rises above the footing level, the correction factor increases and becomes two when the water level reaches the ground surface.

The results are then compared with the correction factor diagrams previously proposed by other researchers. Fig. 6.18 compares variation of $C_w$ with normalized water table depth at $D_f$ =*B*. The figure shows that unlike the diagrams proposed by other researchers, the additional settlement due to water level rise increases at a slower rate once the water level rises above the footing base.

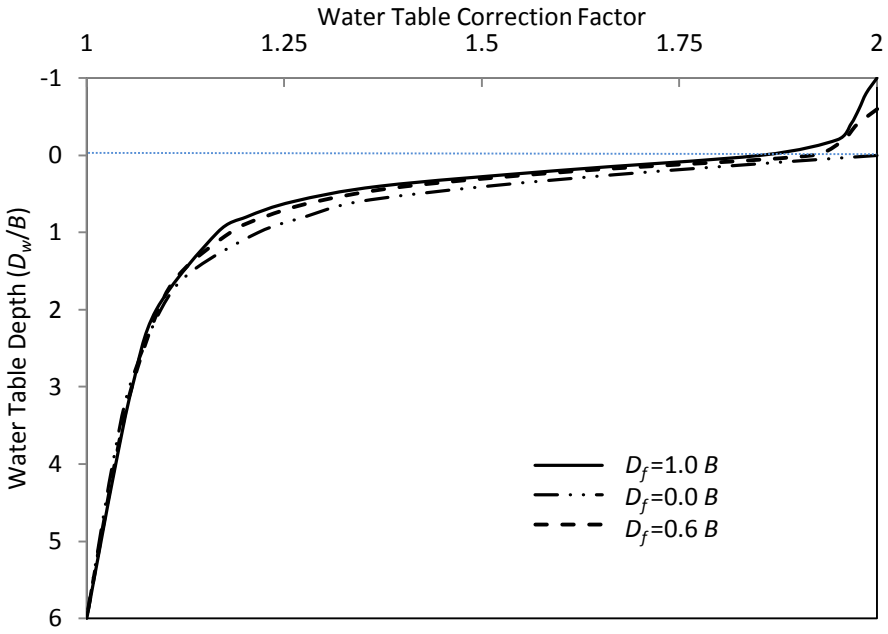


**Figure 6. 17 : Variation of water table correction factor with normalized water table depth at different embedment depths**

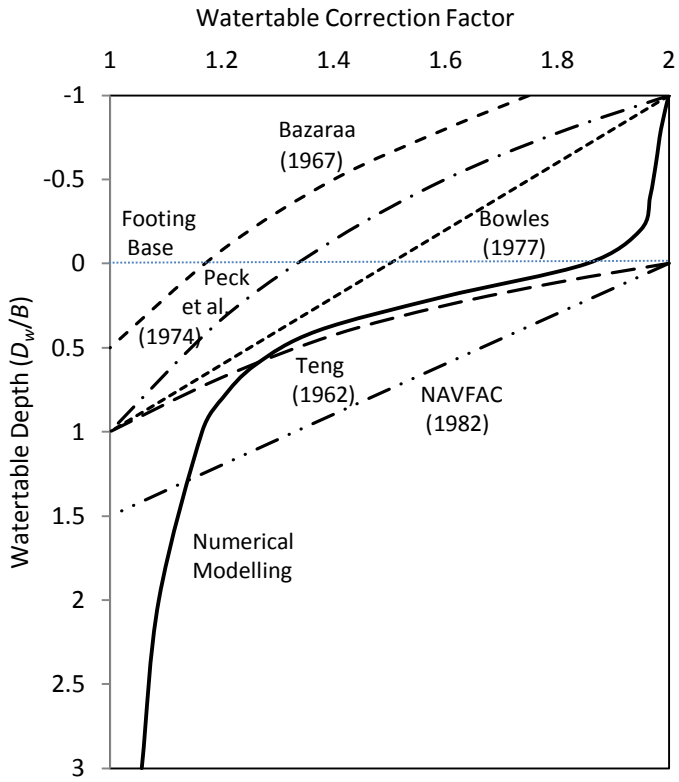


**Figure 6. 18 : Variation of $C_w$ with normalized water table depth at $D_f$ =$B$, based on numerical results and works by other researchers.**

### 6.7.2 Effect of Poisson's ratio

Poisson's ratio is an important soil parameter in predicting the pressure-settlement behaviour of shallow footings on granular soils. It is important to investigate the effect of variation of

Poisson's ratio on additional settlement of shallow footings due to water level rise on granular soils. The drained value of Poisson's ratio is usually taken in the range of 0.25-0.45. However, recent studies show that the drained value of Poisson's ratio corresponding to foundation settlement is significantly less than what was once believed (Mayne and Poulos 1999). Difficulties involved in laboratory triaxial testing (for example, capping problems, seating errors, non-uniformity of stress etc.) gives higher value of Poisson's ratio, ranging from 0.25-0.45 (Lo Presti1995). Accurate measurements are possible these days by mounting local strain devices at midlevel of soil specimen and measuring strain internally (Tatsuoka and Shibuya 1992). Experimental findings from Tatsuoka et al. (1994) showed that drained Poisson's ratio value for elastic continuum solutions ranges from 0.1 to 0.2 in sands. In this study, Poisson's ratio value was taken as 0.1 for loose sands and 0.2 for dense sands while using linear elastic model in FLAC.

Effect of Poisson's ratio on strain influence factor was discussed in section 3.3.2 which showed that the variation of Poisson's ratio affects the strain influence factor diagram for up to a depth of 0.5$B$ below the footing with negligible effect at 0.5$B$ – 6$B$ below the footing. The influence factor diagram was used in Eq. 5.4 where $A_{w}/A_{t}$ was obtained by comparing the area of influence factor diagram that is submerged to the area of total influence factor diagram. This study investigates the effect of Poisson's ratio on $A_{w}/A_{t}$ diagram and hence its effect on water table correction factor. In this study, a circular footing was modelled using linear elastic model in FLAC. The horizontal and vertical boundaries were kept at 6$B$ and 4$B$ away from the footing centre, respectively. Poisson's ratio, $\nu$ = 0.1 and 0.2 was used. The other parameters used were the same as those used in section 6.7.1. From the numerical results, $A_{w}/A_{t}$ at different value of $\nu$ was calculated and plotted against the normalized water table depth, as shown in Fig. 6.19. The figure shows that variation of Poisson's ratio has little effect on $A_{w}/A_{t}$ and hence, on the water table correction factor $C_{w}$ especially when the Poisson's ratio range is considered to be in between 0.1 and 0.2.

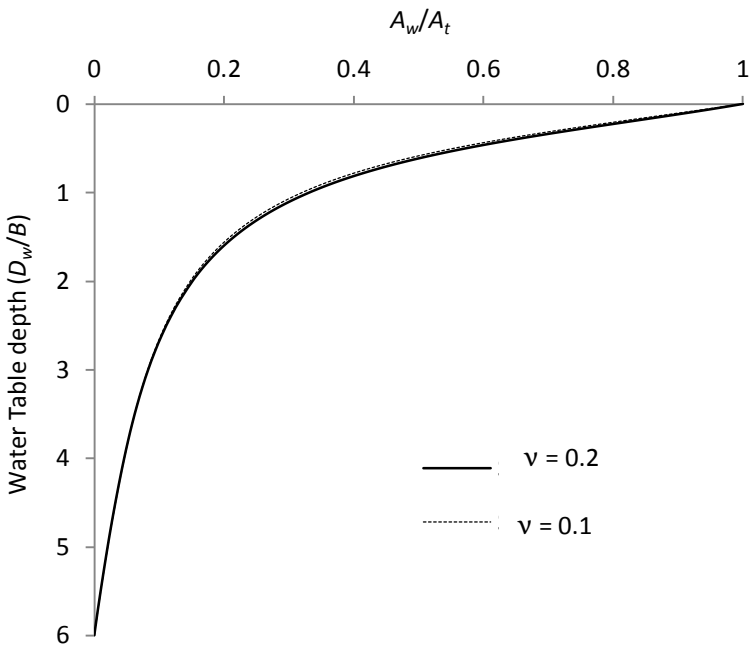


**Figure 6. 19 : Variation of $A_w/A_t$ with water table depth at various Poisson's ratio**

### 6.7.3 Effect of finite layer thickness

Mayne and Poulos (1999) suggested that if a soil mass is underlain by an incompressible stratum, the displacement influence factor of a footing resting on the soil is affected by the depth of thickness of the soil mass ($h_f$). It is important to investigate the effect of finite layer thickness on additional settlement due to water table rise within the soil layer. In this study, the effect of variations of $h_f$ on $C_w$ were investigated by simulating the water level rise on granular soil mass of varying finite layer thickness. A circular footing was modelled using linear elastic model in FLAC and the parameters used were the same as those used in section 6.7.2. Finite layer thickness $h_f$ = 0.5 B, 1*B*, 2*B*, 3*B*, 5*B*, 10*B*, 15*B*, 20*B*, 25*B* and 30*B* was modelled in the study. The $A_w/A_t$ diagram for each finite layer thickness was obtained by comparing the area of influence factor diagram that is below the water level to the total area of influence factor diagram that is above the incompressible layer. Figure 6.20 shows the schematic diagram of influence factor and $A_w/A_t$ where a finite compressible layer is underlain by an incompressible stratum.

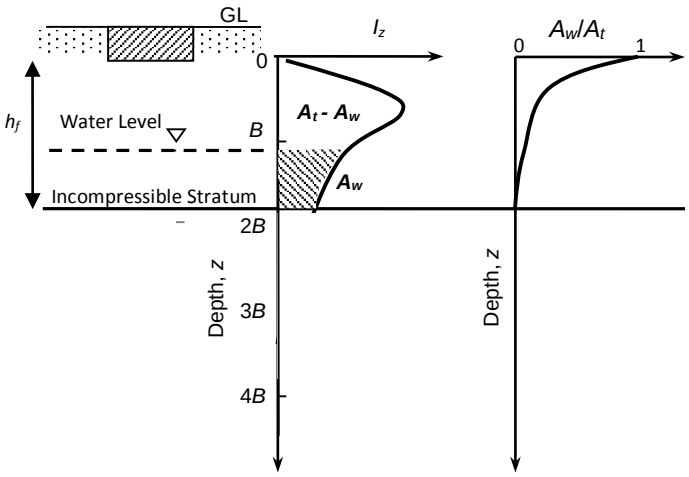


**Figure 6. 20 : Schematic diagram of Influence factor diagram and $A_w/A_t$ diagram for a footing resting on a soil underlain by an incompressible stratum.**

Variation of $A_w/A_t$ plot against the normalized water table depth at different finite layer thickness is shown in Fig. 6.21. The plots indicate that $A_w/A_t$ can be significantly influenced by the thickness of the finite layer. For example, when the water table is at a depth of $2B$, $A_w/A_t$ is 0.074, 0.13 and 0.16 for $h_f = 3B$, $5B$ and $10B$, respectively. $A_w/A_t$ value is important in determining $C_w$ by using Eq. 5.4, and influence of $h_f$ on $A_w/A_t$ indicates that the water table correction factor is influenced by the thickness of the finite compressible layer.

Since the effect of finite compressible layer thickness of water table correction factor is identified, it is important to modify Eq. 5.4 so that the effect of $h_f$ is incorporated into the correction factor calculation. Based on several curve fitting trials, the following equation is proposed to replace $A_w/A_t$ of Eq. 5.4,

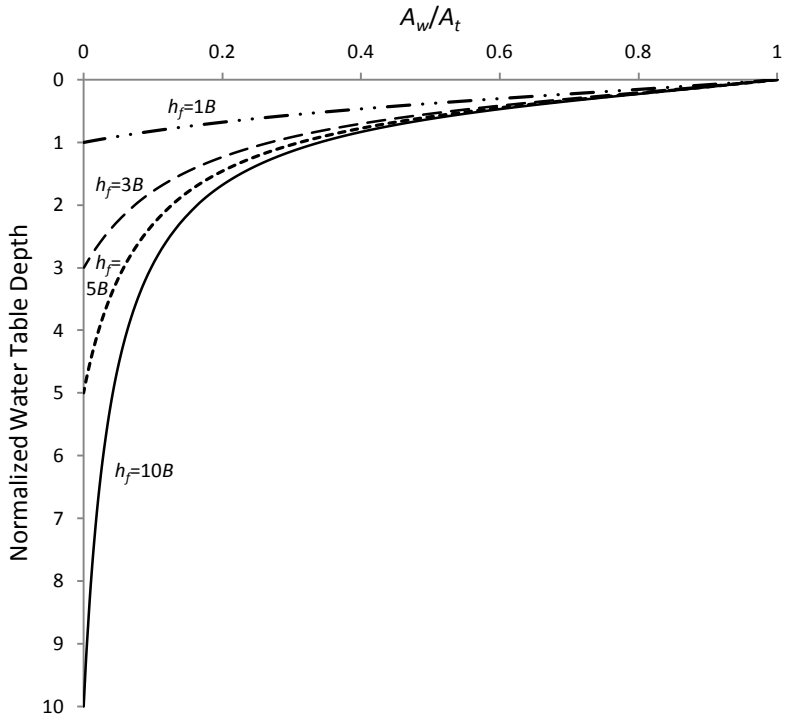


**Figure 6. 21 : Variation of $A_w/A_t$ plot against the normalized water table depth at various values of $h_f$**

$$A_w/A_t = e^{-[C_1*(D_w/B)]^{C_2}} \tag{6.3}$$

Where, $A_w/A_t$= ratio of area of influence factor diagram that is below the water level to the total area of influence factor diagram that is above the incompressible layer, $D_w/B$= normalized water table depth, $C_1$ and $C_2$ are correlation factors used to incorporate the effect of $h_f$ on $C_w$. So, Eq. 5.4 becomes,

$$C_w = 1 + (C_{w,\max} - 1)e^{-[C_1*(D_w/B)]^{C_2}} \tag{6.4}$$

This equation accounts for the water table depth as well as the effect of finite layer thickness on water table correction factor. Correlation factor $C_1$ and $C_2$ can be obtained from Fig. 6.22. Fig. 6.23 compares the correction factor diagram obtained from numerical modelling results and Eq. 6.2 and shows that there is a good agreement between the two.

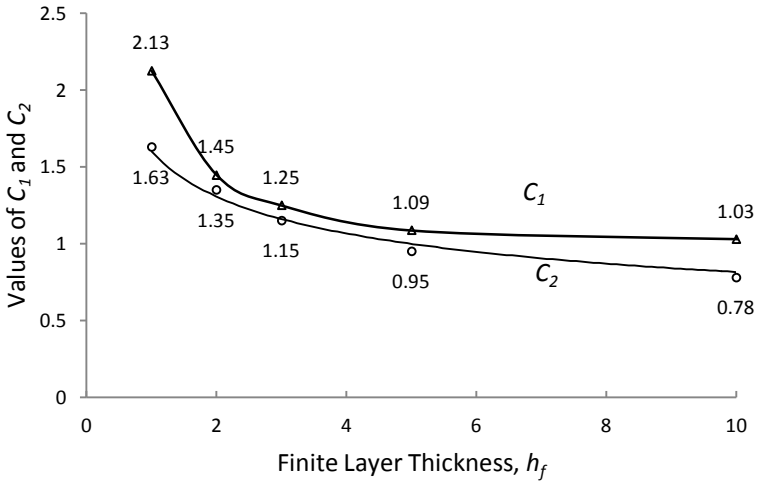


**Figure 6. 22 : Variation of $C_1$ and $C_2$ with $h_f$**

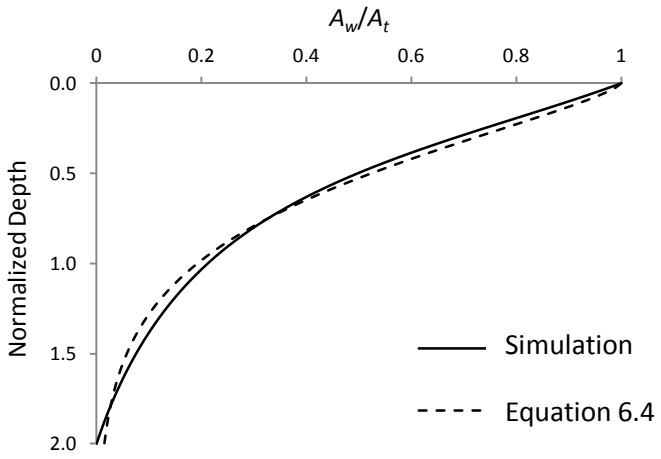


(a)

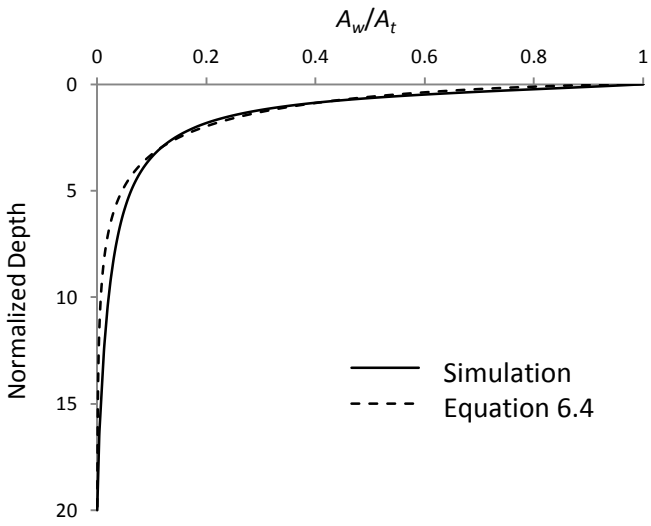


(b)

**Figure 6. 23 : Validation of Eq. 6.4 with numerical modelling results at, a) $h_f = 2B$ and b) $h_f = 10B$**

### 6.7.4 Effect of layered soil profile

Usually, the immediate settlement of a shallow footing resting on granular soils are calculated using theory of elasticity assuming that the footing is placed on a homogeneous elastic medium. In practice, soil mass is not uniform in most cases and there might be two or more different layers of soils those vary with each other in terms of soil types, stiffness and deformation characteristics. The effect of layered soil system on foundation settlement has been discussed in literature (Mayne and Poulos 1999; Razouki and Al-Zubaidy 2010). It is also important to investigate the effect of layered soil profile on the additional settlement occurring by rise in water level. In this section, a simple analytical expression is developed to account for the presence of layered soil profile beneath the footing and its effect on water table correction factor, $C_w$. This was then verified by numerical modelling and laboratory model tests.

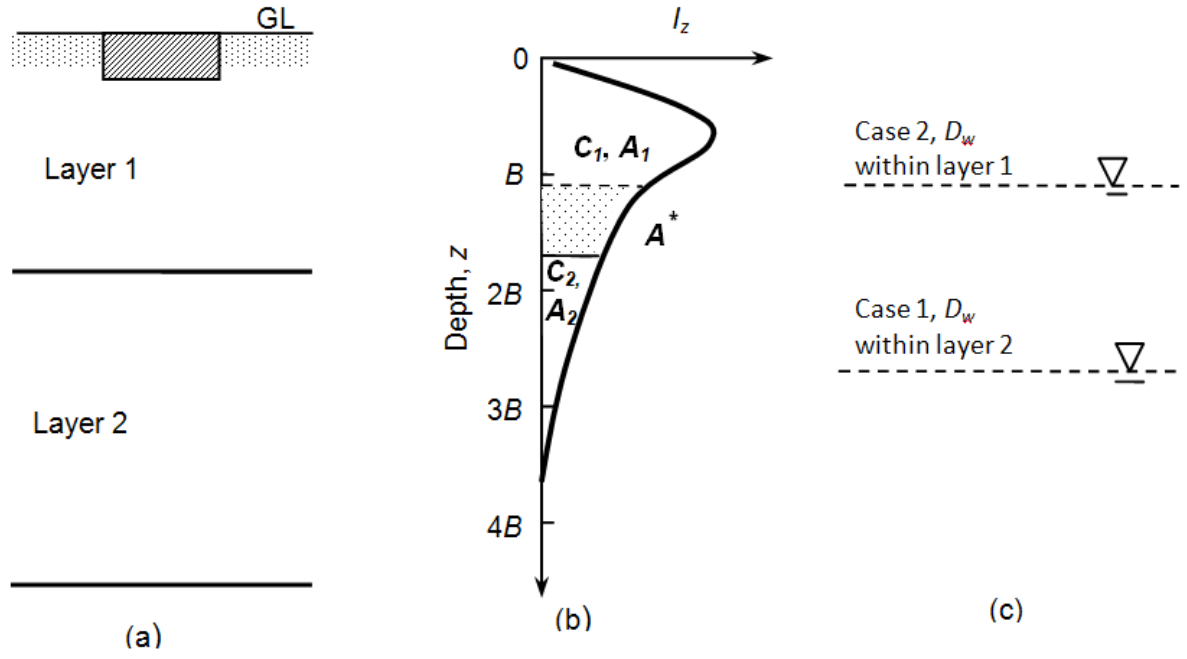


**Figure 6. 24 : Schematic diagram of a two layered soil profile**

The simplest case of a two-layer system was considered in developing the analytical expression. Fig. 6.24(a) shows that the soil below the footing consists of two different layers of granular soils. If it is assumed that the ground water level was initially well below the strain influence zone, two different cases come into consideration in determining additional settlement when the water level rises into the influence zone, case1- when the water level after the rise is within the bottom layer, case 2- when the raised water level is within the upper layer (Fig. 6.24c). Since the soil profile consists of two different types of granular soils,

different maximum values of water table correction factor were assumed for the two layers, namely, $C_1$ for layer 1 and $C_2$ for layer 2 (As shown in Fig. 6.24b). The area of influence factor diagram that is contained within layer 1 can be termed as $A_1$, and the area contained by layer 2 can be termed as $A_2$. For case 2, where the raised water level is in the upper layer, the term $A^*$ refers to the area of influence factor diagram that is submerged and contained within layer 1.

The semi empirical equation for water table correction factor was given in Chapter 5 that was developed from experimental results and strain influence factor diagram,

$$C_w = 1 + (C_{w,\max} - 1)\frac{A_w}{A_t} \tag{5.4}$$

A modified version of Eq. 5.4 is proposed below for two different cases in a two layered soil profile.

### *Case 1, raised water level is within bottom layer*

When the water level after the rise is below the upper layer, only the correction factor of the soil in the bottom layer comes into consideration. Hence, Eq. 5.4 becomes,

$$C_w = 1 + (C_2 - 1)\frac{A_w}{A_t} \tag{6.5}$$

Here, $C_2$ is the maximum value of water level correction factor for the soil in layer 2.

### *Case 2, raised water level is within upper layer*

If the water level rises beyond layer 2 and the raised water level is within layer 1, Eq. 5.4 becomes,

$$C_w = 1 + (C_2 - 1)\frac{A_2}{A_t} + (C_1 - 1)\frac{A^*}{A_t} \tag{6.6}$$

Here, $A^*$= area of influence factor diagram that is submerged and contained within upper layer. This means, $A^* = A_w - A_2$

Here, the second term accounts for the additional settlement occurred in the bottom layer and the third term accounts for the additional settlement due to rise of water level within the upper layer.

When water level rises to the footing base, $A^*$ becomes $A_1$, and $A_w = A_t$. Putting $A^* = A_1$ in Eq. 6.6 and rearranging gives,

$$C_w = C_{w,\max} = \frac{C_1 A_1 + C_2 A_2}{A_1 + A_2} \tag{6.7}$$

### *Validation of proposed expression for a two layer profile*

The expressions in Eq. 6.5, 6.6 and 6.7 can be validated by numerical simulation and laboratory model tests. In this study, FLAC was used to model a circular footing resting on a two layer soil profile. Settlement of the footing at varying water level was obtained and was compared with the analytical expression. Also, an experimental setup similar to the small cylindrical mould test (described in Chapter 4) was used with two layer soil system and the experimental results were compared with the proposed expression.

Firstly, a circular footing was modelled in FLAC that is resting on a two layer soil profile. Linear elastic model was used. Maximum water table correction factor for the upper layer $C_1$ was taken as 8 and for bottom layer $C_2$ as 2. The upper layer extends to a depth of $2B$ below the footing level. For numerical modelling, the Young's modulus of each soil layer was assumed using Eq. 5.13 that relates maximum water table correction factor with SPT number. Leonards (1986) suggested that the soil Young's modulus (in kg/cm$^2$) is eight times the blow count from a standard penetration test. Using this relationship in Eq. 5.13 gives,

$$C_{w,\max} = 67.62 * (E)^{-0.57} \tag{6.8}$$

where, $E$= Soil Young's modulus (in kg/cm$^2$)

Eq. 6.8 can be rearranged to the following,

$$E = e^{\left(\frac{4.214 - \ln C_{w,\max}}{0.57}\right)} \tag{6.9}$$

Eq. 6.9 was used to get Young's modulus of the soil layers. Rise of water level was modelled in FLAC by reducing the soil Young's modulus to half for the submerged soil following Terzaghi's (1943) suggestion. Fig. 6.25 compares numerical results and proposed analytical method for a two layer system. The figure shows that there is a good agreement between the numerical results and the proposed method.

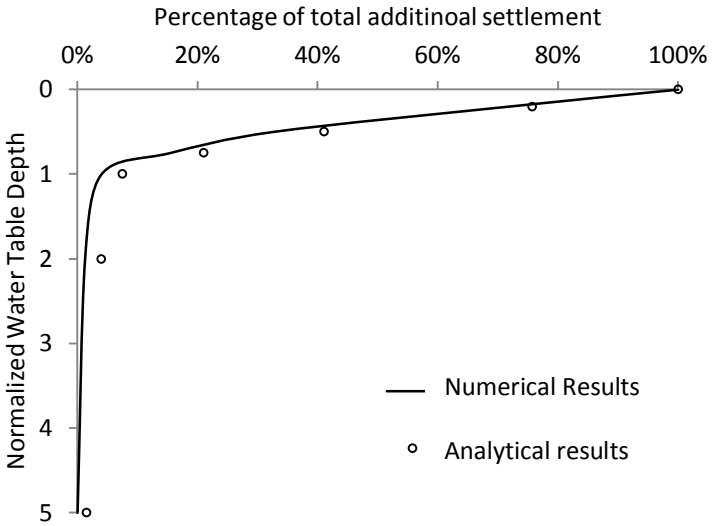


**Figure 6. 25 : Comparison of numerical results and proposed method of water table correction factor determination in a two layer system**

The proposed method was also verified with laboratory experiment using small cylindrical mould. The cylindrical mould that was used in small mould test (as discussed in Chapter 4) was used in this test and the same experimental setup was used. Soil 2 was used in the upper layer and soil 4 was used in the bottom layer. Relative density of both the soils was maintained at 77%, which gives maximum value of correction factor 5.85 for soil 2 and 2.25 for soil 4. A 50 mm diameter model footing was used, and the thickness of upper layer and bottom layer was 60 mm and 120 mm, respectively. The analytical solution using Eq. 6.7 gives the maximum value of correction factor 5.04, when the water level reaches the base of the footing. The correction factor obtained from experimental result was 5.12, which is in good agreement with the proposed method.

### Effect of Gibson Soil Profile

A non-homogenous soil with Young's modulus linearly increasing with depth is referred to as Gibson soil profile. Boswell and Scott (1975), Stark and booker (1997) suggested that a footing resting on soil with elastic modulus increasing with depth is a more generalized problem. The Young's modulus $E_s$ of soil increases linearly by the following equation,

$$E_s = E_0 + k_E.z \tag{6.10}$$

where, $E_0$ = Young's modulus of soil at the base of the footing

$k_E$ = rate of increment of modulus with depth

$z$ = depth

Generally, the non-homogeneity of Gibson soil profile is expressed in terms of a normalized Gibson modulus ratio, $\beta = E_0/(k_E B)$. Numerical studies conducted by Mayne and Poulos (1999) suggested that as $\beta$ tends to infinity, the soil acts like a homogeneous soil mass. In this study, the effect of water table rise on additional settlement of footings resting on Gibson soil has been investigated. In order to study the effect of normalized Gibson modulus ratio on water table correction factor, circular footings of different diameters were used. For all cases, the Young's modulus of soil at the base of the footing $E_0$ was taken as 1 MPa and the rate of increment of modulus with depth $k_E$ was assumed as 1 MPa/meter. Diameters of the circular footings used were 0.01 m, 0.1 m, 1.0 m, 10 m, and 100 m to get results for $\beta$ = 100, 10, 1, 0.1 and 0.01 respectively. Water level was raised from the bottom and the corresponding additional settlement was recorded. Based on the results, the percentage of total additional settlement due to water level rise at various water level depth are plotted in Fig. 6.26 for different values of $\beta$.

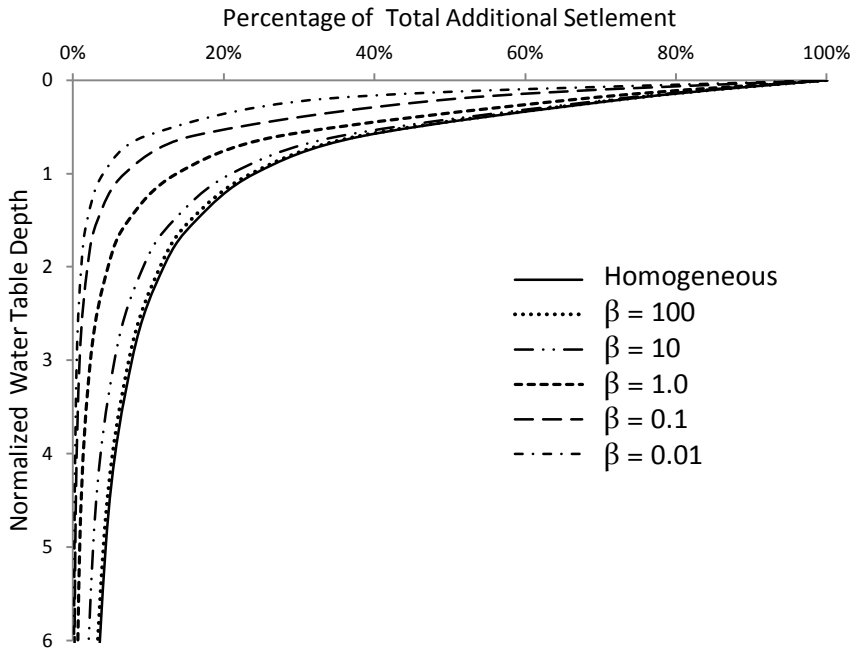


**Figure 6. 26 : Percentage of total additional settlement due to water level rise at various water level depths for different values of β**

The results show that the effect of water level rise can be felt at greater depths for soils having higher normalized Gibson modulus ratio. For example, when the water table is at 1$B$ below the footing level, only 4% of the total additional settlement was observed for a footing

with $\beta$=0.01, whereas 24% of the total additional settlement was found in case of a footing with $\beta$=100. Since higher the value of $\beta$ represents lower diameter of the footing, the result indicates that footings with higher diameter will be less susceptible to water level fluctuation at greater depths. The results also support the findings of Mayne and Poulos (1999) that when $\beta$ tends to infinity, the soil behaviour approaches towards the homogeneity.

## 6.8 Summary and Conclusion

In this Chapter, numerical modelling has been used to investigate the variation of water table correction factor with water table depth. The modelling was carried out using finite difference code FLAC and FLAC$^{3D}$. FLAC was used in modelling two dimensional problems, treating circular and strip footing as axisymmetric and plane strain problems, respectively. FLAC$^{3D}$ was used to model square and rectangular model footings. The simulation undertaken in the study can be divided into three parts.

In the first part, the laboratory model tests described in Chapter 4 was modelled in FLAC and FLAC$^{3D}$. Mesh sensitivity analysis was conducted to ensure that the numerical model effectively represents the laboratory testing condition. The numerical results were then compared with the rational method proposed in Chapter 5 along with the laboratory test data. Comparable results were obtained among the three different techniques. In the second part of the study, three different constitutive models, namely, linear elastic, non-linear elastic and elasto-plastic models were used in modelling the sand behaviour. It was assumed that the Young's modulus reduces by 50% when the dry sand becomes saturated. Based on linear elastic model, it was shown that the settlement doubles when the water table reaches the footing level. However, when non-linear elastic and Mohr-Coulomb constitutive models were used, the additional settlements were significantly more. The nonlinear elastic soil model accounts for the effects of stress level, soil strength and stiffness on the watertable correction factor, so it can be more suitable to be used for practical design. Using hyperbolic non-linear elastic soil model shows that the correction factor varies with the stress level as well as the soil strength and the stiffness. For all models, significant additional settlement due to water table rise was observed when the water level is closer to the footing.

In the third part of this Chapter, effect of various parameters on water table correction factor was studied. Numerical results suggested that depth of embedment and Poisson's ratio has little effect on water table correction factor diagram. Effect of finite layer thickness on additional settlement was investigated, and an equation of water table correction factor has

been proposed to account for thickness of the compressible soil layer. An analytical expression of correction factor for a two layer soil system has been proposed, which was verified by numerical simulation and laboratory modelling results. Numerical studies were also conducted to study the variation of correction factor diagrams in Gibson soil profile.

A finite difference approach is used in this research and linearly elastic, elastoplastic and hyperbolic models were used to model the soil behaviour. However, there remains a scope for further research using more advanced soil models including hierarchical single surface models and disturbed state models. Also, there is a scope for further research by considering anisotropy of granular soils.

# Chapter 7 Summary, Conclusions and Recommendations

This Chapter presents a brief summary of the research carried out in this dissertation as well as conclusions and recommendations for future research.

## 7.1 Summary

The objective of this thesis is to investigate the effect of water level rise on settlement of shallow foundations resting on granular soils.

There are significant uncertainties associated with the prediction of shallow footing settlement on granular soils. This can further increase if there is a probability of future rise of water level beneath the footing. Terzaghi (1943) suggested that the rise of water level to the bottom of the footing doubles the settlement as the soil stiffness reduces to half when the dry soil gets saturated. Since then, various researchers have proposed different techniques to predict the additional settlement based on analytical studies, field tests, laboratory modelling and numerical simulation. Usually the effect of water level rise is accounted for by using a water table correction factor $C_w$, which is multiplied by the settlement in dry condition, to get the settlement when the soil below a certain depth is submerged. The correction factors proposed by various researchers vary in magnitude and with the water table depth. The research conducted on effect of water table rise on footing settlement was largely based on analytical and small scale laboratory test results, and there is a lack of research conducted in comprehensive laboratory tests and numerical modelling. Therefore, a rational method to predict water table correction factor based on comprehensive test results and validated through numerical simulation is crucial to improve the current state-of-the-art.

In this research, analytical, experimental and numerical modelling was carried out to investigate the settlement behaviour of shallow footing subjected to water table rise. Firstly, modified strain influence diagrams were proposed for various footing shapes based on numerical and analytical studies. Then a rational method was proposed to predict water table correction factor based on laboratory test results and proposed strain influence factor diagrams. The method was validated with numerical modelling results. Also, effect of various soil parameters and ground conditions on additional settlement of shallow footings due to water level rise was investigated using laboratory and numerical modelling and theoretical analysis.

In the first part of the study, strain influence factor diagrams for different footing shapes were developed using linear elastic models in FLAC and FLAC$^{3D}$. FLAC was used to develop influence factor diagrams of circular and strip footings, and FLAC$^{3D}$ was used to model square and rectangular footings with various width to length ratios. The results were then compared with simple triangular approximation originally proposed by Schmertmann (1970). The comparison shows that the proposed strain influence factor diagrams vary with the original diagram in terms of initial value at the footing level, depth at which the peak occurs, magnitude of the peak, and the depth to which the diagrams extend. Effect of Poisson's ratio was also investigated for circular and strip footings. The results show that the variation of Poisson's ratio affect the influence factor diagram of a circular footing up to a depth of 0.5*B* below the footing, and up to a depth of *B* below the strip footing. A hyperbolic non-linear elastic soil model was also used to investigate the variation of vertical strain with depth below the footing. Different loading conditions were considered. The result shows that the maximum vertical strain occurs at a depth of 0.3*B* below the footing at all stress levels. To assist design engineers, a simple equation for strain influence factor diagrams was proposed. The equation has the flexibility to account for various footing shapes (i.e., circular, square, rectangular and strip footing) and can be implemented in spread sheets. Also, influence factor at various depths are given in tabular form.

The second part of the study involved comprehensive laboratory modelling of shallow footings subjected to water level rise and development of a rational method based on laboratory test results. The laboratory modelling program was divided in two parts. Initially, a rectangular tank was used to carry out laboratory model tests over wide range of footing shape, soil density and water table depth. A locally available granular soil was used. A circular footing of 100 mm diameter and square and rectangular footings with width $B$ =100 mm and breadth to length ratio = 1.0, 0.75, 0.50, 0.25 were used in the model tests. Sands at two different relative densities ($D_r$= 38% and 77%) were used in the series of model tests. Initially, applied pressure-settlement curves were obtained for footings placed on oven-dried sand. From the load-settlement plot, ultimate bearing capacity and working load of the footings were obtained by using double tangent method. The footings were then subjected to the working load, water table was raised from the bottom of the tank, and the additional settlements were recorded.

The water table correction factor was obtained by comparing the measured additional settlements under water table rise with the initial settlement under working load in dry

condition. The correction factor $C_w$ is higher in loose soils, indicating that the additional settlement due to submergence is more in sands of lower relative density. Eq. 5.4 was proposed based on the modified strain influence factor diagrams and experimental results,

$$C_w = 1 + (C_{w,\max} - 1)\frac{A_w}{A_t} \tag{5.4}$$

where, $A_w$ = area of influence factor diagram that is submerged

$A_t$ = total area of influence factor diagram

$C_{w,max}$ = maximum value of correction factor, which occurs when the water table is at footing level

It was shown that water table rise in granular soils can be successfully modelled by Eq. 5.4 at any water table depth. The result also shows that the additional settlement due to water level rise can be felt up to water level depth of 6*B* below the footing. It was also showed that the strain influence diagrams proposed in Chapter 3 can be successfully used in Eq. 5.4. The $C_w$ - *z* variation is convex upwards, which is supported by the works of Vargas (1961), Brinch Hansen (1966b), and Morgan et al. (2010).

It was established from the settlement tank test results that Eq. 5.4 can be successfully used to predict water table correction factor. It was also established that the shape of the correction factor diagram is convex upward. Table 5.1 or Fig. 5.10 can be used to get the value of $A_w / A_t$ .Soils of different types will have similar trend of water table correction diagram but different values of $C_{w,max}$. Hence, the second part of the laboratory modelling was designed for better understanding of how the $C_{w,max}$ varies for different soils, when the water table is at the base of the footing. Unlike the settlement tank test, a small cylindrical mould was used in this test, and it was not required to record settlement at different water table depths. As a result, much less effort was required in the test which allowed increasing the number of soils used in the test. A total of nine soils were used, and they were chosen so that they can represent wide range of variety in soil gradation, fines content and void ratio range.

The small mould was filled with soils at required density. A circular model footing was used. The test was carried out in dry and submerged conditions. In submerged tests, the water level was raised up to the base of the footing and $C_{w,max}$ was obtained by diving the settlement in wet sand by the settlement in dry sand. Based on the test results, an expression was proposed

in Eq. 5.13, which can be used to obtain $C_{w,max}$ from field SPT value, soil relative density and void ratio. $C_{w,max}$ can be used in Eq. 5.4 to predict water table correction factor at any depth of water table. Effect of fines content was investigated, and the results show that $C_{w,max}$ can significantly increase with increase in fines content. It was found that the ratio of $C_{w,max}$ in loose to dense sand sharply increases with increase in void ratio range and volumetric strain potential. The rational method developed herein to predict the $C_{w,max}$ of different soils can be used in conjunction with the method obtained from settlement tank test to predict the water table correction factor of any regular footing shape resting on soils of any density subjected to water table rise at any depth below the footing.

The third part of the study involves numerical modelling of water table rise in granular soils using explicit finite difference codes FLAC and FLAC$^{3D}$. The simulation undertaken in the study was done in three steps. Firstly, the laboratory test setup of settlement tank test (as described in Chapter 4) was modelled in FLAC and FLAC$^{3D}$. The mesh density was determined by sensitivity analysis to make sure that the simulation effectively represents the soil behaviour in laboratory test condition. The results obtained were compared with the laboratory test results and the correction factor prediction method proposed in Chapter 5. The results showed that there is a good agreement among the proposed method, laboratory test data and the numerical results. In the second part of numerical modelling, shallow footings resting on granular soils and subjected to water level rise were modelled using different constitutive models. Circular and strip footings were modelled using linear elastic model , and the result shows that the settlement gets doubled when the water level rises up to the footing level. Using hyperbolic non-linearly elastic model shows that $C_{w,max}$ can be more than two depending on the stress level and strength and stiffness of the soil. The additional settlement is higher at higher stress level and lower soil stiffness. Results from Mohr-Coulomb elastoplastic model shows that the settlement due to submergence can be significantly higher. This can explain the high additional settlement values recorded in the literature. All the soil models indicate that the water table correction factor diagram is convex upward, which means settlement increases at a higher rate when the water table is in the vicinity of the footing level.

Finally, the effect of various soil parameters and ground conditions on water table correction factor was investigated using numerical results. Variation of foundation embedment depth and Poisson's ratio had little effect on the correction factor diagram. Presence of incompressible stratum at a shallow depth below the footing affects the correction factor

diagrams. This was discussed in details, and a modified water table correction factor equation was proposed to account for the finite layer thickness. Effect of layered soil profile on correction factor was considered, and an analytical expression for correction factor was proposed to account for a two layer soil profile. This was verified by laboratory modelling and numerical results. The non-homogeneity of soil mass and its effect on water table correction factor diagram was also investigated. The result suggests that soils with higher normalized Gibson modulus ratio experience the effect of water level rise at greater depths.

## 7.2 Conclusions

The main conclusions of the study are summarized below in corresponding to the Chapters 3, 4, 5, and 6 of the thesis.

Strain Influence Factor Diagrams for Footings on an Elastic Medium (Chapter 3)

- Schmertmann's (1970) strain influence factors were revisited using explicit finite difference code FLAC and FLAC$^{3D}$, and elastic theory. Based on the results, modified influence factor diagrams for footings resting on elastic medium were proposed for various footing shapes.
- The modified influence factor diagrams were compared with Schmertmann's (1970) original triangular approximation. Unlike the original approximation, the influence factors were 0.72-0.74 at the base of the footing, peaked at around 0.83 at a depth of 0.2*B* to 0.25*B*, and extended to a greater depth.
- The variation of Poisson's ratio influences the strain influence factor diagram up to a depth of 0.25*B* for a circular footing, and up to 1.0 *B* for a strip footing.
- Using hyperbolic non-linear elastic model shows that the depth of maximum vertical strain occurs at 0.3*B* below the footing at any stress level.
- Modified strain influence factors using linear elastic model can be obtained alternatively by using Eq. 3.11 or Table 3.1.

Laboratory Modelling of Shallow Footings and Water Level Rise on Granular Soils (Chapter 4)

- The laboratory test program was divided into two parts- settlement tank test and the small mould test. The settlement tank test was used to deduce the shape of the correction factor diagram and then a rational method for water table correction factor. The small mould test was used to understand the effect of different soil types on $C_{w,max}$.

- The laboratory model described in Chapter 4 can successfully model the rise of water table and its effect on shallow foundation settlement.
- The effect of capillary rise and scale effect on the laboratory model was carefully considered, and the test program was designed to avoid these effects.

Interpretation of Laboratory Test Results (Chapter 5)

- Eq. 5.4 can successfully predict the water table correction factor at any depth of water level. The modified strain influence factor diagrams can be successfully used in Eq. 5.4.
- The water table correction factor is affected by footing shape. Figure 5.10 and Table 5.1 can be used to obtain $A_w/A_t$ for different footing shapes and can be used in Eq. 5.4.
- The laboratory test results validate the proposed analytical expression in Eq. 5.4.
- Footings resting on loose sands experience higher additional settlements due to water table rise than footings resting on dense sands.
- The variation of water table correction factor with water table depth is not linear. Rather, the rate of increment in additional settlement is faster when the water table is closer to the footing. This makes the $C_w$-$z$ curve convex upwards for all footing shapes and at all densities.
- Additional settlement was observed when water table was at 6$B$ below the footing level. The test results show that significant additional settlement can be produced by water table rise even at depths as high as 5$B$.
- $C_{w,max}$ can be obtained from field SPT data, soil relative density and void ratio, as shown in Eq.5.13. This can be used in Eq. 5.4 to predict the additional settlement due to water table rise up to any depth below the footing.
- Percentage of fines content present in the granular soil can significantly affect $C_{w,max}$. The effect is more pronounced in the loose sand than in dense sand.
- The ratio of $C_{w,max}$ on loose sand to dense sand increases sharply with increase in void ratio range and volumetric strain potential.
- $C_{w,max}$ decreases with decreasing roundness, sphericity and regularity. The rate of decline is higher in loose sand that that of dense sand.

Numerical Modelling of Water Table Rise in Granular Soils (Chapter 6)

- The numerical modelling results confirmed the applicability of :

a. The proposed laboratory model developed in Chapter 4 in quantifying the effect of water level rise on shallow foundations settlement in granular soils.
b. The water table correction factor prediction method proposed in Chapter 5 for various footing shapes and water table depths.

- Numerical simulation using different constitutive models reveals that:
  a. When linear elastic model is used, the water table correction factor becomes two as the water table rises up to the footing level.
  b. The non-linear elastic model gives higher additional settlement due to submergence, accounts for the effect of stress level, soil strength and stiffness and it is more suitable to use for practical design.
  c. The additional settlement is significantly higher when Mohr-Coulomb model is used.
- All soil models show that settlement increases at a higher rate when the water level is closer to the footing.
- The maximum value of water table correction factor is dependent on stress level and soil strength and stiffness. The higher the stress level, the higher is the correction factor. On the other hand, higher soil stiffness results in lower value of correction factor.
- Depth of embedment of the footing and Poisson's ratio has little effect on water table correction factor diagram.
- The analytical expression for layered soil profile given in Chapter 6 is validated by numerical and experimental results and can be used by design engineers.
- The thickness of finite compressible layer affects the correction factor diagram and it can be accounted for by the correction factor equation proposed in Chapter 6.

## 7.3 Recommendations for Future Research

Based on the research carried out in this study, the following recommendations have been made for future research. The recommendations are summarized in the sequence of the Chapters 3, 4, 5 and 6in this dissertation.

Strain Influence Factor Diagrams for Footings on an Elastic Medium (Chapter 3)

- Strain influence factor diagrams can be developed for other foundation shapes (for example, triangular, trapezoidal etc.)
- Strain influence factor diagram should be studied by laboratory modelling

- Advanced soil models can be used for numerical modelling
- A simpler and easy to use mathematical expression for strain influence factor diagrams should be proposed.
- The effect of adjacent footings on strain influence factor diagram can be investigated.

Laboratory Modelling of Shallow Footings and Water Level Rise on Granular Soils (Chapter 4)

- More footing shapes should be studied including strip and triangular footings in the laboratory modelling
- Provision for testing at cyclic loading condition.
- Study the effect of footing embedment depth, finite layer thickness and generalized Gibson soil profile. Validate the findings from numerical modelling in Chapter 6.
- A means for testing soils with higher capillary rise without affecting the test results by matric suction can be developed.

Interpretation of Laboratory Test Results (Chapter 5)

- The laboratory test data and proposed rational method can be validated by field test data and settlement data recorded in the literature.
- More soil samples can be used to develop expressions to correlate $C_{w,max}$ with percentage of fines content, void ratio range and volumetric strain potential.
- The effect of uniformity coefficient and coefficient of curvature on water table correction factor should be investigated by conducting test on more soil samples.

Numerical Modelling of Water Table Rise in Granular Soils (Chapter 6)

- The effect of adjacent footings on correction factor should be studied.
- Developing expression for water table correction factor for multilayered soil profile, and validating with numerical and laboratory test data
- Validation of the model with in situ data
- The effect of footing width on additional settlement due to water table rise can be investigated
- A single correction factor equation that can account for all contributing factors those affect additional settlement due to submergence should be developed.
- More advanced soil models (for example, Duncan-Chang soil model) can be used in simulating water table rise in granular soils.

# Reference

Agarwal, K.G., and Rana, M.K. (1987). "Effect of ground water on settlement of footing in sand," *Proceedings, Ninth European Conference on Soil Mechanics and Foundation Engineering*, Dublin, 2, 751-754.

Alpan I. (1964). "Estimating the settlement of foundations on sand." *Civil Engineering and Public Works Review*, 59(700), 1415-1418.

Bathurst, R. J. and Rothenberg, L.(1988). "Micromechanical aspects of isotropic granular assemblies with linear contact interactions", *Journal of Applied Mechanics*, ASME, 55, 17-23.

Bazaraa, A.R. (1967). "Use of the standard penetration test for estimating settlements of shallow foundations on sand," *Ph.D. dissertation*, Department of Civil Engineering, University of Illinois, Champaign-Urbana.

Berardi, R., and Lancellotta, R. (1991). " Stiffness of granular soil from field performance." *Geotechnique*, 41(1), 149-157.

Berry, D. S. (1935). "Stability of granular mixtures." *Proc., 38th Annual Meeting*, Vol. 35, ASTM, Philadelphia, 491–507.

Bolton, M. D., and Lau, C. K. (1989). "Scale effects in the bearing capacity of granular soils." *Proc., 12th Int. Conf. on Soil Mechanics and Foundation Engineering*, Vol. 2, Rio de Janeiro, 895–898.

Boswell, L. F., and Scott, C. R. (1975). ''A flexible circular plate on a heterogeneous elastic half-space: influence coefficients for contact stress and settlement.'' *Geotechnique*, London, 25(3), 604–610.

Bowles, J.E. (1977). *Foundation Analysis and Design, 2nd Ed.*, McGraw-Hill, New York.

Bowles, J.E. (1996). *Foundation analysis and design, 5th ed.*, New York , McGraw-Hill.

Briaud, J.-L., and Gibbens, R.M. (1994). "Predicted and measured behaviour of five spread footings on sand." *ASCE, Geotech. Special Pub*, 41, 255 pp.

Brinch Hansen, J. (1966a). "Stress-strain relationships for sand," *The Danish Geotechnical Institute, Bulletin No. 20*, 8-14.

Brinch Hansen, J. (1966b). "Improved settlement calculation for sand," *The Danish Geotechnical Institute, Bulletin No. 20*, 15-19.

Burland, J.B., and Burbridge, M.C. (1985). "Settlement of foundations on sand and gravel", *Institution of Civil Engineers*, 78 (1), 1325-1381.

Burland, J.B. (1970). "Discussion, Session A." *Proceedings,Conference on Situ Investigations in Soils and Rocks.*British Geotechnical Society, London, England. pp. 61-62.

Cerato, A.B., and Lutenegger, A.J. (2007). "Scale effects of shallow foundation bearing capacity on granular material." *Journal of Geotechnical and Geoenvironmental Engineering*, ASCE, 133(10), 1192-1202.

Coetzee, M. J., Hart R. D., Varona, P. M., and , and Cundall, P. A. (1998). *FLAC Basics*, Itasca Consulting Group Inc., Minneapolis, Minnesota.

Cubrinovski, M., and Ishihara, K. (2002). "Maximum and minimum void ratio characteristics of sands." *Soils Found.*, 426, 65–78.

Cubrinoski, M., and Ishihara, K. (1999)."Empirical correlation between SPT N-value and relative density for sandy soils." *Soils Found.*,395, 61–71.

Dafalias, Y. F.(1986). "Bounding surface plasticity, I: mathematical foundation and Hypoplasticity", *J. Geothech. Eng. Div.*, 12, 966-987.

Darve, F.(1984). "Incrementally non-linear constitutive law of second order and its application to localization", *Mechanics of Engineering Materials*, ed. C. S. Desai and R. H. Gallagher, John Wiley, New York, pp. 179-196.

Das, B.M., and Sivakugan, N. (2011). "*Maximum and minimum void ratios and median grain size of granular soils: their importance and correlations with material properties.*" *In: Porceeding of the International Conference on Advances in Geotechnical Engineering,* pp. 59-73,7-9 November 2011, Perth, WA, Australia.

De Beer, E. E. (1963). "The scale effect in the transposition of the results of deep-sounding tests on the ultimate bearing capacity of piles and caisson foundations." *Geotechnique*, 131, 39–75.

Department of Navy (1982). *Soil Mechanics Design Manual 7.1*. Department of the Navy, Navy Facilities Engineering Command , Alexandria, VA

Douglas, D. J. (1986). "State-of-the-art." *Ground engineering*, 19(2), 2-6.

Drucker, D. C., Gibson, R. E. and Henkel, D. J. (1957). "Soil mechanics and workhardening theory of plasticity", Trans. *ASCE*, 122, 338-346.

Dvorak, A. (1963). "Compressibility of coarse granular soils." *Proceedings, Third European Conference on Soil Mechanics and Foundation Engineering*, 1, 227-232.

Fatt, I. (1958). " Compressibility of sandstones at low to moderate pressures." *Bull. Am. Assoc. Pet.Geol.*, 42: 1924-1957.

Fellenius, B. H., and Altaee, A. (1994). "Stress and settlement of footings in sand. Vertical and horizontal deformations of foundations and embankments."*GSP #40*, Vol. 2, College Station, Tex., 1760–1773.

Ferreira, H.N., and da Silva, C.A.F. (1961). "Soil failure in the Luanda Region, geotechnic study of these soils," *Proceedings, 5th International Conference on Soil Mechanics and Foundation Engineering*, Paris, 1, 95-99.

Gibbs, H. J., and Holtz, W. G. "Research on Determining the Density of Sands by Spoon Penetration Testing." *Proc., 4th International Conference on Soil Mechanics and Foundation Eneineering*, pp 35-39.

Holubec, I., and D'Appolonia, E. (1973). "Effect of particles shape on the engineering properties of granular soils. In: Evaluation of Relative Density and its Role in Geotechnical Projects Involving Cohesionless Soils." *ASTM Spec. Tech. Bull.*, No. 523, pp. 304-318.

Ingles, O.G., and Grant, K.( 1975). Compaction: Effect on properties of coarse sediments. In: G.V. Chilingarian, and K.H. Wolf (Editors), Compaction of Coarse-grained Sediments, I. Elsevier,

Amsterdam, pp. 292-348.

Itasca (2011). *FLAC Verson 7.0: User's guide*. Itasca consulting group, Minneapolis, USA.
Itasca (2012). *FLAC$^{3D}$ Verson 5.0: User's guide*. Itasca consulting group, Minneapolis, USA.

Jenkins, J. T. and Strack, O. (1993). "Mean-field inelastic behaviour of random array of identical spheres", *Mechanics of Materials,* 16, 25-33.

Jeyapalan, J. K., and , and Boehm, R. (1986). "Procedures for predicting settlements in sands. In W. O. Martin (ed.), Settlements of Shallow Foundations on Cohesionless Soils: Design and Performance." *ASCE, Seattle*, 1-22.

Khanna, P.L., Varghese, P.C., and Hoon, R.C. (1953). "Bearing pressure and penetration tests on typical soil strata in the region of the Hirakud Dam project," *Proceedings, 3rd International Conference on Soil Mechanics and Foundation Engineering,* Zurich, 1, 246-252.

Kondner, R.L. , and Zelasko, J.S. (1963). "A hyperbolic stress-strain formulation of sands," *Proceedings, Second PanAmerican Conference on Soil Mechanics and Foundation Engineering,* Sao Paulo, 1, 289-324.
Krumbein, W.C.(1941). "Measurement and geological significance of shape and roundness of sedimentary particles." *J. Sediment,* Petrol., 11: 64-72.

Krumbein, W.C., and Sloss, L.L.( 1963). *Stratigraphy and Sedimentation. 2nd ed.,* Freeman, San Francisco, CA, 380 pp.

Kusakabe, O. (1995). Chapter 6: Foundations. *Geotechnical centrifuge technology,* R. N. Taylor, ed., Blackie Academic & Professional, London,118–167.

Lade, P. V., and Kim, M. K. (1988). "Single hardening constitutive model for frictional materials, II, yield criterion and plastic work contours", *Computers and Geotechnics,* 6(l), 13-29.

Leonards, G.A.(1986). "Settlement of Shallow Foundations on Granular Soils." *Journal of Geotechnical Engineering, July, 1986, Vol. 114, No. 7.*

Liao, S. C., And Whitman, R. V. (1986), "Overburden Correction Factors for SPT in Sand." *ASCE Journal of Geotechnical Engineering,* Vol 112, No. 3, pp. 373-377.

Lopresti, D.C.F. (1995) "General report: measurements of shear deformations of geomaterials", *Pre-failure deformation of geomaterials,* Balkema, Rotterdam, Netherland, Vol. 2, 1067-1088.

Mayne, P.W., and Poulos, H.G. (1999). "Approximate displacement influence factors for elastic shallow foundations.", *Journal of Geotechnical and Geoenvironmental Engineering, ASCE,* 125(6), 453-460.

Meade, R.H.(1966). "Early stages of the compaction of clays and sands." *J. Sediment. Petrol.,* 36:1085-1101.

Meyerhof, G. G. (1956). "Penetration tests and bearing capacity of cohesionless soils." *J. Soil Mech. Found. Div, ASCE,* 82(1), 1-19.

Meyerhof, G. G. (1965). "Shallow foundations." *J. Soil Mech. Found. Div., ASCE,* 91(2), 21-31.
Mohamed, F., and Vanapalli, S. (2006). "Laboratory investigations for the measurement of the bearing capacity of an unsaturated coarse-grained soil." *Proceedings of 59th Canadian Geotechnical Conference,* 219-226

Mohamed, F., Vanapalli, S., and Saatcioglu, M. (2012). "Settlement estimation of shallow footings of saturated and unsaturated sands." *Proceedings of Geocongress, ASCE,* 2552-2561

Morgan, A.B., Sanjay, K.S., and Sivakugan, N. (2010). "An experimental study on the additional settlement of footings resting on granular soils by water table rise," *Soils and Foundations,* 50 (2), 319-324.

Morris, H.C.(1959). " Effect of particle shape and texture on the strength of noncohesive aggregates."*Am. Soc. Test. Mater., Spec. Tech. Publ*., No. 254, pp. 350-364.

Murtaza, G., Athar,M., and Khan, S.M. (1995). "Influence of submergence on settlement of footing on sand," *Journal of the Institution of Engineers (India),* 76 (5), 51-54.

Norris, G. (1977). "The drained shear strength of uniform quartz sand as related to particle size and natural variation in particle shape and surface roughness." *Unpublished Ph.D. Thesis,* University of California, Berkeley, U.S.A., 217 pp.

Oda, M. (1972). "Initial fabrics and their relations to mechanical properties of granular material." *Soil Found*, 12: 17-36.

Ovesen, N. K. (1975). "Centrifugal testing applied to bearing capacity problems of footings on sand." *Geotechnique*, 252_ 394–401.

Papadopoulos, B. P. (1992). "Settlements of shallow foundations on cohesionless soils." *J. Geotech. Eng., ASCE,* 118(3), 377-393.

Patra, C.R., Sivakugan, N., and Das, B.M. (2010). "*Relative density and median grain-size correlation from laboratory compaction tests on granular soil." International Journal of Geotechnical Engineering*, 4 (1). pp. 55-62.

Peck, R. B., and Bazaraa, A.R.S.S. (1969). "Discussion of Settlement of spread-footings on sand." *J.*

*Soil Mech. Found. Div., ASCE,* 95(3), 305-309.

Peck, R.B., Hanson, W.E., and Thornburn, T.H. (1974). *Foundation Engineering, 2nd Ed*., John Wiley & Sons, New York.

Poorooshasb, H. B., Holubec, I., and Sherboume, A. N.(1967). "Yielding and flow of sand in triaxial compression: Part II and III", *Canadian Geotechnicaf Journal*,4(4), 367-397.

Razouki ,S.S., and Al-Zubaidy , D. A. (2010). "Elastic settlement of square footings on a two-layer deposit."*Proceedings of the ICE - Geotechnical Engineering*, Volume 163, Issue 2, 01 April 2010 , pages 101 –106

Rekowski, R. (2001). "Investigation into the effects of rise in water table on shallow foundations in granular soils." *B.E Hons. Thesis*, James Cook University, Townsville, Australia

Richards, B.G., and Greacen, E.L.(1986). " Mechanical stresses on an expanding cylindrical root analogue in granular media." *Aust. J. Soil Res.*, 24: 393-404.

Ridgway, K., and Rupp, R. ( 1969). "The effect of particle shape on powder properties." *J. Pharm. Pharmacol.*, 21 {Suppl.); 30-39.

Roscoe, K. H., Schofield, A. N. and Thurairajah, A.(1963). "Yielding of clays in states wetter than critical", *Geotechnique*, 13, 21 l-224.

Roscoe, K. H. and Burland, J. B. (1968). "On the generalized stress-strain behavior of wet clay", *Engineering Plasticity*, ed. J. V. Hayman and F. A. Leckie, Cambridge University Press, London, 535-609.

Shahin, M. A. (2003). "Use of artificial neural networks for predicting settlement of shallow foundations on cohesionless soils."Ph.D. thesis, The University of Adelaide, Adelaide.

Schmertmann J.H., Hartman J.P., and Brown P.R. (1978). "Improved strain influence factor diagrams.". *J. Geotech. Eng. Div., ASCE*, 104(8), 1131-1135.

Schultze, E., and Melzer K. J. "The determination of the density and the modulus of comressibility of non-cohesive soil by soundings." *Proc., 6th International Conference on Soil Mechanics and Foundation Engineering*, 354-358.

Schultze, E., and E. Menzenbach (1961). "Standard Penetration Test and Compressibility of Soils." *Proceedings, Fifth International Conference on Soil Mechanics and Foundation Engineering*, Paris, Vol. 1, pp. 527-532.

Schultze, E., and Moussa, A. (1961). "Factors affecting the compressibility of sand." *Proceedings of the 5th International Conference on Soil Mechanics and Foundation Engineering 1*, pp. 335-340.

Sivakugan N, and Johnson, K. (2004). "Settlement predictions in granular soils: a probabilistic approach." *Geotechnique*, 54(7), 499-502.

Sivakugan, N., and Das, B.M. (2010). "*Geotechnical Engineering : a practical problem solving approach." J. Ross Publishing, Inc.*, 313pp.

Sivakugan, N., Eckersley, J. and And Li, H. (1998). "Settlement predictions using neural networks.", *Australian Civil Eng. Transactions*, CE 40, 49-52.

Standards Australia (2009). *AS1289.3.6.1-2009, Methods of testing soils for engineering purposes – Soil classification tests – Determination of the particle size distribution of a soil – Standard method of analysis by sieving*

Standards Australia (2009). *AS1289.3.6.3-2003, Methods of testing soils for engineering purposes – Soil classification tests – Determination of the particle size distribution of a soil –* Standard method of fine analysis by using a hydrometer

Standards Australia (1998). *AS1289.5.5.1- 1998, Methods of testing soils for engineering purposes - Soil compaction and density tests - Determination of the minimum and maximum dry density of a cohesionless material - Standard method*

Standards Australia (2013). *AS1289.6.2.1-2001(R2013), Methods of testing soils for engineering purposes - Soil strength and consolidation tests - Determination of shear strength of a soil - Direct shear test using a shear box.*

Standards Australia (2006). *AS 1289.3.5.1-2006, Methods of testing soils for engineering purposes - Soil classification tests - Determination of the soil particle density of a soil - Standard method*

Tan, C. K., and Duncan, J.M. (1991)."Settlement of footings on sands: accuracy and reliability." *Proc., Geotech. Eng. Congress 1991*, 446-455.

Tatsuoka, F., and And Shibuya, S. (1992). "Deformation characteristics of soils and rocks from field

and laboratory tests", *Rep., Inst. of Industrial Science.*, The University of Tokyo, Tokyo, 37 (1)

Tatsuoka, F., Teachavorasinsku, S., Donng, J., Kohata, Y., and Sato, T. (1994). "Importance of measuring local strains in cyclic triaxial tests on granular matrerials", *Dynamic geotechnical testing II, ASTM,* 288-302.

Tatsuoka, F., Okahara, M., Tanaka, T., Tani, K., Morimoto, T., and Siddiquee, M. S. A. (1991). "Progressive failure and particle size effect in bearing capacity of a footing on sand." *Geotech. Spec. Publ.*, No. 27,2, 788–802.

Terzaghi, K. a. P., R.B. (1967). *Soil Mechanics in Engineering Practice, 2nd Edition*, John Wiley and Sons, New York.

Teng, W.C. (1962). *Foundation Design*, Prentice-Hall Inc., New Jersey.

Terzaghi, K. (1943). *Theoretical Soil Mechanics*, John Wiley & Sons, New York.

Terzaghi, K. , and Peck, R.B. (1948). *Soil Mechanics in Engineering Practice, 1st Ed.*, John Wiley & Sons, New York.

U. S. Army Corps of Engineers (1990). "Engineering and Design—Settlement Analysis." *http://www.usace.army.mil/publications/eng-manuals/em.htm* , Washington, D.C.

Vanapalli, S.K., and Mohamed, F.M.O. (2007). "Bearing capacity of model footings in unsaturated soils." *Experimental unsaturated soil mechanics.* Springer-Verlag. Berlin Heidelberg, Germany, 483-493.

Vargas, M. (1961). "Foundations of tall buildings on sands in Sao Paulo, Brazil." *Proceedings of Fifth International Conference on Soil Mechanics and Foundation Engineering*, Paris, 1, 841-843.

Vermeer, P. A., and de Borst, R. (1984). "Non-associated plasticity for soils, concrete and rock", *HERON*, 29, l-64.

Wadel, H.( 1932). "Volume, shape and roundness of rock particles." *J. Geol.*, 40: 443-451.

Yamaguchi, H., Kimura, T., and Fujii, N. (1977). "On the scale effect of footings in dense sand." *Proc., 9th Int. Conf. on Soil Mechanics and Foundation Engineering.* Tokyo, Japan, Vol. 1, 795–798.

Zelasko, J.S., Krizek, R.J., and Edil, T.B.(1975). "Shear behaviour of sands as a function of grain characteristics." *Proceedings of the Istanbul Conference on Soil Mechanics and Foundation Engineering 1*, pp. 55-64.

# APPENDIX A

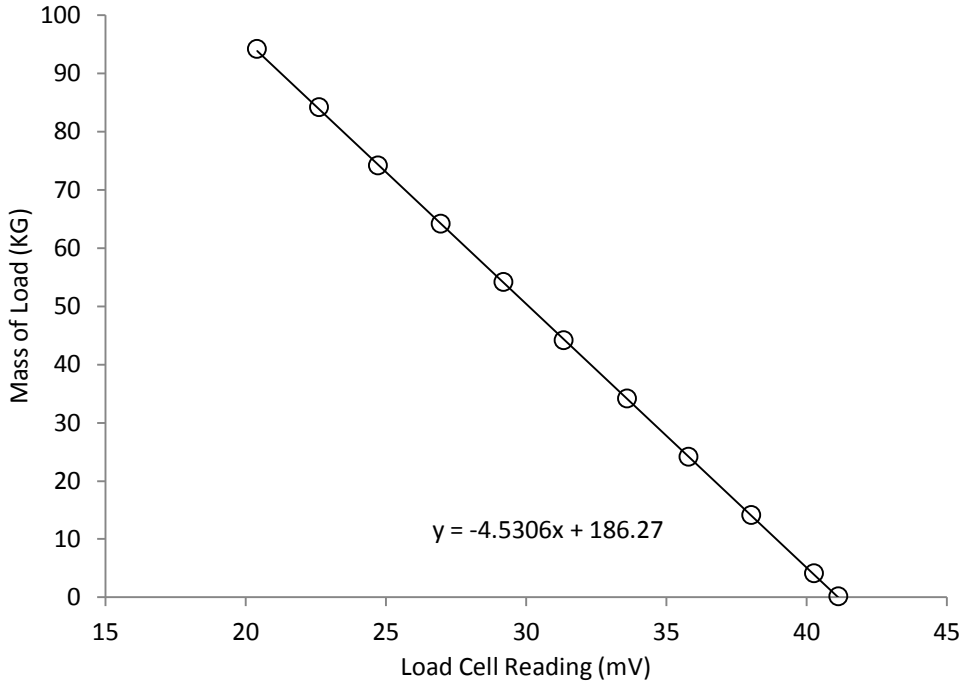


(a)

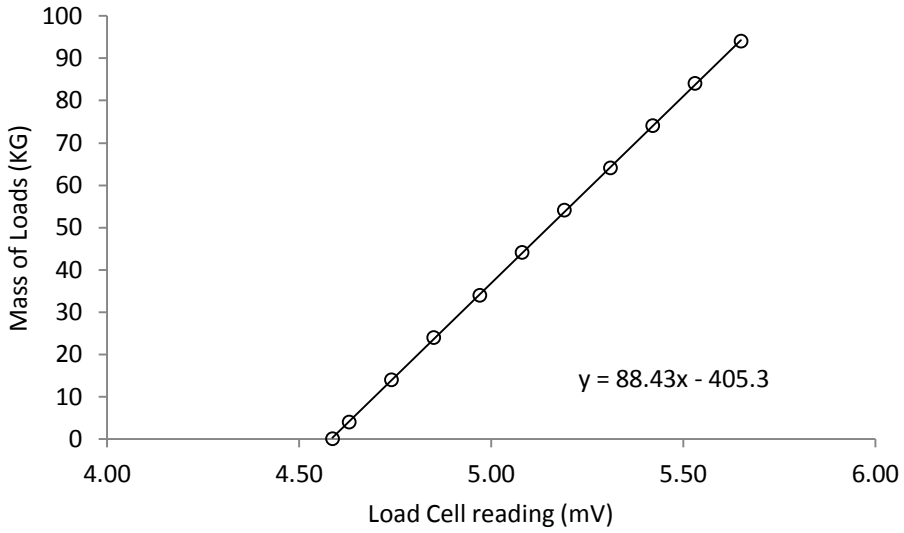


(b)

**Figure A. 1: Load cell calibration for settlement tank test, a) 500 KG load cell, b) 1000 kg load cell**

# APPENDIX B

## Settlement tank test result on loose dry sand

| Footing Shape | Reading in Load Cell (mV ) | Weight (kg) | Applied Force (kN) | Applied Pressure (kPa) | Dial Gauge 1 Reading | Settlement According to Dial Gauge 1 (mm) | Dial Gauge 2 Reading | Settlement According to Dial Gauge 2 (mm) | Average Settlement (in mm) | |
|---|---|---|---|---|---|---|---|---|---|---|
| Rectangular (B/L=.75) | 42.70 | 0.00 | 0.00 | 0.00 | N/A | N/A | 16.13 | 0.00 | 0.00 | |
| | 41.20 | 6.00 | 0.06 | 4.43 | N/A | N/A | 15.85 | 0.28 | 0.28 | |
| | 40.80 | 7.68 | 0.08 | 5.67 | N/A | N/A | 15.31 | 0.82 | 0.82 | |
| | 40.60 | 8.52 | 0.08 | 6.29 | N/A | N/A | 15.12 | 1.01 | 1.01 | |
| | 39.30 | 13.98 | 0.14 | 10.31 | 41.32 | N/A | 14.72 | 1.41 | 1.41 | |
| | 38.40 | 17.76 | 0.17 | 13.10 | 40.73 | 2.00 | 14.04 | 2.09 | 2.05 | |
| | 37.40 | 21.96 | 0.22 | 16.19 | 39.81 | 2.92 | 13.00 | 3.13 | 3.03 | |
| | 36.30 | 26.57 | 0.26 | 19.60 | 39.24 | 3.49 | 12.33 | 3.80 | 3.65 | |
| | 35.40 | 30.35 | 0.30 | 22.39 | 38.69 | 4.04 | 11.73 | 4.40 | 4.22 | |
| | 34.50 | 34.13 | 0.33 | 25.17 | 37.86 | 4.87 | 10.83 | 5.30 | 5.09 | |
| | 33.50 | 38.33 | 0.38 | 28.27 | 36.91 | 5.82 | 9.83 | 6.30 | 6.06 | |
| | 32.70 | 41.69 | 0.41 | 30.75 | 36.00 | 6.73 | 8.88 | 7.25 | 6.99 | |
| | 31.80 | 45.46 | 0.45 | 33.53 | 34.52 | 8.21 | 7.31 | 8.82 | 8.52 | |
| | 31.00 | 48.82 | 0.48 | 36.01 | 32.93 | 9.80 | 5.62 | 10.51 | 10.16 | |
| | 30.10 | 52.60 | 0.52 | 38.80 | 31.02 | 11.71 | 4.67 | 11.46 | 11.59 | |
| | 29.80 | 53.86 | 0.53 | 39.73 | 30.79 | 11.94 | 3.42 | 12.71 | 12.33 | |
| | 29.10 | 56.80 | 0.56 | 41.89 | 28.82 | 13.91 | 1.41 | 14.72 | 14.32 | |
| | 28.60 | 58.90 | 0.58 | 43.44 | 28.07 | 14.66 | 0.74 | 15.39 | 15.03 | |
| Square | 42.60 | 0.00 | 0.00 | 0.00 | 28.20 | 0.00 | 34.20 | 0.00 | | 0.00 |
| | 42.40 | 0.97 | 0.01 | 0.95 | 28.27 | -0.07 | 34.01 | 0.19 | | 0.06 |
| | 40.40 | 9.36 | 0.09 | 9.19 | 27.70 | 0.50 | 33.21 | 0.99 | | 0.75 |
| | 38.60 | 16.92 | 0.17 | 16.60 | 26.87 | 1.33 | 32.49 | 1.71 | | 1.52 |
| | 37.50 | 21.54 | 0.21 | 21.13 | 25.82 | 2.38 | 31.34 | 2.86 | | 2.62 |
| | 36.50 | 25.73 | 0.25 | 25.25 | 24.92 | 3.28 | 30.38 | 3.82 | | 3.55 |
| | 35.60 | 29.51 | 0.29 | 28.95 | 24.05 | 4.15 | 29.48 | 4.72 | | 4.44 |
| | 34.90 | 32.45 | 0.32 | 31.83 | 22.30 | 5.90 | 27.69 | 6.51 | | 6.21 |
| | 33.80 | 37.07 | 0.36 | 36.36 | 19.52 | 8.68 | 24.88 | 9.32 | | 9.00 |
| | 32.70 | 41.69 | 0.41 | 40.89 | 16.62 | 11.58 | 22.00 | 12.20 | | 11.89 |
| | 31.80 | 45.46 | 0.45 | 44.60 | 13.09 | 15.11 | 18.15 | 16.05 | | 15.58 |
| | 31.00 | 48.82 | 0.48 | 47.89 | 10.81 | 17.39 | 16.21 | 17.99 | | 17.69 |

| Footing Shape | Reading in Load Cell (mV ) | Weight (kg) | Applied Force (kN) | Applied Pressure (kPa) | Dial Gauge 1 Reading | Settlement According to Dial Gauge 1 (mm) | Dial Gauge 2 Reading | Settlement According to Dial Gauge 2 (mm) | Average Settlement (in mm) |
|---|---|---|---|---|---|---|---|---|---|
| Rectangular (B/L=.5) | 4.59 | 0.59 | 0.01 | 0.00 | 39.10 | 0.00 | 0.00 | 0.00 | 0.00 |
| | 4.68 | 8.55 | 0.08 | 4.19 | 38.66 | 0.44 | 30.37 | | 0.44 |
| | 4.77 | 16.51 | 0.16 | 8.10 | 37.72 | 1.38 | 29.63 | 1.18 | 1.28 |
| | 4.87 | 25.35 | 0.25 | 12.44 | 36.29 | 2.81 | 28.17 | 2.64 | 2.73 |
| | 4.93 | 30.66 | 0.30 | 15.04 | 35.86 | 3.24 | 27.73 | 3.08 | 3.16 |
| | 5.01 | 37.73 | 0.37 | 18.51 | 35.03 | 4.07 | 26.91 | 3.90 | 3.99 |
| | 5.07 | 43.04 | 0.42 | 21.11 | 34.13 | 4.97 | 26.03 | 4.78 | 4.88 |
| | 5.13 | 48.35 | 0.47 | 23.71 | 33.30 | 5.80 | 25.19 | 5.62 | 5.71 |
| | 5.19 | 53.65 | 0.53 | 26.32 | 32.42 | 6.68 | 24.32 | 6.49 | 6.59 |
| | 5.26 | 59.84 | 0.59 | 29.35 | 31.08 | 8.02 | 23.00 | 7.81 | 7.92 |
| | 5.32 | 65.15 | 0.64 | 31.95 | 29.75 | 9.35 | 21.67 | 9.14 | 9.25 |
| | 5.36 | 68.68 | 0.67 | 33.69 | 28.76 | 10.34 | 20.70 | 10.11 | 10.23 |
| | 5.43 | 74.87 | 0.73 | 36.73 | 27.13 | 11.97 | 19.07 | 11.74 | 11.86 |
| | 5.49 | 80.18 | 0.79 | 39.33 | 25.11 | 13.99 | 17.09 | 13.72 | 13.86 |
| | 5.51 | 81.95 | 0.80 | 40.20 | 24.11 | 14.99 | 16.11 | 14.70 | 14.85 |
| | 5.56 | 86.37 | 0.85 | 42.36 | 22.77 | 16.33 | 14.78 | 16.03 | 16.18 |
| | 5.62 | 91.68 | 0.90 | 44.97 | 20.20 | 18.90 | 13.21 | 17.60 | 18.25 |

| Footing Shape | Reading in Load Cell (mV ) | Weight (kg) | Applied Force (kN) | Applied Pressure (kPa) | Dial Gauge1 Reading | Settlement According to Dial Gauge 1 (mm) | Dial Gauge2 Reading | Settlement According to Dial Gauge 2 (mm) | Average Settlement (in mm) | |
|---|---|---|---|---|---|---|---|---|---|---|
| Circular | 4.58 | -0.29 | 0.00 | 0.00 | 18.99 | 0.00 | 30.55 | 0.00 | 0.00 | |
| | 4.68 | 8.55 | 0.08 | 10.68 | 17.87 | 1.12 | 29.43 | 1.12 | 1.12 | |
| | 4.72 | 12.09 | 0.12 | 15.10 | 16.68 | 2.31 | 28.28 | 2.27 | 2.29 | |
| | 4.76 | 15.63 | 0.15 | 19.52 | 14.48 | 4.51 | 26.09 | 4.46 | 4.49 | |
| | 4.79 | 18.28 | 0.18 | 22.83 | 13.02 | 5.97 | 24.64 | 5.91 | 5.94 | |
| | 4.83 | 21.82 | 0.21 | 27.25 | 10.46 | 8.53 | 22.03 | 8.52 | 8.53 | |
| | 4.86 | 24.47 | 0.24 | 30.56 | 8.35 | 10.64 | 19.87 | 10.68 | 10.66 | |
| | 4.89 | 27.12 | 0.27 | 33.88 | 5.48 | 13.51 | 17.00 | 13.55 | 13.53 | |
| | 4.92 | 29.78 | 0.29 | 37.19 | 2.88 | 16.11 | 14.32 | 16.23 | 16.17 | |
| | 4.93 | 30.66 | 0.30 | 38.30 | 1.29 | 17.70 | 12.74 | 17.81 | 17.76 | |
| Rectangular (B/L=0.25) | 4.58 | -0.29 | 0.00 | 0.00 | 34.96 | 0.00 | 27.19 | 0.00 | | 0.00 |
| | 4.79 | 18.28 | 0.18 | 4.48 | 34.59 | 0.37 | 27.06 | 0.13 | | 0.25 |
| | 4.85 | 23.59 | 0.23 | 5.78 | 34.20 | 0.76 | 26.69 | 0.50 | | 0.63 |
| | 4.97 | 34.20 | 0.34 | 8.39 | 33.76 | 1.20 | 26.26 | 0.93 | | 1.07 |
| | 5.05 | 41.27 | 0.40 | 10.12 | 33.42 | 1.54 | 25.91 | 1.28 | | 1.41 |
| | 5.20 | 54.54 | 0.53 | 13.37 | 32.46 | 2.50 | 24.93 | 2.26 | | 2.38 |
| | 5.34 | 66.92 | 0.66 | 16.41 | 31.76 | 3.20 | 24.23 | 2.96 | | 3.08 |
| | 5.42 | 73.99 | 0.73 | 18.15 | 31.23 | 3.73 | 23.69 | 3.50 | | 3.62 |
| | 5.54 | 84.60 | 0.83 | 20.75 | 30.25 | 4.71 | 22.73 | 4.46 | | 4.59 |
| | 5.67 | 96.10 | 0.94 | 23.57 | 28.96 | 6.00 | 21.44 | 5.75 | | 5.88 |
| | 5.77 | 104.94 | 1.03 | 25.74 | 28.37 | 6.59 | 20.84 | 6.35 | | 6.47 |
| | 5.83 | 110.25 | 1.08 | 27.04 | 27.25 | 7.71 | 19.75 | 7.44 | | 7.58 |
| | 5.98 | 123.51 | 1.21 | 30.29 | 25.78 | 9.18 | 18.29 | 8.90 | | 9.04 |
| | 6.17 | 140.31 | 1.38 | 34.41 | 23.50 | 11.46 | 16.08 | 11.11 | | 11.29 |
| | 6.35 | 156.23 | 1.53 | 38.32 | 20.76 | 14.20 | 13.38 | 13.81 | | 14.01 |
| | 6.47 | 166.84 | 1.64 | 40.92 | 19.50 | 15.46 | 12.10 | 15.09 | | 15.28 |
| | 6.70 | 187.18 | 1.84 | 45.91 | 15.85 | 19.11 | 8.47 | 18.72 | | 18.92 |
| | 6.81 | 196.91 | 1.93 | 48.29 | 11.53 | 23.43 | 4.13 | 23.06 | | 23.25 |

## Settlement tank test result on dense dry sand

| Footing Shape | Reading in Load Cell (mV ) | Weight (kg) | Applied Force (kN) | Applied Pressure (kPa) | Dial Gauge 1 Reading | Settlement According to Dial Gauge 1 (mm) | Dial Gauge 2 Reading | Settlement According to Dial Gauge 2 (mm) | Average Settlement (in mm) | | |
|---|---|---|---|---|---|---|---|---|---|---|---|
| Square Footing | 4.59 | 0.00 | 0.00 | 0.00 | 26.30 | 0.00 | 35.64 | 0.00 | 0.00 | | |
| | 4.63 | 4.13 | 0.04 | 4.05 | 26.24 | 0.06 | 35.56 | 0.08 | 0.07 | | |
| | 4.67 | 7.67 | 0.08 | 7.52 | 25.92 | 0.38 | 35.32 | 0.32 | 0.35 | | |
| | 4.81 | 20.05 | 0.20 | 19.67 | 25.76 | 0.54 | 35.05 | 0.59 | 0.57 | | |
| | 4.88 | 26.24 | 0.26 | 25.74 | 25.43 | 0.87 | 34.80 | 0.84 | 0.86 | | |
| | 4.98 | 35.08 | 0.34 | 34.41 | 25.05 | 1.25 | 34.39 | 1.25 | 1.25 | | |
| | 5.14 | 49.23 | 0.48 | 48.29 | 24.55 | 1.75 | 33.90 | 1.74 | 1.75 | | |
| | 5.29 | 62.49 | 0.61 | 61.31 | 23.86 | 2.44 | 33.32 | 2.32 | 2.38 | | |
| | 5.34 | 66.92 | 0.66 | 65.64 | 23.65 | 2.65 | 33.04 | 2.60 | 2.63 | | |
| | 5.45 | 76.64 | 0.75 | 75.19 | 23.15 | 3.15 | 32.52 | 3.12 | 3.14 | | |
| | 5.64 | 93.45 | 0.92 | 91.67 | 22.13 | 4.17 | 31.50 | 4.14 | 4.16 | | |
| | 5.83 | 110.25 | 1.08 | 108.15 | 20.61 | 5.69 | 30.00 | 5.64 | 5.67 | | |
| | 5.92 | 118.21 | 1.16 | 115.96 | 19.86 | 6.44 | 29.15 | 6.49 | 6.47 | | |
| | 5.98 | 123.51 | 1.21 | 121.16 | 17.85 | 8.45 | 27.30 | 8.34 | 8.40 | | |
| | 6.00 | 125.28 | 1.23 | 122.90 | 15.61 | 10.69 | 25.00 | 10.64 | 10.67 | | |
| | 5.78 | 105.83 | 1.04 | 103.81 | 8.78 | 17.52 | 17.86 | 17.78 | 17.65 | | |
| | 5.77 | 104.94 | 1.03 | 102.95 | 4.35 | 21.95 | 13.64 | 22.00 | 21.98 | | |
| Circular Footing | 4.59 | 0.00 | 0.00 | 0.00 | 43.90 | 0.00 | 37.78 | 0.00 | | 0.00 | |
| | 4.68 | 8.55 | 0.08 | 10.68 | 43.64 | 0.26 | 37.56 | 0.22 | | 0.24 | |
| | 4.78 | 17.40 | 0.17 | 21.73 | 43.21 | 0.69 | 37.08 | 0.70 | | 0.70 | |
| | 4.92 | 29.78 | 0.29 | 37.19 | 42.12 | 1.78 | 36.05 | 1.73 | | 1.76 | |
| | 5.06 | 42.16 | 0.41 | 52.65 | 41.25 | 2.65 | 35.10 | 2.68 | | 2.67 | |
| | 5.22 | 56.30 | 0.55 | 70.33 | 39.60 | 4.30 | 33.48 | 4.30 | | 4.30 | |
| | 5.36 | 68.68 | 0.67 | 85.79 | 38.12 | 5.78 | 32.05 | 5.73 | | 5.76 | |
| | 5.36 | 68.68 | 0.67 | 85.79 | 37.52 | 6.38 | 31.45 | 6.33 | | 6.36 | |
| | 5.34 | 66.92 | 0.66 | 83.58 | 36.52 | 7.38 | 30.38 | 7.40 | | 7.39 | |
| | 5.34 | 66.92 | 0.66 | 83.58 | 34.28 | 9.62 | 28.12 | 9.66 | | 9.64 | |
| Rectangular Footing ($B/L$=0.5) | 4.59 | 0.59 | 0.01 | 0.29 | 31.41 | 0.00 | 45.08 | 0.00 | | | 0.00 |
| | 4.74 | 13.86 | 0.14 | 6.80 | 31.32 | 0.09 | 44.99 | 0.09 | | | 0.09 |
| | 5.04 | 40.39 | 0.40 | 19.81 | 31.06 | 0.35 | 44.70 | 0.38 | | | 0.36 |
| | 5.28 | 61.61 | 0.60 | 30.22 | 30.84 | 0.57 | 44.54 | 0.54 | | | 0.56 |
| | 5.58 | 88.14 | 0.86 | 43.23 | 30.52 | 0.89 | 44.29 | 0.79 | | | 0.84 |
| | 5.94 | 119.97 | 1.18 | 58.85 | 29.91 | 1.50 | 43.72 | 1.36 | | | 1.43 |
| | 6.32 | 153.58 | 1.51 | 75.33 | 29.34 | 2.07 | 43.15 | 1.93 | | | 2.00 |
| | 6.56 | 174.80 | 1.71 | 85.74 | 28.71 | 2.70 | 42.53 | 2.55 | | | 2.63 |
| | 6.98 | 211.94 | 2.08 | 103.96 | 27.50 | 3.91 | 41.30 | 3.78 | | | 3.85 |
| | 7.29 | 239.35 | 2.35 | 117.40 | 26.32 | 5.09 | 40.07 | 5.01 | | | 5.05 |
| | 7.58 | 265.00 | 2.60 | 129.98 | 24.95 | 6.46 | 38.70 | 6.38 | | | 6.42 |
| | 7.86 | 289.76 | 2.84 | 142.13 | 22.08 | 9.33 | 35.81 | 9.27 | | | 9.30 |
| | 8.06 | 307.45 | 3.02 | 150.80 | 19.91 | 11.50 | 33.62 | 11.46 | | | 11.48 |
| | 7.92 | 295.07 | 2.89 | 144.73 | 17.26 | 14.15 | 30.97 | 14.11 | | | 14.13 |
| | 7.86 | 289.76 | 2.84 | 142.13 | 15.21 | 16.20 | 28.94 | 16.14 | | | 16.17 |
| | 7.70 | 275.61 | 2.70 | 135.19 | 10.66 | 20.75 | 24.40 | 20.68 | | | 20.72 |

## Settlement tank test result on loose saturated sand

| Footing Shape | Dial Gauge 1 Reading | Settlement According to Dial Gauge 1 (mm) | Dial Gauge 2 Reading | Settlement According to Dial Gauge 2 (mm) | Average Settlement (in mm) | Correction Factor | Height of Watertable from bottom (in mm) | Normalized Water Table Depth | | | | |
|---|---|---|---|---|---|---|---|---|---|---|---|---|
| | | | | | | | | Rectangular ($B/L$=0.25) | Rectangular ($B/L$=0.5) | Rectangular ($B/L$=1.0) | Rectangular ($B/L$=0.75) | Circular |
| Rectangular (B/L)=0.25 | 46.34 | 1.28 | 28.92 | 0.93 | 1.15 | 1.00 | 0.00 | 5.99 | | | | |
| | 45.86 | 1.76 | 28.43 | 1.42 | 1.59 | 1.38 | 100.00 | 4.98 | | | | |
| | 45.31 | 2.31 | 27.87 | 1.98 | 2.15 | 1.87 | 200.00 | 3.98 | | | | |
| | 44.60 | 3.02 | 27.18 | 2.67 | 2.85 | 2.47 | 300.00 | 2.97 | | | | |
| | 43.37 | 4.25 | 25.94 | 3.91 | 4.08 | 3.55 | 400.00 | 1.96 | | | | |
| | 41.50 | 6.12 | 24.07 | 5.78 | 5.95 | 5.17 | 500.00 | 0.94 | | | | |
| | 41.25 | 6.37 | 23.82 | 6.03 | 6.20 | 5.39 | 520.00 | 0.74 | | | | |
| | 40.79 | 6.83 | 23.35 | 6.50 | 6.67 | 5.80 | 540.00 | 0.53 | | | | |
| | 40.39 | 7.23 | 22.95 | 6.90 | 7.07 | 6.14 | 560.00 | 0.33 | | | | |
| | 39.99 | 7.63 | 22.54 | 7.31 | 7.47 | 6.50 | 580.00 | 0.13 | | | | |
| | 39.71 | 7.91 | 22.30 | 7.55 | 7.73 | 6.72 | 593.00 | 0.00 | | | | |
| Rectangular (B/L=0.5) | 41.99 | 0.89 | 49.47 | 0.89 | 0.89 | 1.00 | 0.00 | | 5.74 | | | |
| | 41.90 | 0.98 | 49.39 | 0.97 | 0.98 | 1.10 | 75.00 | | 5.00 | | | |
| | 41.76 | 1.12 | 49.25 | 1.11 | 1.12 | 1.25 | 175.00 | | 4.00 | | | |
| | 41.39 | 1.49 | 48.87 | 1.49 | 1.49 | 1.67 | 275.00 | | 3.00 | | | |
| | 40.55 | 2.33 | 48.02 | 2.34 | 2.34 | 2.62 | 375.00 | | 2.00 | | | |
| | 39.05 | 3.83 | 46.53 | 3.83 | 3.83 | 4.30 | 475.00 | | 1.00 | | | |
| | 38.63 | 4.25 | 46.15 | 4.21 | 4.23 | 4.75 | 499.00 | | 0.76 | | | |
| | 38.42 | 4.46 | 45.89 | 4.47 | 4.47 | 5.02 | 517.00 | | 0.58 | | | |
| | 38.21 | 4.67 | 45.74 | 4.62 | 4.65 | 5.22 | 535.00 | | 0.40 | | | |
| | 37.53 | 5.35 | 45.01 | 5.35 | 5.35 | 6.01 | 575.00 | | 0.00 | | | |
| Square (B/L=1) | 10.23 | 0.67 | 41.61 | 0.67 | 0.67 | 1.00 | 0.00 | | | 5.89 | | |
| | 10.05 | 0.85 | 41.36 | 0.92 | 0.89 | 1.32 | 90.00 | | | 4.99 | | |
| | 9.94 | 0.96 | 41.22 | 1.06 | 1.01 | 1.51 | 190.00 | | | 3.99 | | |
| | 9.73 | 1.17 | 40.96 | 1.32 | 1.25 | 1.86 | 290.00 | | | 2.99 | | |
| | 9.10 | 1.80 | 40.35 | 1.93 | 1.87 | 2.78 | 390.00 | | | 1.98 | | |
| | 7.79 | 3.11 | 39.01 | 3.27 | 3.19 | 4.76 | 490.00 | | | 0.97 | | |
| | 7.44 | 3.46 | 38.66 | 3.62 | 3.54 | 5.28 | 510.00 | | | 0.76 | | |
| | 7.05 | 3.85 | 38.29 | 3.99 | 3.92 | 5.85 | 530.00 | | | 0.56 | | |
| | 6.74 | 4.16 | 37.96 | 4.32 | 4.24 | 6.33 | 550.00 | | | 0.36 | | |
| | 6.39 | 4.51 | 37.60 | 4.68 | 4.60 | 6.86 | 570.00 | | | 0.15 | | |
| | 5.90 | 5.00 | 37.13 | 5.15 | 5.08 | 7.57 | 585.00 | | | 0.00 | | |
| Rectangular (B/L=0.75) | 9.75 | 1.37 | 33.01 | 0.92 | 1.15 | 1.00 | 0.00 | | | | 5.89 | |
| | 9.47 | 1.65 | 32.76 | 1.17 | 1.41 | 1.23 | 90.00 | | | | 4.99 | |
| | 9.32 | 1.80 | 32.58 | 1.35 | 1.58 | 1.38 | 190.00 | | | | 3.98 | |
| | 9.05 | 2.07 | 32.32 | 1.61 | 1.84 | 1.61 | 290.00 | | | | 2.98 | |
| | 8.31 | 2.81 | 31.61 | 2.32 | 2.57 | 2.24 | 390.00 | | | | 1.97 | |
| | 6.75 | 4.37 | 30.18 | 3.75 | 4.06 | 3.55 | 490.00 | | | | 0.96 | |
| | 6.55 | 4.57 | 29.96 | 3.97 | 4.27 | 3.73 | 510.00 | | | | 0.76 | |
| | 6.25 | 4.87 | 29.69 | 4.24 | 4.56 | 3.98 | 530.00 | | | | 0.55 | |
| | 5.92 | 5.20 | 29.39 | 4.54 | 4.87 | 4.25 | 550.00 | | | | 0.35 | |
| | 5.50 | 5.62 | 29.01 | 4.92 | 5.27 | 4.60 | 570.00 | | | | 0.15 | |
| | 5.16 | 5.96 | 28.69 | 5.24 | 5.60 | 4.89 | 585.00 | | | | 0.00 | |
| Circular | 14.20 | 0.64 | 27.39 | 0.59 | 0.62 | 1.00 | 0.00 | | | | | 5.79 |
| | 14.10 | 0.74 | 27.29 | 0.69 | 0.72 | 1.16 | 100.00 | | | | | 4.79 |
| | 14.00 | 0.84 | 27.20 | 0.78 | 0.81 | 1.32 | 200.00 | | | | | 3.79 |
| | 13.85 | 0.99 | 27.14 | 0.84 | 0.92 | 1.49 | 300.00 | | | | | 2.79 |
| | 13.56 | 1.28 | 26.73 | 1.25 | 1.27 | 2.06 | 400.00 | | | | | 1.79 |
| | 12.76 | 2.08 | 25.96 | 2.02 | 2.05 | 3.33 | 500.00 | | | | | 0.78 |
| | 12.48 | 2.36 | 25.68 | 2.30 | 2.33 | 3.79 | 520.00 | | | | | 0.58 |
| | 12.24 | 2.60 | 25.43 | 2.55 | 2.58 | 4.19 | 540.00 | | | | | 0.37 |
| | 11.92 | 2.92 | 25.13 | 2.85 | 2.89 | 4.69 | 560.00 | | | | | 0.17 |
| | 11.20 | 3.64 | 24.40 | 3.58 | 3.61 | 5.87 | 577.00 | | | | | 0.00 |

## Settlement tank test result on dense saturated sand

| Footing Shape | Dial Gauge 1 Reading | Settlement According to Dial Gauge 1 (mm) | Dial Gauge 2 Reading | Settlement According to Dial Gauge 2 (mm) | Average Settlement (in mm) | Correction Factor | Height of Watertable from bottom (in mm) | Normalized Water Table Depth | | |
|---|---|---|---|---|---|---|---|---|---|---|
| | | | | | | | | Square Footing ($B/L$=1.0) | Rectangular Footing ($B/L$=0.5) | Circular Footing |
| Rectangular (B/L=0.5 ) | 28.87 | 1.30 | 42.40 | 1.26 | 1.28 | 1.00 | 0.00 | | 5.99 | |
| | 28.84 | 1.33 | 42.38 | 1.28 | 1.31 | 1.02 | 100.00 | | 4.99 | |
| | 28.78 | 1.39 | 42.34 | 1.32 | 1.36 | 1.06 | 200.00 | | 3.99 | |
| | 28.68 | 1.49 | 42.24 | 1.42 | 1.46 | 1.14 | 300.00 | | 2.99 | |
| | 28.44 | 1.73 | 42.02 | 1.64 | 1.69 | 1.32 | 400.00 | | 1.98 | |
| | 27.64 | 2.53 | 41.24 | 2.42 | 2.48 | 1.93 | 500.00 | | 0.98 | |
| | 27.47 | 2.70 | 41.06 | 2.60 | 2.65 | 2.07 | 520.00 | | 0.77 | |
| | 27.15 | 3.02 | 40.72 | 2.94 | 2.98 | 2.33 | 540.00 | | 0.57 | |
| | 26.98 | 3.19 | 40.57 | 3.09 | 3.14 | 2.45 | 560.00 | | 0.37 | |
| | 26.50 | 3.67 | 40.11 | 3.55 | 3.61 | 2.82 | 580.00 | | 0.16 | |
| | 25.98 | 4.19 | 39.57 | 4.09 | 4.14 | 3.23 | 593.00 | | 0.00 | |
| Square | 30.86 | 1.50 | 45.81 | 1.50 | 1.50 | 1.00 | 0.00 | 5.99 | | |
| | 30.79 | 1.57 | 45.74 | 1.57 | 1.57 | 1.05 | 100.00 | 4.98 | | |
| | 30.69 | 1.67 | 45.64 | 1.67 | 1.67 | 1.11 | 200.00 | 3.98 | | |
| | 30.64 | 1.72 | 45.58 | 1.73 | 1.73 | 1.15 | 300.00 | 2.98 | | |
| | 30.49 | 1.87 | 45.42 | 1.89 | 1.88 | 1.25 | 400.00 | 1.98 | | |
| | 30.08 | 2.28 | 45.02 | 2.29 | 2.29 | 1.52 | 500.00 | 0.98 | | |
| | 29.87 | 2.49 | 44.81 | 2.50 | 2.50 | 1.66 | 520.00 | 0.78 | | |
| | 29.68 | 2.68 | 44.61 | 2.70 | 2.69 | 1.79 | 540.00 | 0.57 | | |
| | 29.38 | 2.98 | 44.31 | 3.00 | 2.99 | 1.99 | 560.00 | 0.37 | | |
| | 28.86 | 3.50 | 43.80 | 3.51 | 3.51 | 2.34 | 580.00 | 0.16 | | |
| | 27.99 | 4.37 | 42.91 | 4.40 | 4.39 | 2.92 | 593.00 | 0.00 | | |
| Circular | 30.04 | 0.81 | 42.76 | 0.81 | 0.81 | 1.00 | 0.00 | | | 5.97 |
| | 29.99 | 0.86 | 42.72 | 0.85 | 0.86 | 1.06 | 100.00 | | | 4.97 |
| | 29.82 | 1.03 | 42.59 | 0.98 | 1.01 | 1.24 | 300.00 | | | 2.97 |
| | 29.67 | 1.18 | 42.45 | 1.12 | 1.15 | 1.42 | 400.00 | | | 1.97 |
| | 29.01 | 1.84 | 41.82 | 1.75 | 1.80 | 2.22 | 500.00 | | | 0.96 |
| | 28.76 | 2.09 | 41.60 | 1.97 | 2.03 | 2.51 | 520.00 | | | 0.76 |
| | 28.56 | 2.29 | 41.42 | 2.15 | 2.22 | 2.74 | 540.00 | | | 0.56 |
| | 28.26 | 2.59 | 41.12 | 2.45 | 2.52 | 3.11 | 560.00 | | | 0.35 |
| | 27.58 | 3.27 | 40.46 | 3.11 | 3.19 | 3.94 | 580.00 | | | 0.15 |
| | 27.17 | 3.68 | 40.05 | 3.52 | 3.60 | 4.44 | 594.00 | | | 0.00 |

# Appendix C

## Double tangent method applied in settlement tank tests

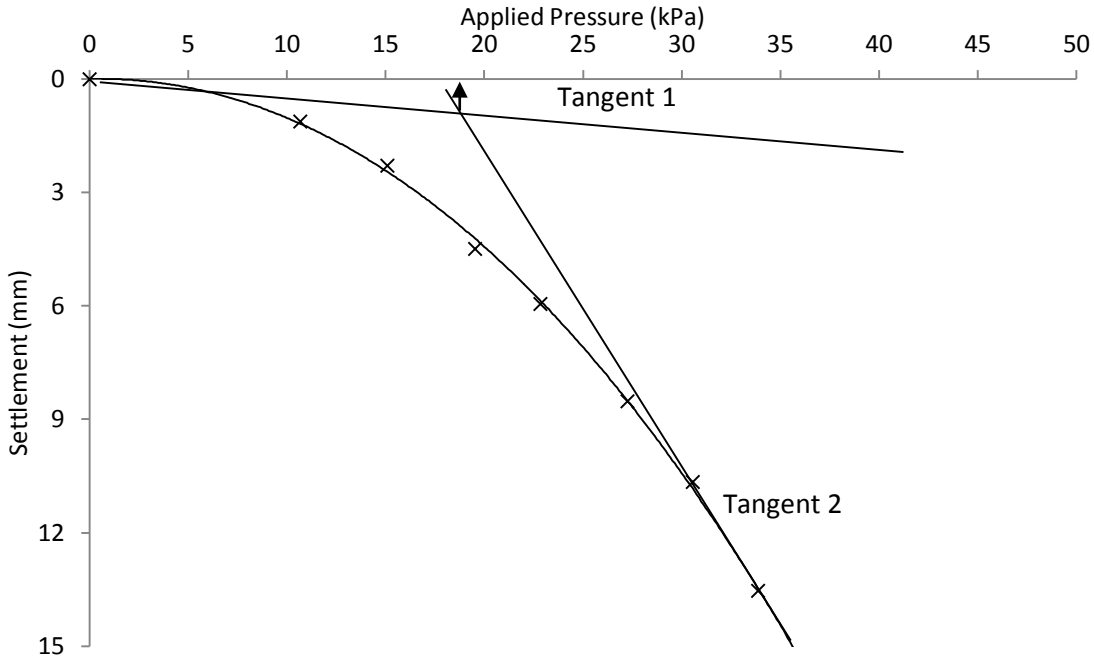


(a)

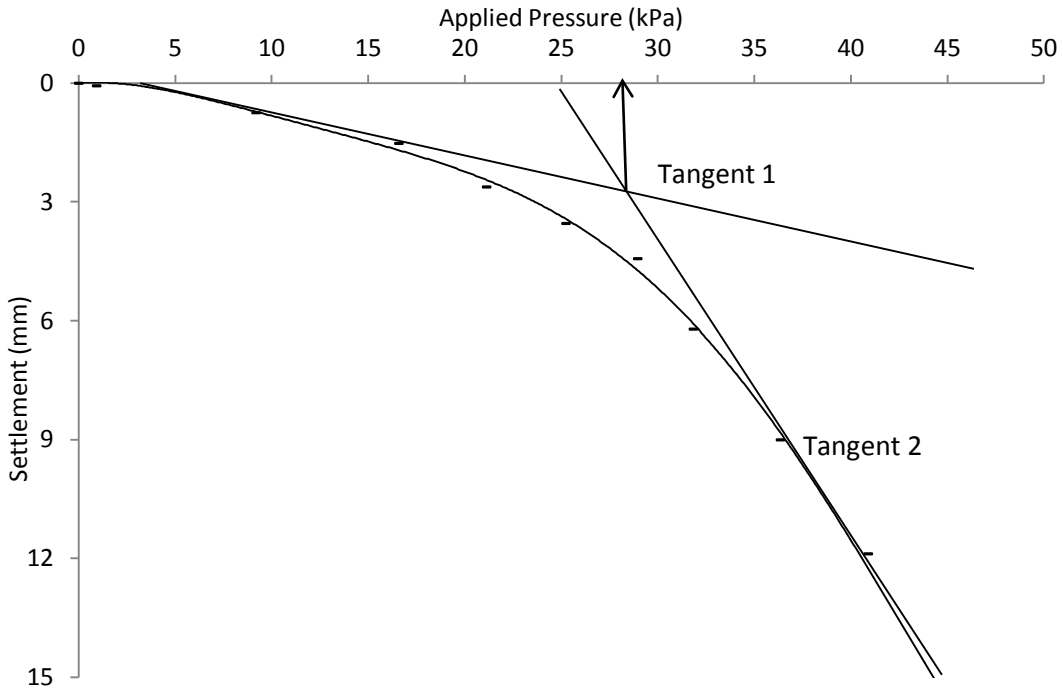


(b)

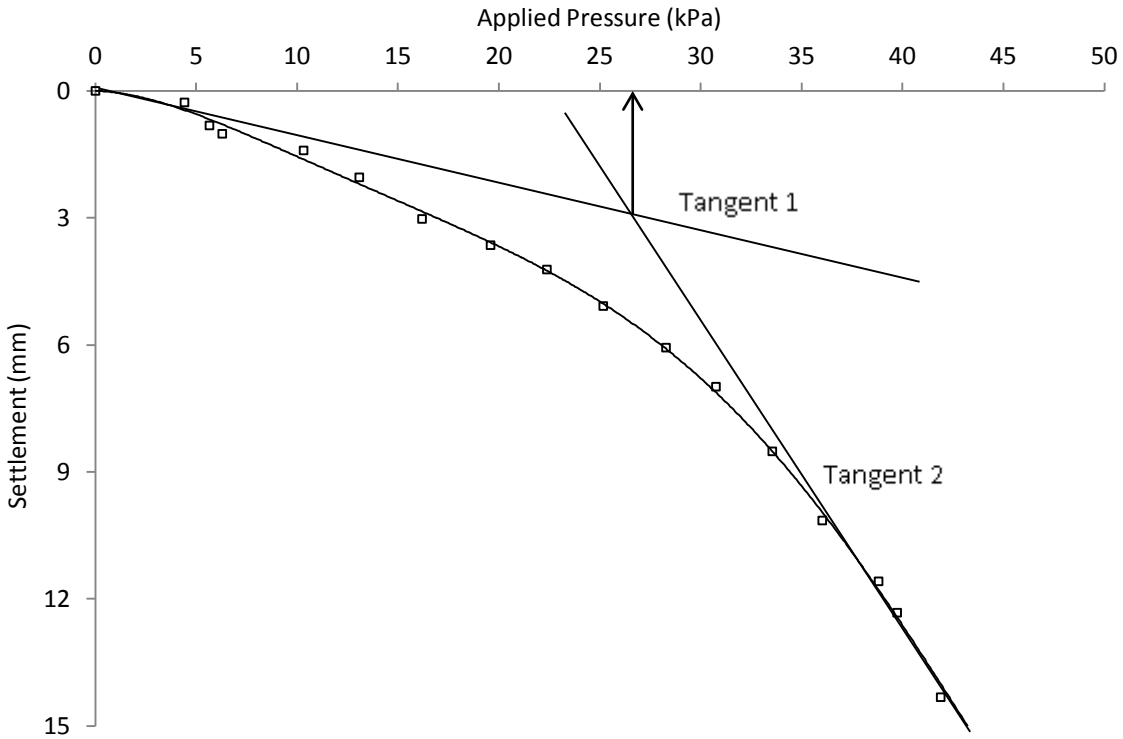
Applied Pressure (kPa)
0
5
10
15
20
25
30
35
40
45
50
Settlement (mm)
0
3
6
9
12
15
Tangent 1
Tangent 2

(c)

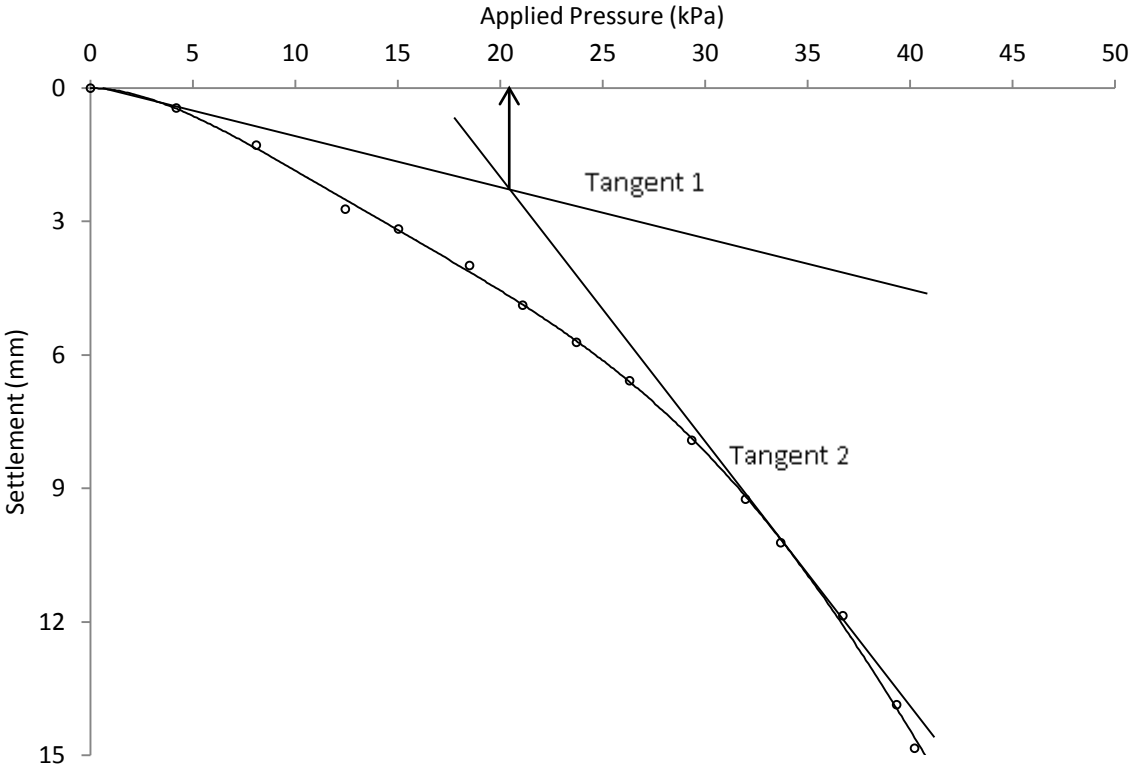
Applied Pressure (kPa)
0
5
10
15
20
25
30
35
40
45
50
Settlement (mm)
0
3
6
9
12
15
Tangent 1
Tangent 2

(d)

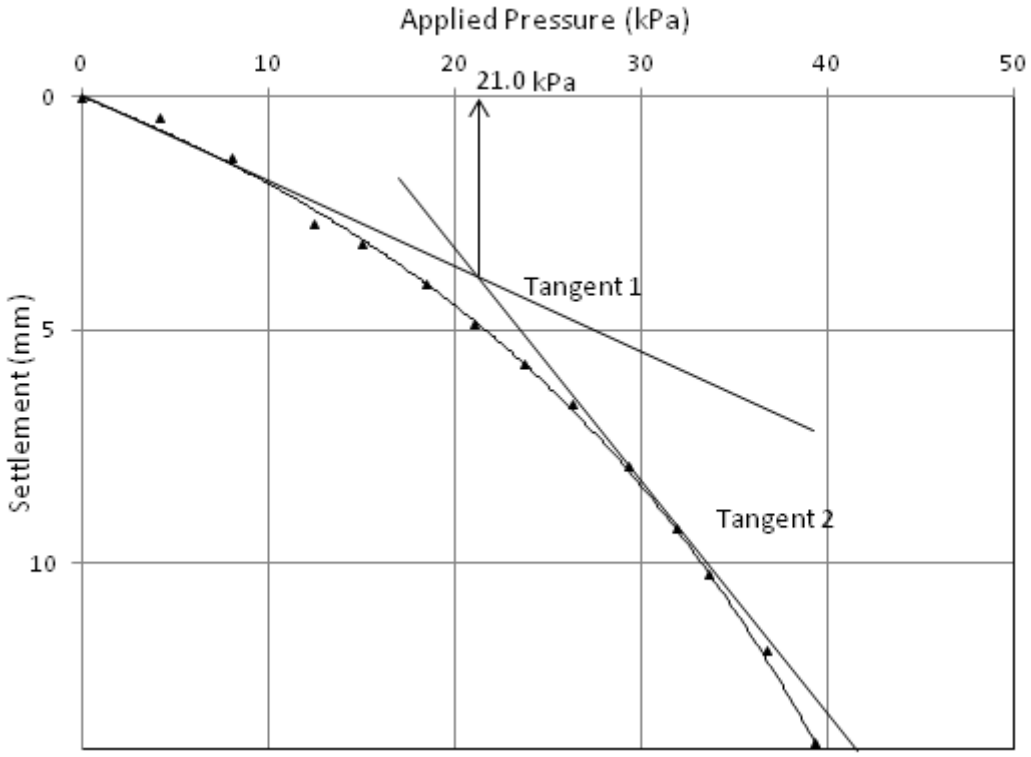


(e)

**Figure C. 1: Bearing capacity determination using double tangent method for footings resting on dry loose sand, a) circular footing, b) square footing, c) rectangular footing (B/L=0.75), d) rectangular footing (B/L=0.5), e) rectangular footing (B/L=0.25)**

## Appendix D1

FLAC code for laboratory model circular footing

```
;==============================
; Laboratory model circular footing
; Water level at 1B below the footing level
;==========================
new
; configure
        config axisymmetry
;generate grid
        grid 72 82
        m e i=1,20 j=1,20
        m e i=1,20 j=22 41
        m e i=1,40 j=43 82
        m e i=42 61 j=22 61
        m e i=63 72 j=22 31
        gen 0,0 0,.4 .4,.4 .4,0 i=1,21 j=1,21
        gen 0 .4 0 .5 .1 .5 .1 .4 i=1,21 j=22 42
        gen 0 .5 0 .6 .1 .6 .1 .5 i=1,41 j=43 83
        gen .1 .4 .1 .6 .2 .6 .2 .4 i=42 62 j=22 62
        gen .2 .4 .2 .6 .4 .6 .4 .4 i=63 73 j=22 32

; define Young's modulus, Poisson's ratio, density
def install
        loop i (1,izones)
                loop j (1,jzones)
                        yc = (y(i,j)+y(i,j+1))/2.0
                        zz = 0.6 - yc
                        if zz > 0 then
                        abc = 15.495e6
                        else
                        abc = 0
                        end_if
```

```
                    if zz > 0 then
                    cc=884.6
                    else
                    cc=1434
                    end_if
                    y_mod = y_zero - abc
                    shear_mod(i,j) = y_mod / (2.0*(1.0+p_ratio))
                    bulk_mod(i,j) = y_mod / (3.0*(1.0-2.0*p_ratio))
                    density(i,j) = cc
                    end_loop
                end_loop
        end
        set p_ratio=0.2 y_zero=20e6
install

;attach
        attach aside from 1,21 to 6,21 bside from 1,22 to 21,22
        attach aside from 6,21 to 11,21 bside from 42,22 to 62,22
        attach aside from 11,21 to 21,21 bside from 63,22 to 73,22
        attach aside from 1,42 to 21,42 bside from 1,43 to 41,43
        attach aside from 21,22 to 21,42 bside from 42,22 to 42,42
        attach aside from 41,43 to 41,83 bside from 42,42 to 42,62
        attach aside from 62,22 to 62,62 bside from 63,22 to 63,32

; initial and boundary condition
        set gravity 9.81
        fix x i=73
        fix x i=21 j=1,21
        fix y j=1
        fix x j=1
        plot hold model grid bou lm attach yell
        solve
        ini ydisp=0 xdisp=0
; apply pressure and solve
```

```
apply pressure=5e3 from 1,83 to 21,83
solve
plot hold model grid
print ydisp i=1
```

## Appendix D2

FLAC code for full scale model circular footing with $D_f$ = 1.0$B$

```
;==============================
; Full scale model circular footing
; Embedment depth,  Df = 1.0B
; Water level at ground surface
;==========================
new
; configure
        config axisymmetry
;generate grid
        grid 72 103
        m e i=1,20 j=1,20
        m e i=1,20 j=22 41
        m e i=1,40 j=43 82
        m e i=42 61 j=22 81
        m e i=63 72 j=22 36
        m e i=1, 10 j=84 103
        gen 0,0 0,4 4,4 4,0 i=1,21 j=1,21
        gen 0 4 0 5 1 5 1 4 i=1,21 j=22 42
        gen 0 5 0 6 1 6 1 5 i=1,41 j=43 83
        gen 1 4 1 7 2 7 2 4 i=42 62 j=22 82
        gen 2 4 2 7 4 7 4 4 i=63 73 j=22 37
        gen .5 6 .5 7 1 7 1 6 i=1 11 j=84 104

; define Young's modulus, Poisson's ratio, density

        def install
                loop i (1,izones)
                        loop j (1,jzones)
                        yc = (y(i,j)+y(i,j+1))/2.0
                        zz = 7 - yc
                        if zz > 6 then
```

```
                    abc = 10e6
                    else
                    abc = 0
                    end_if
                    if zz > 6 then
                    cc=884.6
                    else
                    cc=1434
                    end_if
                    y_mod = y_zero - abc
                    shear_mod(i,j) = y_mod / (2.0*(1.0+p_ratio))
                    bulk_mod(i,j) = y_mod / (3.0*(1.0-2.0*p_ratio))
                    density(i,j) = cc
                    end_loop
                end_loop
        end
        set p_ratio=0.2 y_zero=20e6
        install

;attach
        attach aside from 1,21 to 6,21 bside from 1,22 to 21,22
        attach aside from 6,21 to 11,21 bside from 42,22 to 62,22
        attach aside from 11,21 to 21,21 bside from 63,22 to 73,22
        attach aside from 1,42 to 21,42 bside from 1,43 to 41,43
        attach aside from 21,22 to 21,42 bside from 42,22 to 42,42
        attach aside from 41,43 to 41,83 bside from 42,42 to 42,62
        attach aside from 62,22 to 62,82 bside from 63,22 to 63,37
        attach aside from 11 84 to 11 104 bside from 42 62 to 42 82
        attach aside from 21 83 to 41 83 bside from 1 84 to 11 84

; initial and boundary condition
        fix x i=73
        fix x i=21 j=1,21
        fix y j=1
```

```
        fix x j=1
        plot hold model grid bou lm attach yell
        ini ydisp=0 xdisp=0

; apply pressure and solve
        apply pressure=100e3 from 1,83 to 21,83
        solve
```